AN ANALYSIS OF SHIP AVAILABILITY AFTER AN EARTHQUAKE-TSUNAMI: A CASE STUDY IN BRITISH COLUMBIA

by

Lauryne Rodrigues

Submitted in partial fulfillment of the requirements
for the degree of Master of Applied Science

at

Dalhousie University
Halifax, Nova Scotia
April 2023

Dalhousie University is located in Mi'kma'ki, the
ancestral and unceded territory of the Mi'kmaq.
We are all Treaty people.

TABLE OF CONTENTS

List of Tables

List of Figures

Abstract

Maritime logistics play a vital role in supporting emergency relief logistics for communities that are dependent on this transportation mode. By its geographical nature, this concerns specifically island populations. The viability of performing post-disaster operations depends on the availability of infrastructure elements, such as ports, waterways navigation support, and ship availability. During an earthquake event, especially when followed by a tsunami, there is a substantial risk of damage to vessels operating in coastal areas. This research investigates this risk in a Cascadia-type Earthquake event in British Columbia. In particular, a model is proposed to estimate the probability of ships being unavailable to support the humanitarian supply chain operations in the disaster response phase. The study uses spatial analysis tools with vessel movement data from the Automatic Information System. First, their origin and destination ports are determined, and routes and trajectories patterns are extracted from the data. Then, the model investigates the risk of damage to ferries and tugs on points along a specific path. The developed model considers various spatial and attribute components, such as the distance from collapsing structures, tsunami zone, safe depth areas, tsunami arrival time, and other nautical features. The results indicate that many small ferries and some tugs have a substantial probability of being unavailable to support emergency logistics, whereas larger ferries are less affected. Various results, such as the probability of certain parts of the fleet being unavailable, maps of dangerous navigational areas, and routes with reduced transportation capacity, can be used as a resource to support disaster preparedness and mitigation actions. Despite some uncertainties related to exact ship location and tsunami data and some model simplifications, the findings can thus be used to inform regional emergency preparedness decision-making and related risk management.

List of Abbreviations and Symbols Used

AIS - Automatic Identification System

EMBC - Emergency Management in British Columbia

ERL - Emergency Response Logistic

GIS - Geographic Information System

GRT - Gross Register Tonnage

IMO - International Maritime Organization identification code

MEOPAR - Marine Observation, Prediction and Response

MMSI - The Maritime Mobile Service Identity

MTSs - Maritime Transportation Systems

MVM - Marine Vessel Movement model

RUSEMARIE - Earthquake- Tsunami Loss Prediction Model for Marine Vessels

SIREN - Shipping Resilience: Strategic Planning for Coastal Community Resilience to Marine Transportation Risk project

SOG - Speed Over Ground

TAT- Tsunami Estimated Arrival time

TTD - Travel Time to a Safe Area

Acknowledgments

Developing and writing this thesis dissertation during the Covid-19 pandemic was challenging. For that reason, my support network was crucial to this project's completion. So, I would like to take a moment to show my gratitude to the people who were on my side during this period.

First, I would like to acknowledge my supervisor, Dr. Floris Goerlandt, and co-supervisor Dr. Ronald Pelot, for their patience, guidance, and encouragement. This thesis steps were constructive due to mutual self-respect, constructive feedback, attention to detail, and resilience. I want to highlight the professor concern for student mental health, always being open to listening, and the support words that helped increase confidence during this process.

It is also important to point out that this project was realized with funding support from the Marine Observation, Prediction and Response (MEOPAR) Network of Centres of Excellence and by the Province of British Columbia in the context of the 'Shipping Resilience: Strategic Planning for Coastal Community Resilience to Marine Transportation Risk (SIREN) project. The AIS database was provided by exactEarth Ltd., but it is also important to remember and thank R. Casey Hilliard for helping me understand AIS in this project's first steps.

I owe my gratitude to Brazilian Industrial Engineering friends Rafael and Luana, who destined to get together one more time for an academic journey. A special thank you to Luana, a great project co-worker, and friend.

Finally, I would like to express my profound gratitude to my mother, Lucinea, for all her encouraging words and for constantly reminding me that I am capable. She teaches me how to be strong. Furthermore, for my husband, Thiago, I do not have enough words to express my gratefulness for you to embark on this journey, for endless patience, and for being my emotional anchor.

Chapter 1
Introduction

Impacts on major ports and damaged vessels can cause marine transportation disruption, severely affecting coastal communities. The Great Earthquake and Tsunami event of 2011 in Japan is an example of this situation, where 28,612 marine vessels were damaged, and 319 ports had their facilities compromised [1]. Island communities rely on maritime supplies, and this dependency increases in case of disaster events. Depending on the disaster scale, the destruction of the local suppliers could generate a shortage of food, fuel, and medicines [2]. In the Japan 2011 event, the Kochi municipality had an Emergency Response Logistic (ERL) plan, which included essential supplies for affected people, amounting to a need for 2,300 tons of food per day [3]. Offering emergency supplies and restocking these affected coastal communities could present significant challenges when ports and vessels are unavailable.

One of the roles of an emergency response logistics plan is understanding the available resources. Hence, investigating the number of marine vessels available to support these island communities in post-disaster emergency logistics is essential to improve risk assessment and management. However, there currently is no technique to estimate these numbers. This research proposes a method to estimate the probability of a vessel being damaged due to an earthquake-tsunami event, applied to a specific scenario based on a Cascadia subduction zone Earthquake off the coast of British Columbia, affecting marine traffic near Vancouver Island.

In the following introductory subsections, details about the research problem will be tied to the scope of the study. In addition, the project objectives and questions will be presented. Finalizing the introduction chapter, the last subsection gives an overview of the thesis structure.

1.1 Research problem and scope of the study

The West Coast of Canada is adjacent to the Pacific, North America, and the Juan the Fuca plates [4]. As a result, there is a megathrust fault among these tectonic plates, the

Cascadia Subduction Zone. This active seismic zone turns British Columbia into one of the high-risk areas for the occurrence of earthquakes and tsunamis, which is confirmed by coastal geological sediments found on Vancouver Island, and evidence from previous seismic activity [5]. There are various research studies about the initial area of an earthquake along the 600 miles of the Cascadia zone, with models predicting an earthquake of at least magnitude 8.5 to occur in the next 500-600 years, with an event up to magnitude 9.2 occurring in the next 2500 years. Research also suggests earthquake-triggered tsunamis are highly likely to occur in such earthquake events [6].

Vancouver Island is susceptible to these catastrophic natural events and, simultaneously, is a coastal community that relies on maritime transportation to receive supplies [2], [7]–[9]. It was estimated in 2012 that 90% of all food is delivered by ferry and that the major city on the island, Victoria, has just three days of food due to just-in-time supply chain configuration [10]. Hence, while the coastal maritime supply chain in British Columbia is resilient to small-scale disruptions [11], the supply of goods to Vancouver Island is vulnerable to large-scale disruptions, e.g., in cases when ports or transportation assets are damaged in natural disasters[12].

Hence emergency response authorities will need to rely on ships to distribute supplies, although the communities would be vulnerable to shortages in case of an earthquake-triggered tsunami event [2]. For this reason, estimating if a ship will be damaged, and understanding the effects of earthquake-tsunami events on the availability of the fleet, is an essential part of the emergency response logistic plan for coastal communities.

This study focuses on the possibility of using a ship to support emergency response logistics. Hence, any damage that incapacitates a ship to promptly support deliveries in the immediate disaster response phase is of concern. So, even though different damage levels can be expected to occur, in this research, the terms damage, availability, and operability will be used interchangeably to denote whether or not a vessel is available for emergency logistics operations in the immediate response phase. There are different types of damage related to tsunamis for vessels: sinking or grounding, stranding, collision, loss of stability, and structural damage [1].

Studies related to damaged ships due to earthquakes and tsunamis s are sparse, with most of them performed in the context of Japan's 2011 Earthquake. There is no consensus and understanding about the exact damage mechanisms to a ship due to a tsunami in relation to its dynamic motion characteristics. Most studies on damages related to tsunami events focus on static structures for buildings, ports, and bridges [13], [14]. The recent developments in this field include the loss function of ships near ports due to currents [15], [16]. The latest advances in this field are motivated by innovations in data availability, computational power, and improved tsunami simulation models. Most studies focus on post-disaster data analyses, addressing damage according to ship size, tonnage, and material, further relating the vessel damage to tsunami velocity and wave height. These studies, thus, are limited to data analyses of past occurrences, which are not directly useful to estimate the damage to vessels in other contexts and geographical areas.

A better insight into the damage to ships, considering the route on which vessels operate and the evacuation time, would provide helpful information. The ship's safety will depend on various elements, such as ship dimensions, the collapse of nearby structures, tsunami parameters, and evacuation time to safe depths [15]. It is essential to fill this knowledge gap to understand what could happen to vessels in a voyage when an earthquake-tsunami event occurs. Such insights are helpful for the emergency response planners, as well as for the marine industry sector, to enhance emergency response plans by estimating the number of ships available for humanitarian logistics. This information can improve risk assessment and emergency preparedness, and response management, ultimately improving community resilience.

1.2 Thesis objective

Given the lack of research regarding ship availability in British Columbia following a major disaster, more specifically in the context of a Cascadia Earthquake event, this study aims to understand, investigate, and evaluate the damaged marine vessels by developing a novel model and by applying this to various datasets in British Columbia. This study is based on the day-to-day operation patterns in the study area, which are interpreted in the context of the described natural disaster event. In addition to that, this thesis proposes a new methodology to estimate the probability of a vessel having a function for humanitarian supply chain logistics operations being damaged by a natural disaster. The research sub-questions enumerated below will be answered in the following pages.

- **RQ1**: How many ships will be unavailable to support humanitarian supply chain operations in Vancouver Island coastal area?
- **RQ2:** What is the relation between ships groups sizes and damage probability considering Vancouver maritime logistic operations?
- **RQ3:** What are hazardous sea areas or routes for a ship to navigate in case of a tsunami in a Cascadia earthquake-tsunami scenario?
- **RQ4:** Which regions of Vancouver Island will likely be exposed to a reduced ship capacity for emergency logistics deliveries due to ships not being available in the immediate disaster response phase?
-

1.2 Thesis organization

The overall structure of the study takes the form of six chapters. The first chapter of this thesis presents the purpose and rationale behind the intended topic. Then, Chapter 2 offers a thematic literature review detailing earthquakes and tsunamis, especially the Cascadia event in British Columbia, and their impacts on marine assets. It will also review previous studies of ship damage. Next, in the methodology section, Chapter 3, the datasets used for the analysis will be specified, along with the two methods utilized, thus directing the theoretical research context to the vessel damage analysis technique.

The fourth section will present the research findings, focusing on the key thesis themes: movement data, availability estimation, and risk maps from post-processed results. Finally, the results will be discussed in Chapter 5, relating the findings to the research sub-questions. Future research applications will also be presented in the discussion, for example, using this study's results to network models. To summarize the thesis, the conclusion in Chapter 6 will highlight the main points of the previous chapters.

Chapter 2
Literature review

During an earthquake event, especially when followed by a tsunami, there is a substantial risk of damage to vessels operating in coastal areas. The viability of post-disaster operations depends on the availability of essential infrastructure and assets, such as ports, waterways navigation services, and ship availability. So, this literature review aims to understand relevant aspects of earthquake-tsunami events, their impacts on coastal areas and maritime transport systems, current studies on ship damage, and emergency logistics with vessels.

This chapter will conduct a thematic literature review to outline and provide a basis for understanding key aspects of maritime transportation and the impacts of earthquake-tsunami events for building the model to answer the research questions outlined in the introduction. The literature review will not focus on other types of natural disasters, such as hurricanes or socio-technical vessel accidents, without a natural disaster context. It starts by describing earthquake studies in British Columbia, focusing on the Cascadia-type earthquake. Next, the widespread impacts on maritime assets, specifically ports, sea areas, and waterways, will be examined. This is followed by more detailed studies on ship damages, recognizing that most of these investigations relate to the Japan 2011 Great Tohoku Earthquake. In addition, existing methods and techniques for vessel loss estimation will be reviewed. Then, maritime transportation as a critical point in emergency logistic response to coastal communities will be established, through the lens of a past event study case. These themes together set the scope and provide an information basis to develop and construct the proposed damage analysis technique.

2.1 Earthquakes in British Columbia

Earthquake events are related to tectonic plates, which are gradually moving. Sometimes when two or more plates move, friction is generated, and edges get stuck. When the force of the movement is greater than friction, energy is released to the earth's crust resulting in shakes, called earthquakes [17]. When an earthquake happens in shallow depths with high intensity and with an epicenter near populated areas, this combination of factors can result in a catastrophic event [8]. Several big earthquakes happened in the last years; for example, Nepal in 2015 endured a severe earthquake with 7.8 magnitude, causing approximately 9000 estimated deaths, Japan in 2011 experienced a 9.0 magnitude event, resulting in 15,690 deaths, Haiti in 2010 had a 7.0 magnitude earthquake with a devastating death toll of 316,000 people, and China in 2008 was hit by a 7.8 magnitude earthquake, resulting in 87,600 deaths [18]. In these past events, besides the loss of life, the direct damage to buildings, houses, and roads was very extensive. In all cases, there was significant additional damage caused by post-earthquake impacts such as tsunamis, landslides, and fires [19]. The west coast of Canada is situated to active tectonic plates, and hence is vulnerable to the similar impacts and consequences [12].

The Geological Survey of Canada recorded more than 1,000 earthquakes on the west coast yearly [20]. This is because of intense seismic activity in and near the Cascadia Subduction Zone area on the west coast of Canada, where the Pacific, North America, and Juan de Fuca plates produce friction [5]. In the last 70 years, more than 100 earthquakes of magnitude 5 or greater were registered on Vancouver Island's offshore region, and their magnitude was enough to cause damage if near the coast [20]. The Cascadia Subduction Zone has a 1,400 km length and 5 km depth [21]. Focusing on this zone, studies discovered from past geological data that there are 3 possible sources of an earthquake that also generates tsunamis. The northern segment could happen every 500-800 years along Vancouver Island to Washington State in the U.S. with a magnitude between 8.5 and 9. Major earthquake events in the central segment have an estimated return period of 500 to 600 years, between southern Washington and northern Oregon, with a magnitude of 8.5. A long-narrow segment with a 1,100 km possible rupture happens every 2500 years along the Vancouver Island coast, passing toward Oregon, with a magnitude of 9.1 to 9.2 [22]–[24].

In some studies, the long-narrow Cascadia is also called big-one or worst case due to the megathrust fault size, magnitude, and effects on a vast population along the 1100 km of coast[25],[21]. Geological evidence shows the damage and flooding in a Cascadia earthquake-tsunami event which occurred in 1700 A.D. reached seven Japanese shorelines, with waves of 1 to 5 m in Japanese coastal locations, proving its very significant energy, destructive power, and geographical reach [26].

Large tsunamis originate on tectonic plates located in the ocean. When a sub-sea earthquake happens, sea soil is displaced, and the vertical force generates water movement towards all directions in the entire water column. The water movement produces waves that travel along the ocean. The waves increase in size, i.e. have a larger wave height, when moving from deep ocean areas towards shallow coastal waters [27]. The last tsunami in the Pacific Ocean near British Columbia happened in the 2012 Haida Gwaii earthquake, with a magnitude of 7.7. This tsunami had run-ups over 7 m in several inlets, with maximum wave heights reaching up to 13 m. Due to low population density, with even extensive non-populated areas, with only some man-made structures in coastal areas, the damage was minimal despite the intense tsunami [28].

However, tsunamis can cause significant damage. For instance, in the 2011 Tohoku earthquake with magnitude 9.0 off the Japanese coast, a tsunami was observed a maximum run-up of 38 m in a narrow valley, generating 11m/s currents after 10 minutes in some channels. The worst event registered involved outflow currents over 3 m/s to 11 m/s for over 2 minutes in the Kesennuma Bay narrows. This rapid current increase was impossible for any vessel to navigate [29]. Some studies for a Cascadia worst case scenario estimate tsunamis running up to 25 m along 8 Vancouver Island communities facing the Pacific Ocean [30] while in some narrow areas maximum currents of 12 m/s are likely [24]. These high run-ups and currents can severely damage marine assets.

2.2 Impacts of earthquake and tsunami on maritime assets

According to Berle et al., a formal vulnerability assessment evaluates systems as they currently function, and asseses the impacts of a disruptive event. For maritime transportation systems as part of a logistics network, they highlight that better methodologies are needed to investigate and identify their vulnerabilities and mitigation actions [31]. Cheng et al. performed an extensive study of coastal shipping disruptions, presenting several details about the impacts of earthquakes and tsunamis on maritime assets. They investigated information on natural hazards and damage to ports, vessels, and navigation channels [2]. The Japan Association of Marine Safety performed a study on navigation safety measures in the event of significant earthquake-tsunami strikes. The tsunami safety measures for maritime assets include research ports and vessel assessment impacts [32]. Different types of failures can disrupt a maritime transportation system in a variety of ways [33]. Earthquake damage to ports requires several months or sometimes years to be fully repaired. Furthermore, their vulnerability increases due to coastal storms and tsunamis [2]. If boats and ships do not leave port, they could be damaged due to the effects of high local currents and impacts with other floating or land-based structures. They can become a hazard because if they become unmoored, becoming floating debris [34], [35]. In addition, waterway navigation channels can also be other maritime areas that can be disrupted due to the presence of debris or destruction of essential navigation services [33].

Several waterway elements affect navigation after an earthquake-triggered tsunami, such as landslides, bridge collapse, destruction of aids to navigation (AtoN), and debris [36]. The ground shaking of earthquakes can trigger submarine landslides, altering shallow and narrow channels' navigation operability, as well as triggering landslides-tsunamis, causing higher waves with shorter wavelengths [37]. In addition, inland landslides could block channels and rivers, blocking navigational ways, especially to barges [19]. In the same way, the collapse of bridges on waterways could block a ship's route [38]. Besides that, earthquakes and tsunamis can damage AtoNs, which support mariners shipping through the waterways. Subsequent landslides in waterway areas can also destroy navigational infrastructure, impacting the safety of navigation[39].

Lighted/unlighted buoys, minor lights/beacons, and day beacons are mostly placed in water and have a high possibility of damage, leaving waterways unsafe and making it more difficult for emergency supplies transportation [36]. A real example of the importance of AtoNs is after Hurricane Katrina, where malfunctioning AtoNs resulted in 11 port closures [40]. After a tsunami reaches a city, when the water recedes, lots of land debris floats back to the sea. According to a study, considering the unlimited availability of resources, at least 24 hours is necessary to fix AtoNs and reinstate waterways to good navigation conditions [36]. These points, together with port and ship damages, affect the ability of maritime emergency response logistics, as there can be delays to the operability of certain shipping routes to support emergency logistics [41].

2.2.1 Ports impacts

Port infrastructure is vulnerable to damage from different types of hazards, and past earthquakes and tsunamis have caused damage to ports worldwide [42]. For example, the earthquake-tsunami disaster in Japan in 2011 destroyed 10 major ports and over 300 fishing ports [2]. The earthquakes generate ground shaking, leading to liquefaction, lateral spreading, collapsing infrastructures, and landslides [19]. Besides that, ground shaking affects wharves, cranes, yards, and land transportation structures [2]. In contrast, tsunami damages to ports include washout of structures, including ships, the impact of debris, floods, wage structural damage, and spells of oil or gas leading to fires [43]. A comprehensive study of damage related to Earthquake-tsunami on modern port infrastructure was performed after the Tohoku, Japan Earthquake-tsunami disaster [44]. Sumer et al. realized an extensive study of earthquake-induced liquefaction around marine structures, including tsunami information and previous studies and methods [43].

Quay walls, piers, docks, breakwaters, buried pipelines, sheet-piled structures, storage facilities, waterfront buildings, and other structures are located in coastal areas, usually inside ports. When such structures are located near an earthquake epicenter, they are exposed to shaking effects from seismic activity. Shaking of soil can result in liquefaction, resulting in loss of stability and integrity of these structures, which can lead to their partial or total collapse [43]. An overview of how liquefaction works in this area is given in Sumer et al. In addition, they point out that many researchers and engineers studied the liquefaction mechanism induced by seismic activity in the last years, given the catastrophic effects of recent earthquakes. They conclude that despite good measurements, and building codes and guidelines put in place in the ports, the liquefaction phenomenon is still not fully scientifically understood [43].

As explained in Section 2.1, one of the effects of earthquakes is tsunamis, a great threat to marine structures in ports. Sumer et al. described that due to their sheer size forces, tsunami threats to ports involve three main elements: soil, structure, and wave interaction.

Tsunamis also affect quays, walls, and piled structures. However, the tsunami-induced liquefaction information is challenging to identify, because the subsequent flooding and successive waves obliterate evidence of direct liquefaction processes, leading to challenges to differentiate earthquake and tsunami liquefaction when these events are successive. Other tsunami effects addressed in previous research include: waves moving entire structures from the foundation and dragging these to land, damage to buildings from impact with ships brought in from shore and other debris accumulated as the wave moves inland, weakening of foundations and piles with erosion from receding waves, overturning of structures by force from receding waves or pressure from advancing waves, and damage from large ships colliding with docks [19], [32], [43], [45], [46]. Another consequence of tsunamis in ports is the generation of (often strong) currents.

Currents happen "when a free surface flow is forced through a geometric constriction" [44]. Tsunami-induced currents differ from regular ocean currents, yet they can cause significant damage to ports [47]. Regular currents are caused, for example, by tidal flow through an inlet, possibly generating some minor damage. In contrast, currents generated by tsunamis have spatial and temporal scales because tsunamis involve significantly higher waves, which reach the coast with repeated force over a short time period [44]. Due to the infrequency of tsunamis and precise data, there is limited specific knowledge about this type of current. Many past records of tsunami currents mention them as whirlpools, which were also found in some glyphs and carvings of Indigenous peoples in the Pacific Northwest, characterizing these as monsters [48]. Currents were also observed in areas with no flood and no waves [49]. For example, at Salalah Port during the 2004 tsunami in India, the maximum tsunami elevation was 1.5 m [50]. However, the currents were strong enough to break all 12 mooring lines of a large freighter[51]. Lynett et al. grouped some observations and created a model of tsunami-induced currents in ports and harbors [15], [44].

Damage types associated with strong currents include breaking of mooring lines and damages to docks and ships. Lynette et al., in another study, collected data from four different tsunamis in Japan, California, New Zealand, and the Galapagos Islands and created a damage index correlating with the tsunami current [44]. With currents smaller than 3 knots, no damage is expected, while currents with speeds over 9 knots can cause extreme damage, where more than 50% of docks and ships are estimated to be damaged. For example, several docks near the harbor entrance in Crescent City Harbor in California in November 2006 were damaged because of tsunami currents from a magnitude 8.3 earthquake in the Kuril Islands [52]. The same happened to other ports in California following the magnitude 8.8 Maule, Chile Earthquake in 2010 [53]. Due to its power and potential to lead to significant damage, there is an increase studies focusing on tsunami-induced currents, such as [15], [44], [49], [29],[54].

Ports are the center of commercial and social activity of coastal communities. Hence, they are essential infrastructure hubs for emergency response logistics. However, as they are vulnerable to earthquake-induced tsunami disasters, it is important to increase ports' resilience so they can function to support emergency response operations [19]. As mentioned in the above paragraphs, some of the damage consequences of earthquakes and tsunamis are vessels being affected by debris from ports or the opposite vessels colliding with port structures. Therefore, comprehending the aspects around port damage helps understand its relation with ship damage.

2.2.2 Types of ship damage cause

The earthquake and tsunami damages for static objects, such as ports and buildings, are easier to measure and study than motion objects. Vessels are moving objects, and the damage mechanism is more chaotic, especially for tsunamis that can initiate the vessel's movement [14], [16], [55]. Despite the complexity of exact damage mechanisms, if boats and ships do not leave the port, they could become unmoored and become floating debris, colliding with others structures [34], [35]. Suga et al. studied the drifting of ships at Kesennuma City in Japan's 2011 catastrophe, where 17 ships were stranded on land, and 23 sank. In their research, they used tsunami modeling with a drift model to analyze the damage data [56]. So, evidence shows that ships are damaged in earthquake-tsunami events, especially near ports, due to tsunami hazards.

Earthquakes can cause devastating damage to ports and other structures, and as a result, vessels are damaged or destroyed [35]. Once an earthquake occurs, the ground and structures can shake violently, resulting in the breakdown of port quay walls, the destruction of the deck and other structures, and the dislocation of mooring systems [34]. When a vessel is docked at a port and an earthquake suddenly occurs, structures start to collapse. The damage probability to vessels increases with increasing probabilities of port infrastructure collapse, such as cranes [43]. Another possible damage for vessels from static structures is from bridges, as happened during an earthquake when some vessels were navigating under the bridge when it collapsed, and the vessels sank [43]. So, this literature suggests to include structural damage analyses to understand damage to vessel assets.

Earthquakes generate shockwaves due to violent water motions besides tsunamis. So, the general sea level rise as a consequence of earthquakes will have multiple impacts [57]. The difference between high and low water levels generate by flooding reduces the safe distance between ships and bridges [58]. Water level elevation and lowering increase material degradation, intensifies the exposure of decks on wharves and piers. In addition, an earthquake causes hull motion, increasing the pressure on the vessel's mooring lines, and increasing the risk of mooring breakage, which can turn ships into heavy loose colliding debris [56], [59],[32]. There is a mutual threat relation between damage for ports and vessels because if unmoored and adding waves from the tsunami, vessels can collide in ports with buildings, bridges, and other structures. For example, during Hurricane Katrina, casino barges broke free and damaged several buildings [35]. Another example is during the Samoa Tsunami, with low flow depths, a moored barge caused damage to a pier because, during the Tsunami drawdown, it got up under the pier and then raised it with the tsunami run-up [35]. Hence, according to several studies, all ships and barges should evacuate to deep water when it is possible in case of earthquake-tsunami events, because of their high potential of turning to float debris, often resulting in an impact to other structures, and often also sinking of the vessels at the coastline [2], [34], [35].

Most studies about ship damage are related to tsunami elements. First, the water drawdown, run up, flooding, and run down elements, and subsequent waves; second, the tsunami currents power [35]. So, when ships are near ports, where usually the ocean depth is lower, the wave's amplitudes increase. In medium-high depth areas, waves have high velocity [23]. Suppasri et al. [55] identified the main causes of damage. Grounding is when there is a difference in water level, where the initial water level is lower than the tsunami run down, resulting in a vessel grounding at the sea bottom. Stranding is when the bottom vessel elevation is higher than the pier, dock, and terminal elevation. A study using 1000t vessels calculated that a tsunami wave of 3.5m is able to cause stranding. Loss of stability is the inverse of the vessel's opposition to being inclined or its tendency to go back to a vertical position, where it is found that a small vessel of less than 10 t remains stable only with a tsunami velocity below 1-2 m/s. Also, loss of stability can happen when vessels encounter tsunami waves in the ocean region away from the coast. Another damage cause, already mentioned above, was the failure of the mooring rope. These causes of damage can lead to vessels sinking, stranding, allision, and collision, according to analyses of 20,000 vessel data, mainly boats from the Japan 2011 Earthquake [1].

A number of studies examined the relationship between tsunami currents and ship damage [44], [49], [54], [60], [61]. Tsunami current forces can break the moorings, resulting in a ship being pulled away from the port. For example, in the 2004 Tsunami in Oman, after 90 minutes of tsunami arrival, a 285 m long container ship was pulled by strong currents. It drifted for hours and spinned 3 times before sinking in a sand bank[62]. The same happened in other locations, for instance Madagascar and Reunion Island, where similar incidents were registered for large vessels [50], [63]. On Reunion Island, a 196 m freighter collided with docks and damaged cranes due to strong currents [63]. These studies suggest that better warning systems for vessels evacuating the coastline and being at safe depth areas could reduce vessel damage.

2.3 Studies of ship damage

There are several studies about ship damage involving accidents and difficult weather conditions [64], but only a few for ship damage related to earthquake and tsunami natural disasters. Studies about earthquake-tsunamis can be divided into two types: analyses of historical data from previous disasters and the development of safety guidelines. In addition, both types consider only tsunami parameter information for their analyses.

Governments and maritime organizations made most of the studies focusing on guidelines, through publishing reports [32], [65]–[69]. The guide's instructions are divided into local tsunamis (10-30 minutes ETA) and distance tsunamis (3-4 hours ETA) and the ships' location if they are moored or at sea. In these guides, it is also possible to find information about evacuation areas, such as the safe depth. Some guidelines suggested that the safe depth is 55 meters, others are 182 m, and few include current tsunami information. A gap in these reports is the classification between small and large vessels, because there is no definition of the size of these categories. The Japan Association of Marine Safety created the most extensive guide in 2015, presenting research on navigation safety measurements in the event of significant earthquake-tsunamis strikes [32].

The Japan Association of Marine Safety provides a study flow for tsunami safety measures, with information about the identification of ports and vessels characteristics and usage, damage characteristics of historic tsunamis, and assessment of tsunami impacts on vessels. They also include regional disaster prevention plans and establish safety and evacuation measures. They highlighted an interesting piece of information, that some large vessels require tugboat assistance to leave port in case of evacuation. Consequently, they need to prepare additional measures to cope with Tsunami evacuation. Iwanaga and Matsuura studied the evacuation information and damage related to Japan's catastrophe in 2011. Using AIS data, they analyzed that several ships started the evacuation process after 30 minutes after the earthquake struck, showing that the tsunami pushed some ships [70].

Most studies on ship damage due to the Earthquake-tsunami disaster are related to the great Japan 2011 catastrophe. Using this natural disaster vessel dataset, Suppasri studied the relation between tsunami height and velocity with vessel damage to develop loss damage calculations[55]. In the same way, Muhari identified some types of damage, such as sinking, drifting, stranding, collision, and others, to improve loss probability functions [1]. According to Lee et al., the damage to ships in waves, such as tsunamis, involves loss of structural integrity, motion, and stability analyses to inform mitigation strategies [59]. A study also used the Japanese disaster information that analyzed the drift motion of large vessels, simulated the drifting, and compared the results [56]. They created hazard maps for ship drift and stranding on land and discussed damage prevention and mitigation.

The studies described above consider a position for the ship at the moment of an earthquake-tsunami event. However, it is difficult to predict where will be the ship's position when the tsunami strikes, due to the dynamic characteristics of both elements, and because of the unpredictability of earthquake events. All studies focused on tsunami damage and consequences, especially near ports. Most research in this field aimed to analyze data from previous events, especially Japan's 2011 natural disaster, leading to damage probability considering this event's characteristics. In contrast, as indicated in the introduction, our research aims to address plausible ship damage for an event, which has not occurred since 1700 A.D, but which is predicted to likely manifest in the next 100 to 300 years.

2.4 Marine vessels loss estimation studies

The Japan 2011 earthquake-tsunami catastrophe and the data related to ship damage and its analyses generate the possibility of developing a loss function probability for ship damage related to this natural disaster. Suppasri et al. and Muhari et al. develop vessel loss probability models, relating simulated tsunami data with marine vessel loss data [1],[55],[71].

Suppasri et al. took data from 20,000 small vessels damaged by the Great Japan tsunami and developed loss functions to calculate the probability of vessel damage. They used 5 critical parameters: tsunami height, simulated velocity, and arrival time, with vessel parameter data including tonnage and material type. Using data from the tsunami, and damage ratios developed by Shuto with median values from the samples, they developed loss functions using linear regression analyses. Linear regression and normal distributions were used in other fragility studies to calculate loss function for buildings, bridges, and roads. The studies used two scenarios, maximum tsunami height and maximum flow velocity, and compared vessels at the port with less than 5 t inboard and outboard motors vessels and 5-20 tones located near, far away, and unknown location from the tsunami. For a tsunami height of 5 m located near the vessels, the damage probability was 85% for less than 5 t outboard vessels, 70% for inboard vessels, and 25 % for 5-20 t vessels. In contrast, for a flow velocity of 5 m/s located near a vessels, the damage probability was 95% for less than 5 t outboard vessels, 85% for inboard vessels, and 55 % for 5-20 t vessels. They concluded that vessels away from the tsunami source had lower damage probability because vessels had time to evacuate and tsunami parameters were lower than near the tsunami source. It was also suggested that a study with a combination of tsunami parameters would be better, as well as information about the damage mechanisms and uncertainties analyses.

Muhari assessed the tsunami hazards in ports and vessels using tsunami models and damage information. The study aimed to develop a new loss function to estimate the potential damage to marine vessels caused by the tsunami using a multivariate statistical modeling method. The loss functions were based on ordinal regression utilizing various explanatory variables. From the tsunami model, heights and velocities were used as input for loss estimation calculations. The variables for vessel loss estimation utilized were as follows: condition before the tsunami, location after the tsunami, tonnage, material, type of engine, and type or cause of damage. The vessel data used to calculate the loss estimation probability were made using only vessels with less than 5 tonnes, boats, and fishing vessels. In the results, there is more than 50% probability of damage, with losses being more than 90% certain if the tsunami height exceeds 1.9 m and velocity is 2.1 m/s. The loss probability rises to 75% for moored ships with tsunami heights bigger than 3.65 m and velocity 3.8 m/s, and the highest loss probability of 90% with an 8 m wave height and 5 m/s velocity. The study points out that their tsunami data were invalid due to a lack of data. It also indicates that future research should elaborate on other loss estimation information for small, large, and medium vessels.

Comparing both studies described above, the work by Muhari applied the suggestions made by Suppasri, such as applying both tsunami height and velocity simultaneously. They both consider historic damage from Japan for small vessels to develop the damage probability information and loss functions, and used data from the vessels at port. Muhari used only vessels that were anchored and moored before the tsunami. Both studies show a 80-90% damage probability, comparing the same variables for tsunami height and velocity for small vessels, with heights around 5-8 m and 5 m/s. In conclusion, their use of different vessel variables in combination with tsunami information inspired the methodology applied in the current research, as further explained in Section 3 below.

2.5 Emergency response logistics for coastal dependent communities

Coastline cities and their population heavily count on vessels for the transportation of people and goods. After a natural disaster, the need for food, fuel, and medicine increases, while interruptions in transportation systems increase significantly [2]. Islands and coastal cities can suffer severe impacts due to maritime transportation disruption due to their dependency on it [72], [73]. In a short-term period, a few days, depending on the scale of the natural disaster, a severe shortage can happen in this just-in-time logistic system world [2], [8]. For example, after Hurricane Katrina in 2005 and Sandy in 2012, the fuel shortage left communities vulnerable and affected emergency response time [74], [75]. Despite the high consequences, the risks related to disastrous consequences for coastal communities have received relatively little academic focus to date.

Due to coastal communities' vulnerability, some studies were performed to understand how to mitigate the risk. Valenzuela et al. performed a study to understand how disaster risk is observed and identified in these communities to provide a better assessment and guide for risk governance and management [76], [77]. Recently, studies have focused more on coastal communities' emergency management phases. This includes work on mitigation, e.g. developing tsunami information guidelines for populations and vessels on the U.S. coast [78], assessment of preparedness strategies, e.g., impacts of maritime distribution transportation to hospital supplies on the B.C. coast [9], development of response plans such as evacuation decisions in China coast[79], and analysis of recovery and restoration through modeling of earthquake impacts in the district of north Vancouver [80]. Hence, the current research, which focuses on the vulnerability of maritime assets to the impacts of a Cascadia-type earthquake-tsunami event, will also help inform the risk assessment for coastal communities and provide information that could be used for the four phases of emergency disaster management, providing estimates of vessel damage information.

2.6 Performance of ships after an earthquake

Organized and resilient maritime transportation systems with effective pre-disaster measures can also provide valuable post-disaster mobility solutions [38], whereas disorganized systems can increase the vulnerability of coastal communities [2]. In 1989 in San Francisco, after the Loma Prieta earthquake, ferries were used to evacuate and transport emergency supplies [81]. The Bay Bridge had structural damage, and ferries became a vital transportation link. They were organized to transport people between bays, transporting 15,000 passengers only a few hours after the event and keeping this ongoing service during the emergency recovery phase [82].

Another efficient use of ferries was observed during the Japan great Earthquake, where larger ferries, bigger than 5,000 GRT, were used to transport about 6,000 personnel and 2,000 vehicles to the disaster area in the first 6 days [3]. These major ferries assisted in the deployment of Search and Rescue teams. They were chosen due to great transportation capacity and limited resource availability, with port facilities and fuel resources being scarce in the immediate post-disaster phase. Reports show that during the 4 months of the recovery phase, 48 ferries made 899 Emergency Response Logistic shipments, carrying almost 60,000 people and more than 16,000 vehicles. Other examples of the use of ferries for emergency response logistics include the 2004 Indian Ocean tsunami in Indonesia, New York after Hurricane Sandy in 2012, Queensland in the Australia flood in 2011, and Indonesia during the Boxing day tsunami in 2004 [83].

Barges and tugs were also used for emergency logistics during the 2010 Haiti Earthquake. They were used for relief operations for thousands of tonnes of food and aid [84]. Different studies, reports, papers, and guidelines for an emergency response using maritime transportation suggest the use of barges and ferries as a transportation mode for coastal communities [3] [8], [77], [84]–[87]. Major ferries and barges have a good size and power to carry supplies and heavy emergency equipment, and they are considered a good fit for emergency response. Nevertheless, while there is some work building on historic disaster data, there is currently no method to estimate the extent to which vessels become damaged after an earthquake-tsunami event, for a plausible scenario which has not yet occurred.

2.5 Literature review conclusions

The main inspiration behind the current research stems from the Japan Society for Maritime Safety tsunami damage framework. That points out the importance of identifying the current maritime transportation systems characteristics according to the studied area, past tsunami damage information and impacts, including regional prevention information, assessment of the tsunami impacts to ports and vessels, and evacuation actions. The rationale behind the RUSEMARIE model, which is used to estimate whether a vessel in a given location is likely to be damaged by an earthquake-tsunami event, is inspired by guidelines and information reviewed in the preceding sections. In addition, the use of tsunami and vessel variables as a basis for the RUSEMARIE model is based on empirical findings from the two-loss probability damage studies described in Section 2.4 above, as well as the differentiation for different vessel sizes and groups. This information basis will shape the methodology described in Section 3 to address the research questions of Section 1.2.

Much of the work in this area is still limited by the low number of earthquake-tsunami natural disasters in the last decades. Because of that, there are not much data to perform analyses comparing different scenarios or simulations with historical data. In addition, most studies focus on tsunami damage for static structures, while there is less information available about vessels, which are moving objects with different shapes, materials, and hydrodynamic characteristics than static land structures. There is also a lack of understanding of specific damage types and the extent to vessels, which can be related to shakes and tsunamis wiping out much information with waves. Furthermore, the understanding of tsunami currents is still an ongoing field of study. Despite some attempts to address this issue, there is a lack of data regarding other catastrophic events with different geographical elements compared with the Japan 2011 earthquake. This lack of knowledge is also a reality for the general study of ship damage.

The overall previous work on ship damage related to risk analyses has not explicitly addressed the issue of combining earthquake damage, different damage levels, movement of the vessels through their trajectory analyses, different vessel sizes, and providing information for a future natural disaster. This research tries to understand how these elements can be used together, aimed at providing better background knowledge for disaster preparedness risk assessment and management. Hence, this thesis's work will help address some of the mentioned gaps. In particular, a knowledge-based model will be developed to assess damage to maritime assets based on vessel movement data and simulated data of an earthquake-tsunami event.

Chapter 3
Methodology

The research methodology used in this work concerns a case study, focused on analyzing vessels damaged by a particular scenario of an earthquake followed by a tsunami. The case study is located in British Columbia, for which the scenario Cascadia L1 with the worst-case tsunami in this study area, is considered [22]–[24], [88]. This specific study case was selected due to the high probability of widespread destruction of infrastructure in the region, and a corresponding likelihood of high impact on ships. No earlier analysis of impacts of earthquake and tsunami events on vessels is known to have been performed in this study area. In addition, this work is part of the SIREN project, which aims to understand how natural disasters affect coastal communities and the maritime transportation system in British Columbia, also giving the Cascadia Earthquake and tsunami event an important role[89].

To be able to answer the research questions, such as how many ships would be unavailable following the disaster event, and what are the dangerous marine areas for ship navigation for an earthquake-tsunami event, a quantitative modeling approach is used. In addition, in the data collection and analysis research phase, some steps apply a qualitative design to establish a knowledge base for the possible availability of ships in case of an earthquake-tsunami event. This qualitative approach was exploratory because this project focuses on emergency preparedness risk management, particularly to estimate the damage risk for different vessel groups and tsunami zone levels. No earlier work has focused on establishing a systematic knowledge base to enable quantitative modeling for this phenomenon. Hence, this study uses a mix of positivism and interpretivism as underlying research philosophies to examine the data about the earthquake-tsunami event, and to develop quantitative models to understand ship damage[90].

In this section, the data and methods used in this research are explained in detail. Figure 1 outlines the steps applied to estimate the risk of damage to vessels operating in the study area during an earthquake-tsunami event. The methodology section is divided into two parts. The first part introduces the dataset utilized in the research and in what way they relate to the developed models. In addition, the data preprocessing steps are presented considering the study case definitions, resulting in an input data dataset, represented by box 1 in Figure 1, and earthquake-tsunami impact scenario information, shown in box 3. The second part, explained in section 3.2, describes the two developed models. The first of these is the Marine vessel movement (MVM) model (box 2), which generates ship routes from historical data. Furthermore, these vessel movement results are used in the developed Earthquake- Tsunami loss prediction model for marine vessels (RUSEMARIE) (box 4), together with the Cascadia impact scenario (box 3) to assess ship availability. These procedures utilize spatial analysis tools as a core approach to generate the output data results (box 5) in the form of maps, figures, and tables. In addition, details are provided about the implementation, descriptive statistics methods, and critical evidence methods. Figure 1 below represents the integration of the main five stages of the work related to the proposed case of study and furthermore helps understand how the following section is structured.

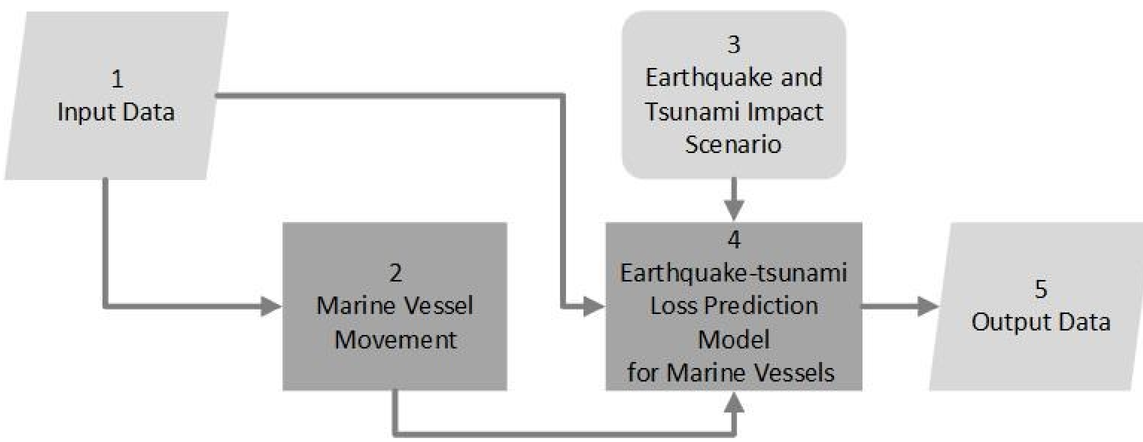

Figure 1- Research overview where each box represents parts of the research, starting with input data, going through the three methodology parts, and ending at output data.

3.1 Data

For this study, the following vital data were extracted considering the selected study area in British Columbia, with data from different sources described in their respective sections. Figure 2 represents the data elaboration process used in this research. Some data, such as the bridges and ports' damage status, were derived from the Coastal Community Resilience to Marine Transportation Risk (SIREN) project [12]. The data is described in the following subsections according to the order of use in the models. First, the Vancouver study area will be introduced, and the main limitations related to the considered communities and the selected ship fleet described. Next, the Automatic Identification System (AIS) data will be described, detailing the database approach and sampling strategy. Attention is given to how ports and coastline information are linked with the AIS data. These sets of information will be used in Marine Vessel Movement model (box 2 in Figure 1). Then, the subsequent data subsections will describe the additional data applied to the RUSEMARIE model (box 4 in Figure 1). This section includes the earthquake and tsunami data and their expected damage to bridges and port structures, vessel safety guidelines for tsunami events, and bathymetric data. The data files associated with the data indicated above include geographical data , preprocessed using GIS more specifically ArcGIS Pro software. Which it is software used to view, edit, process, create, and analyze data with geographical attributes that can inform thought map, figures, graphs, tables, and other graphical documents.

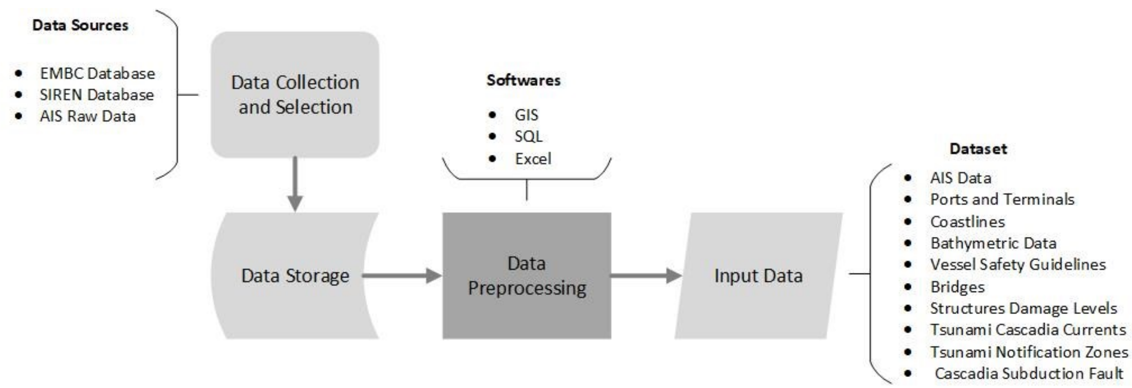

Figure 2- Input data overview outline, which contains details about the databases used, software and final datasets

Most data used in the study have been obtained from the Emergency Management in British Columbia (EMBC) database and as previously mentioned, from the SIREN project. The data collection and selection were completed according to the scope and focus of the case study, composed of Excel files and geographic information file format, and few data from expert reports. These were stored in and preprocessed using ArcGIS software, while some of the AIS data pre-selection was performed using DB Browser for SQLite due to the size of the dataset. SQL is a programing language to manage big databases. Some preprocessing activities include selecting specific data according to the scenario features and study area, matching dataset information, and joining tables. After these steps, a final database was created and further analyzed, by linking the data to the developed models. More detailed information will be provided in the following subsections.

3.1.1 Vancouver study area

British Columbia, more specifically the sea areas near Vancouver Island and Vancouver, as represented in the map area in Figure 3, was chosen due to the high probability of an earthquake triggering a tsunami event in this region, as well as the vulnerability of communities to disruptions to maritime logistics. The Vancouver Island communities are more likely to be impacted by this natural event due to their location. Moreover, they are dependent on resources shipped from the mainland area near Vancouver by vessels (ferries and barges).

The Vancouver study area was divided into 6 regions. Figure 3 shows the boundaries of these regions based on the 2016 census division taken from the EMBC database [91]. The regions used consider adaptations to encompass geography, population, maritime transportation, and tsunami characteristics. The regions are comprised of 130 communities using census subdivisions as applied in the SIREN project, including 13 small islands and major cities located on Vancouver Island, such as Victoria and Nanaimo (see Appendix 1 for a map and table showing the subdivisions). Together, these communities include almost 800,000 people according to the 2016 census division [92]. However, there was a population growth of 8.2%, according to the 2021 census for Vancouver Island [93]. People in these communities rely on maritime transportation for their daily supply of goods, and an earthquake-tsunami Cascadia event could severely impact them.

The communities were divided into 6 regions for analysis and discussion, as these have different characteristics and access to maritime transportation. In addition, the region's area will be used to answer the fourth research question: which regions of Vancouver Island will likely have a reduced ship capacity for emergency deliveries due to ships not being available? Figure 6 shows the 6 regions, and Table 1 shows the respective communities and population numbers. The Sunshine Coast region comprises of two islands in the middle of the Strait of Georgia, located in the sea between Gulf Island and Vancouver mainland, and has the smallest population. In contrast, the most populated region is South Island, where Victoria, a central city of Vancouver Island, is located. The geographical descriptions of each region can be found in Table 1

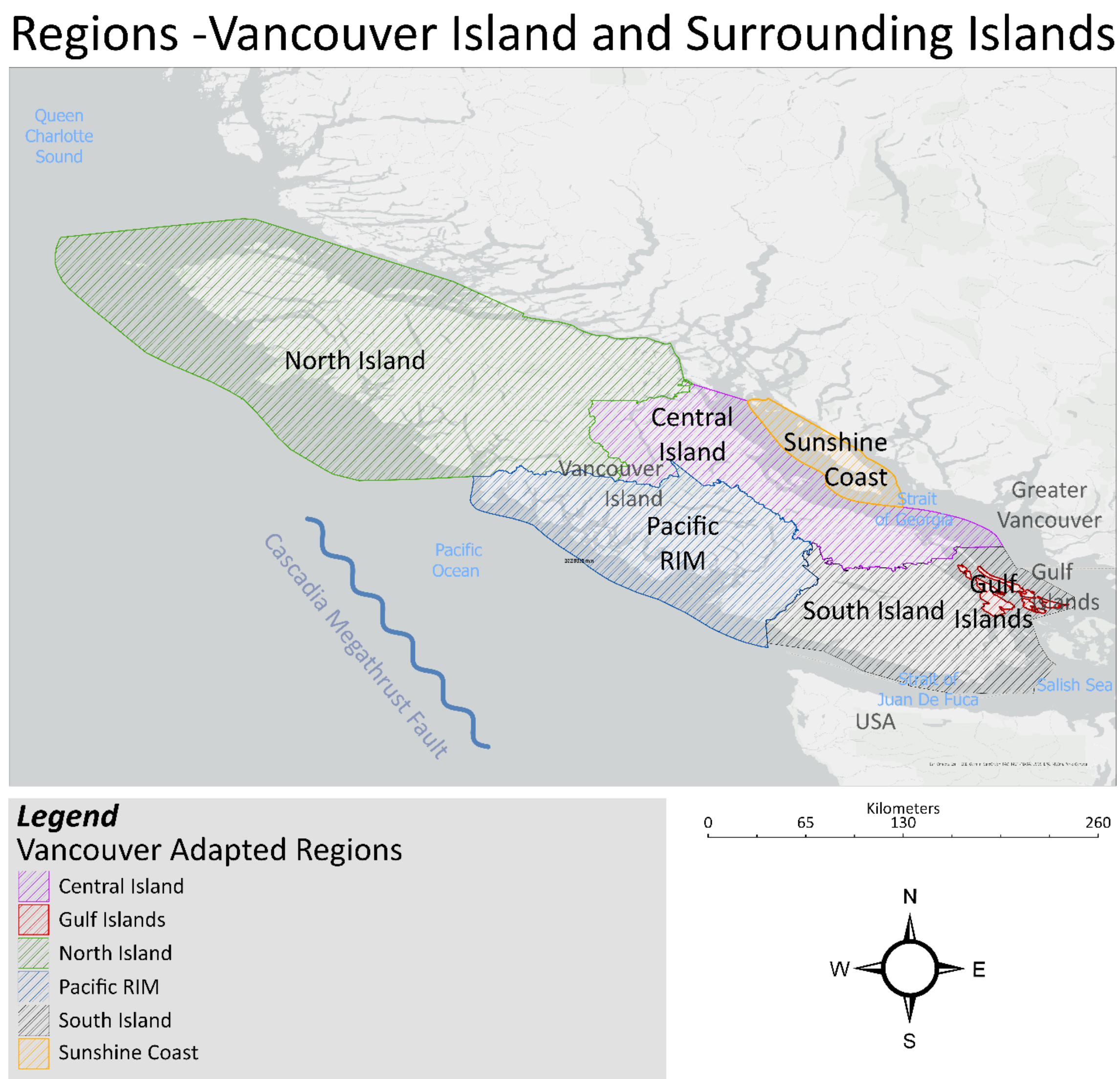

Figure 3- Six regions composed of Vancouver Island and surrounding island communities. The boundaries and names were adapted from census divisions considering census subdivisions' population numbers. (Data Source [20]).

Table 1 - Vancouver Island region information with population numbers, numbers of communities in each region, and their geographical descriptions. (Data Source [20,21])

Regions Name	Population (2016)	Adapted Sub-divisions (Communities)	Geographical Description
Sunshine Coast	1,475	2	Two islands in the middle of the Strait of Georgia are in the sea area between Vancouver Island and the mainland.
South Island	451,358	48	South of Vancouver Island, surrounded by the Strait of Juan De Fuca, where the city of Victoria is located.
Pacific RIM	30,981	23	Area exterior to the Pacific Ocean covering Tofino on the coast and Port Hardy in the middle of Vancouver Island.
North Island	12,214	20	North of Vancouver Island, some areas face the Pacific Ocean but also cover a northern area strait.
Gulf Islands	16,057	8	The region is composed of eight islands located between Great Vancouver and Victoria.
Central Island	262,267	29	The Vancouver Island area facing the Strait of Georgia comprises three small islands and Vancouver Island cities.
Total	774,352	130	

The Vancouver study area has an intense maritime transport activity. However, for the current research, only ships that could support emergency response logistics to Vancouver Island and other island communities were selected, aligning with the SIREN project aims and dataset [19]. The initial ship dataset is composed of two types: roll-on/roll-off ferries that carry passengers, cars, and trucks, and tug-barge combinations, which consist of flat-deck barges that can carry a variety of cargo. In total, 62 ships are gathered from the SIREN dataset that contains information to connect with AIS data set, but only 57 ships have tracks on this chosen research area. This selected fleet is applied in the marine vessel movement and availability estimation analyses.

3.1.2 AIS data and coastline information

The Automatic Identification System (AIS) is a system used to identify and track vessels, which consists of a broadcast device placed on ships, as well as towers, satellites, and stations that receive the signal messages [94]. The International Maritime Organization implemented AIS in 2000, and five years after, the system became mandatory for commercial vessels according to their size [95]. In this project, the AIS database was obtained from data collected using satellite devices and was provided by exactEarth and MEOPAR. According to IMO, the satellite data provide precise point location information with a 10 m tolerance [96].

Ships navigating internationally with a Gross Register Tonnage (GRT) of at least 300 GRT or bigger, national cargo vessels with at least 500 GRT, and all passenger vessels, irrespective of their size, are required to carry AIS devices [97]. These devices broadcast 27 message types categorized into different groups: position reports, base station reports, static and voyage data, binary communication messages, UTC/date details, safety information, and other navigation elements [98].

Message types 1, 2, 3, 18, and 27 are dynamic position data and will be used to generate trajectory information. Furthermore, this research will use messages 5 and 24, which contain static data. The dynamic position data comprises some essential elements, which are necessary for this study: message ID, time stamp, MMSI, IMO, heading, SOG, COG, longitude, and latitude. In addition, static information includes ship name, MMSI, IMO, ship type, length, and breadth. The definitions of each above the above terms and abbreviations can be found in Table 2 below, which also shows the units.

Table 2- AIS field description divided into dynamic and static data. (Based on [97]*)*

	Field name	Field description
Dynamic AIS data	SOG	The speed over ground (knots)
	Longitude	The longitude position of the ship (number)
	Latitude	The latitude position of the ship (number)
	Date stamp	Record of the time moment (DD/MM/YY)
	Heading	The direction of the ship's bow (number)
	COG	The course of ground (degree)
	Message type	The type of message data being broadcasted (number)
	Field name	**Field description**
Static AIS data	Ship Name	The name of the Vessel (letters)
	MMSI	The Maritime Mobile Service Identity (number)
	Ship Type	The type of the Vessel (code)
	Length	The length of the Vessel (meter)
	Width	The width of the Vessel (meter)
	IMO	The vessel name code (number)

Using the fields of the dynamic messages with geographic information (latitude and longitude) it is possible to display and work with data XY point format. Together with the time stamp, the points can be used to reconstruct a vessel track dataset, making it possible to generate trajectories to be used in the Marine Vessel Movement model. Moreover, the static data were used to categorize ships in groups according to their size and type, and as transitional data to connect the SIREN ship database mentioned above with AIS dynamic messages. So, the AIS dataset will be used to generate a ship itinerary, i.e. origin and destination ports, and as a basis for analyzing tracks from trajectories to generate a path. This information is important for the current research because the RUSEMARIE model performs a damage calculation using the path as the core dataset, with a spatially-based analysis performed upon the points on the path, using on other information layers.

The AIS data is the pillar information to answer the research questions: (RQ1) How many ships will be unavailable to support humanitarian supply chain operations in Vancouver Island coastal area?; (RQ2) What is the relation between ships groups sizes and damage probability considering Vancouver maritime logistic operations?; and (RQ3) What are hazardous sea areas or routes to a ship navigate in case of a Tsunami in a Cascadia scenario?

The data provided by exactEarth contains a total of 127,275,014 points representing dynamic vessel data, spanning a period from January 1, 2018, to December 31, 2018, and a geographic area comprising the West Coast of Canada, the coast of British Columbia, together with some data from ships leaving Vancouver to Washington, US, and some arriving from overseas. Figure 4 provides a graphic overview of the complete AIS database, distinguishing ferries and tug-barge combinations.

Next, a sampling procedure was performed using the ArcGIS tool Sampling data due to processing time, GIS running capacity, and memory limitations [28]. Only AIS points of the 57 SIREN ship database were selected to align with the project aims, resulting in almost 13.5 million points being selected. Then the files were divided by vessel types, distinguishing ferries and tugs, each one containing 9.6 and 3.7 million points respectively. As ferries follow the same routes but with more frequent travels, 25% of all data points were selected for further analysis; this data is enough to analyze ship trajectories. Because the studied tug-barge combinations do not perform daily navigation operations and display a larger variety of routes taken, 50% of the tug-barge data were randomly selected. The time stamp between points of the population is on average 40 seconds for tugs and 20 seconds for ferries, after the sampling procedure the time between points is on average 90 seconds for tugs and 45 seconds for ferries. So, the sampling strategy does not affect the results due to the redundancy of points, due sampling rate[99]. As previously mentioned, AIS points have an accuracy of 10 meters, as pointed out by Devogele et al. in their study about maritime monitoring [100], which is considered sufficient for analysis of the regional maritime transport system in the current work.

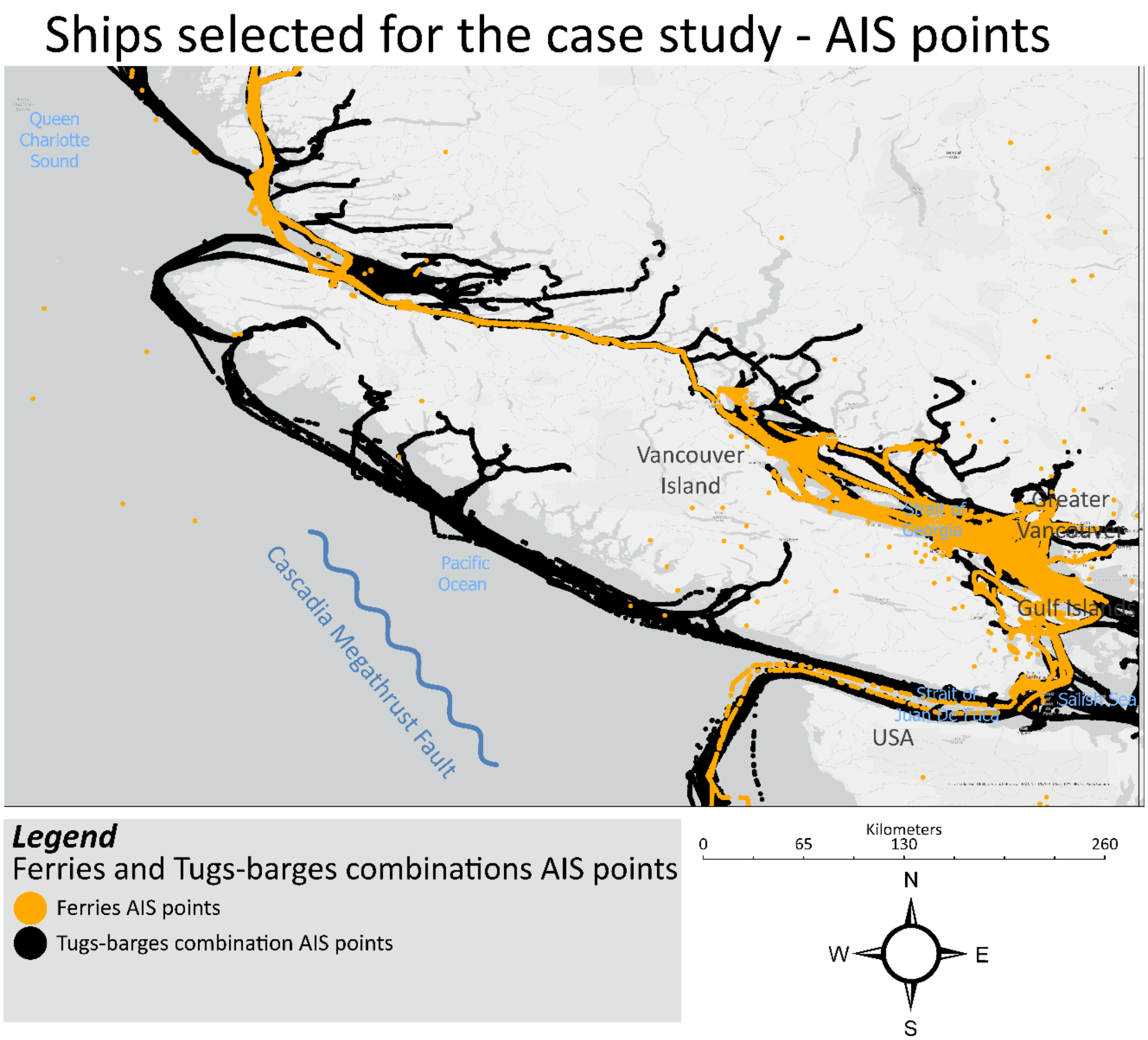

Figure 4- Research selected ferries and tug-barges combination AIS points, ships based on SIREN project limitations.

In conclusion, the sampling strategy does not affect the reliability of the results of the MVM model and post-data processing steps and analyses. Figure 5 shows the total population and sample data for the selected ships. In the first map, the ferries points are exhibited with high density. The green square points show the population data, while the yellow circle represents the sample. So, as can be observed, the sample data with 25% of the population is still representative of the information. In the second map, the tug-barge combination shows that their density is lower than for the ferries, and that the sample of 50% is sufficiently representative to serve as a basis for constructing an accurate path.

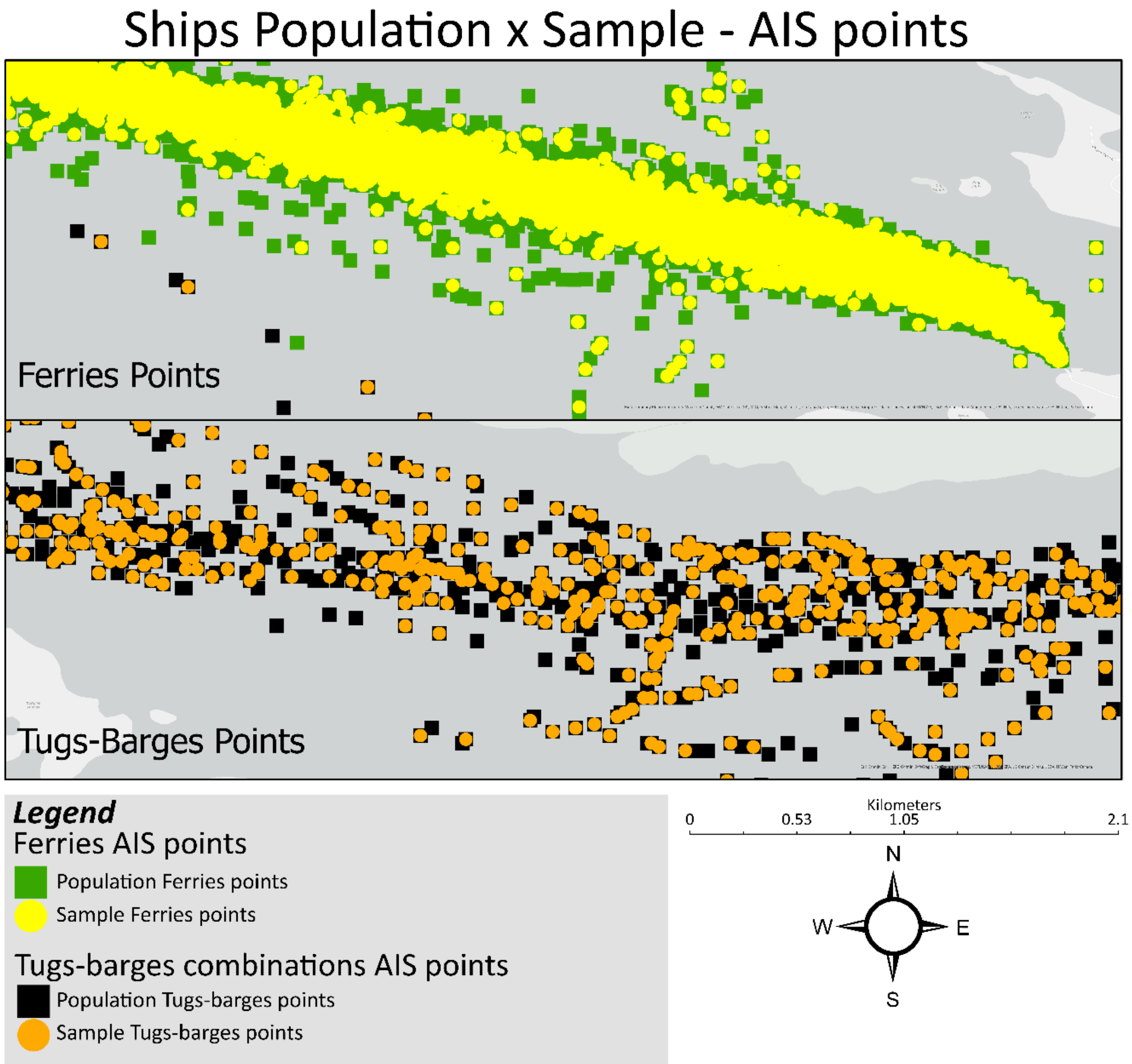

Figure 5- This map illustrates the population and sample of the AIS data for both ship types, demonstrating that the sampling procedure kept the accuracy of information.

The AIS data has outliers that were treated using data preprocessing techniques as has been done in previous work [99], [101], [102]. Some of the outliers preprocessing approaches used a land boundary to process the information, such as the coastline data. A cleaning step was used to manage the points located on land, duplicated records, improper latitude and longitude standards, and ranges outside of the standard for heading, SOG, and COG data fields.

The British Columbia coastline data were collected from the EMBC database, represented in Figure 6, in red color [103]. This polygon shapefile is used to clean AIS points located on a land surface, with these points considered erroneous outliers. In addition, the shapefile was also used in both models, MVM and RUSEMARIE, as a basis to delimit the AIS routes and estimate the ship travel path and ship travel time to safe areas. The coastline data do not allow trajectories to pass over small islands and keep them in the sea area. It is also essential in narrow areas, such as bays, rivers, and inlets. Thus, the coastline data function as support information for the path construction from the AIS points on the MVM model and also for determining the time needed to navigate to safety areas, as used in the RUSEMARIE model.

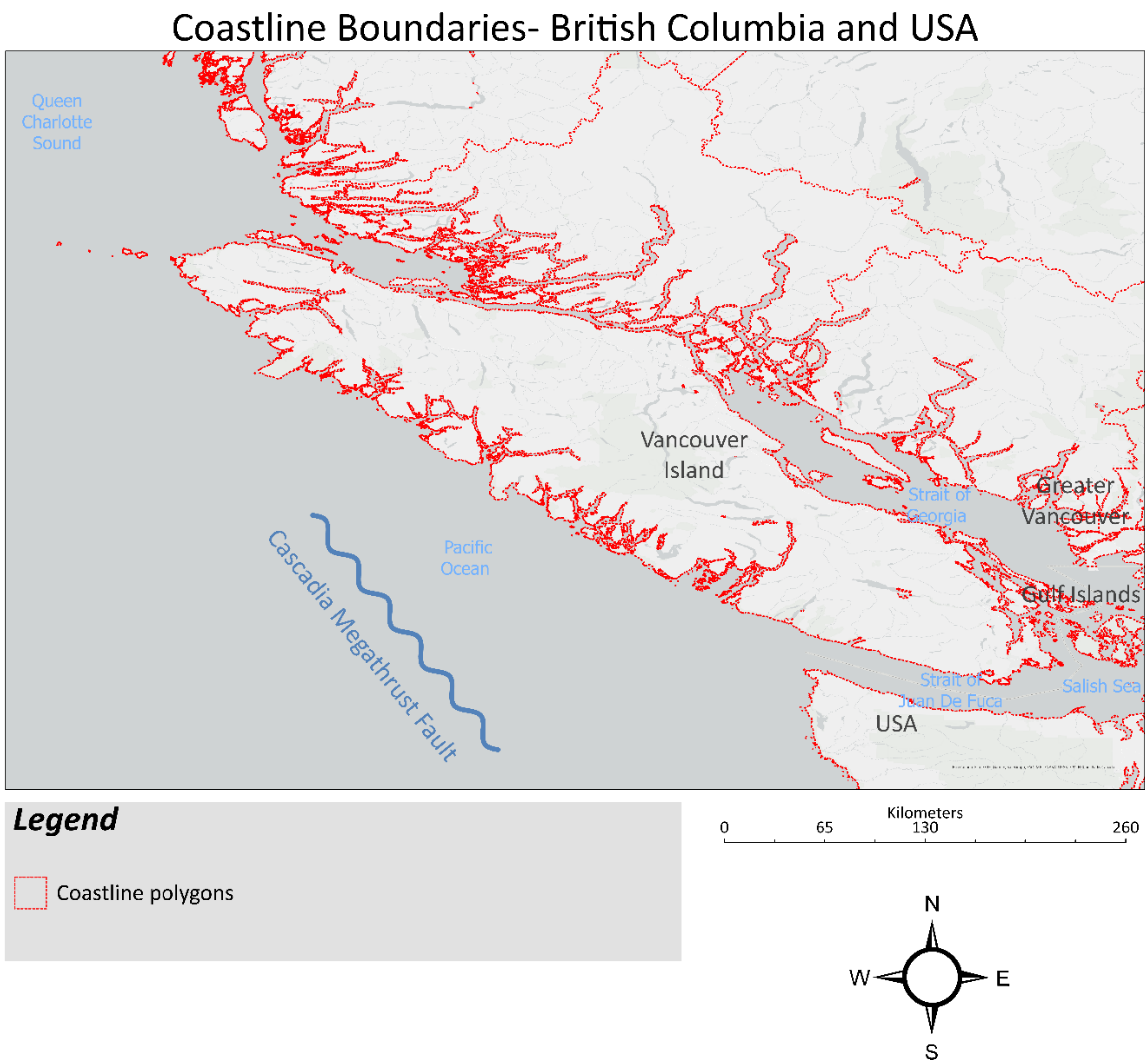

Figure 6- Coastline boundaries from the study area used in the MVM and RUSEMARIE models to avoid overlay at land areas. (Data Source [32]).

3.1.3 Ports/terminal data

The ports and terminal data for British Columbia are a compilation of two databases: EMBC [104] and SIREN database [12], and are used for determining stop points for the vessel trajectories derived from the AIS database. The preprocessing steps to generate the final ports and terminal data consist of the following steps. The Excel data obtained through the SIREN dataset consist of 164 ports that were added and plotted on map files using ArcGIS. It was grouped with the EMBC shapefiles dataset consisting of marinas, moorages, anchorages, and ports, with almost 5000 marine structures, where all duplicated locations were cleaned. Afterward, this data is used alongside the AIS dataset for the 57 selected vessels, analyzing their stop points near the coastline, with stop points identified when the vessel speed was 0 knots.

It was possible to match the marine structures with the stop points from the AIS dataset, resulting in 71 ports, marine structures, and 61 additional locations. These additional locations represent tugs-barges stop points, such as decks and ramps, that are not as such considered ports or terminals in the previously mentioned databases, and are hence not included in those datasets. Nevertheless, they were identified as stop locations for tug-barge combinations, because of their ability to travel in shallow water areas. However, in this thesis, we will use the same terminology (port or terminal), to include official ports and terminals as well as the additionally identified stop points. The final dataset comprises 132 ports, represented in Figure 7.

The information used in this study consists of locations name, geographical areas, longitude, latitude, region, and classification (Ferries terminal, Tugs-barges terminal, and Ferries-tugs terminal). The port information will be used in the two tools applied in the MVM model to define the origin and destination port in a path, because the available AIS database does not include this information. In the RUSEMARIE model, the port data is used to calculate the distance between a port and a ship's point. More details about the damage relation between ports and ships will be provided in Section 3.2.2, also how calculations will be performed

From the total 132 ports, the data set is formed by 29 ferry terminals where only ferry vessels stop, 91 tug terminals only tug-barges combinations stop, and 12 ferries-tug terminals where both vessel types are able to stop. Referring to Figure 7, there are 69 ports in the Greater Vancouver are, 2 ports are located on the Sunshine Coast, 18 ports on South Island, 1 on Pacific RIM, 17 on North Island, 8 on the Gulf Islands, and 17 on the Central Island area. There are only tug-barges combination ports facing the Pacific Ocean, while most of the ports are located in the Greater Vancouver area, more specifically alongside Fraser River and on other local rivers/inlet locations near more densely populated areas.

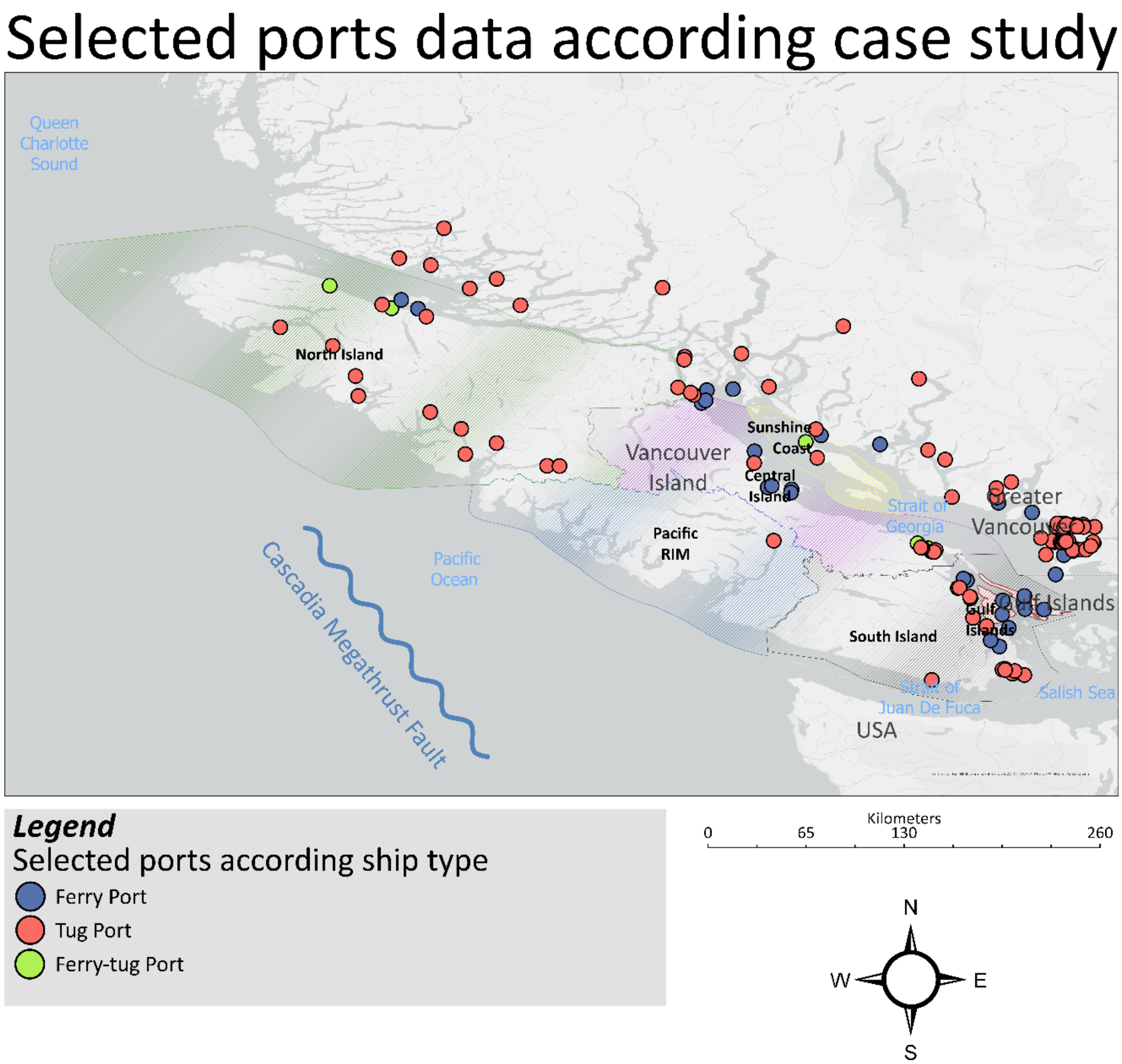

Figure 7 - 132 ports selected to be used as ports dataset in the research, it is composed stop points to ferries and tug-barges combination.

3.1.4 Earthquake and Tsunami impact for Cascadia scenario

This subsection will describe the data collected to develop a realistic scenario for a Cascadia Earthquake and Tsunami event, see also Subsection 2.1. These data represent the Earthquake and Tsunami Impact Scenario (Figure 1, box 3) and can be divided into two groups: earthquake data and tsunami data. It starts with baseline information, followed by information about the possible impact, as demonstrated in Figure 8 below. First, the Cascadia Subduction Zone and megathrust fault are presented, followed by Tsunami Cascadia zones and alert system, their connection with the Cascadia Earthquake and tsunami, and the ensuing damage impacts to bridges and ports. Then, the ocean current areas are presented, with their respective magnitudes and velocities. These four groups of information are the core information to develop the scenario applies in the research case study.

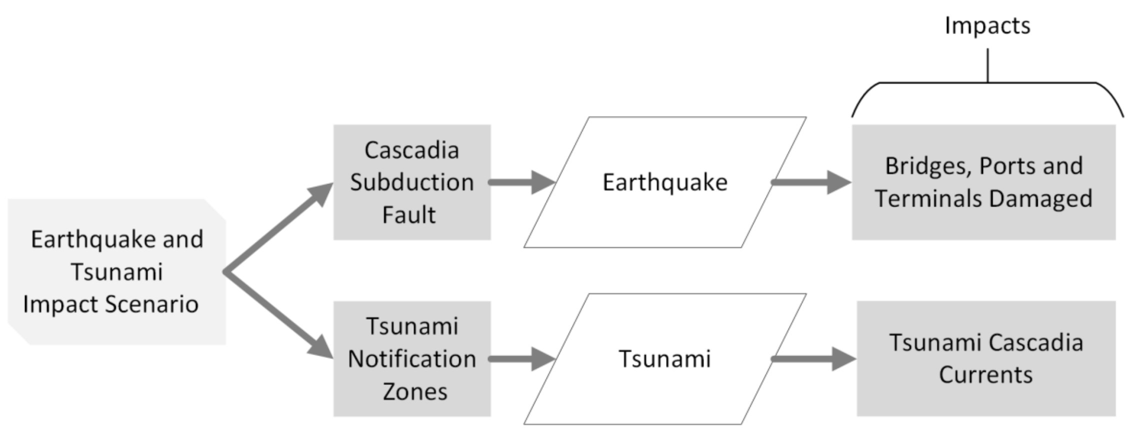

Figure 8-Cascadia scenario data structure, giving an overview of Earthquake and Tsunami and their impacts.

The Cascadia Subduction Zone is used as a basis for the case of study, and provides the context for the megathrust fault data, represented by the blue curved line in Figure 9. The Cascadia Subduction Zone, represented in Figure 9, spans 1,400 km, located a mere 100 km from the coast of Tofino city in the Pacific RIM region. For this work, the central megathrust long-narrow scenario with a rupture of 1,100 km will be used, because it is considered the one with most impact on the Vancouver coast due to its significant damage[25][21]. In addition, the megathrust fault will be used as a reference line to calculate the tsunami arrival time, so that the calculation can consider different start points in the line, depending on the closest location of a given ship point trajectory. It is essential to know the location of the Cascadia megathrust fault, and consequently, the start line of the tsunami, so that the tsunami arrival time and travel time to a safe area can be compared to see if a vessel has sufficient time to evacuate to a safe sea area.

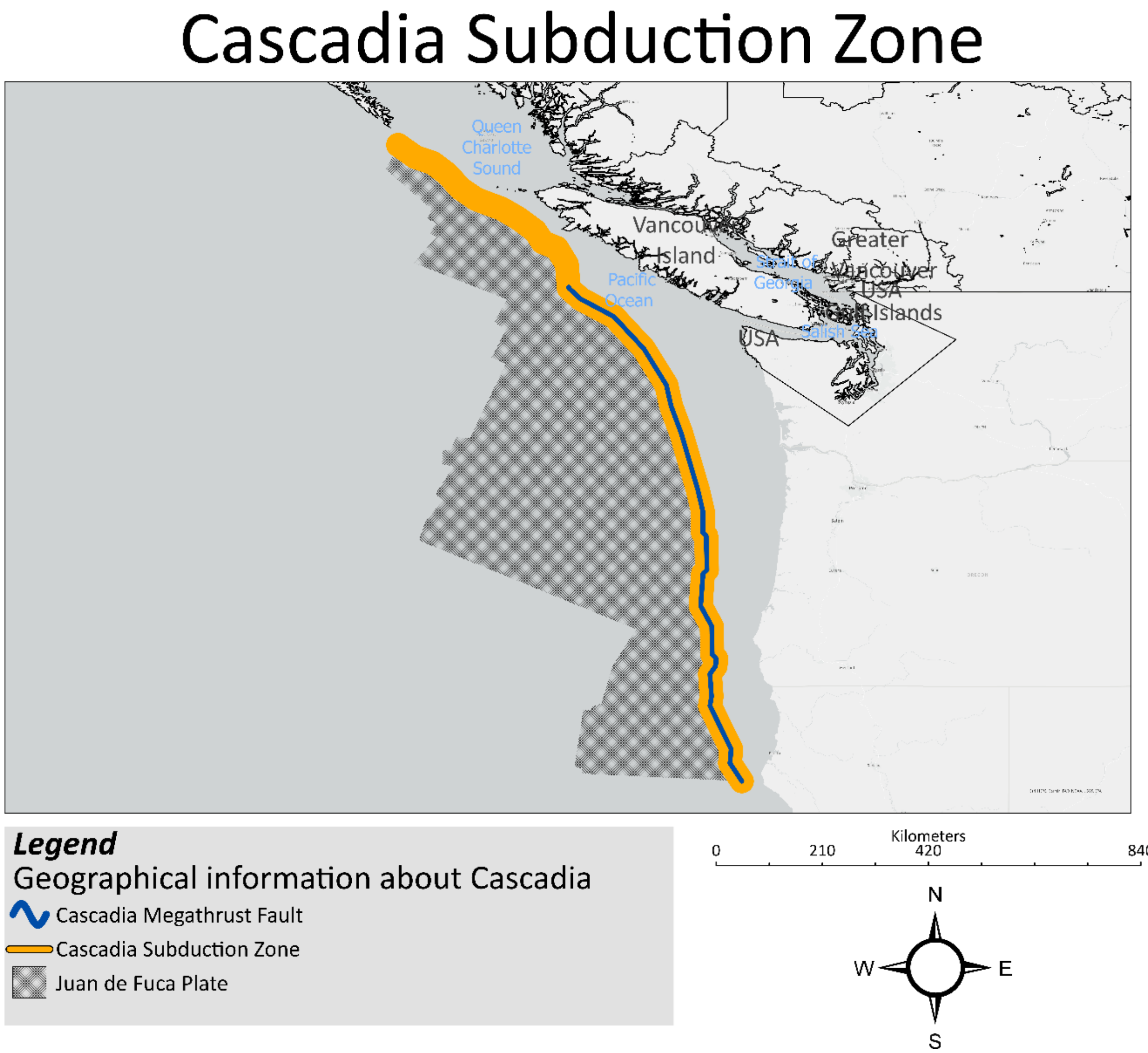

Figure 9- Map representing Cascadia scenario information, with details about the Cascadia Subduction Zone and Megathrust Fault. (Data Source [105])

Emergency Management in British Columbia created Tsunami Notification Zones, which are illustrated in Figure 10, to support the broadcasting of information related to tsunamis as relevant for each zone, primarily to transmit warnings and alerts [106]. There are five notification zones: Greater Vancouver, Vancouver Island, Graham Island, Gulf

Islands, and surrounding islands. First, Zone A, located at North Coast BC, comprises Graham Island, being the indigenous name Haida Gwaii. Zone B includes the central region of BC and northwest of Vancouver Island. Zone C at the west coast of Vancouver Island and stretches out into the Pacific Ocean, Zone D situated south of Vancouver Island at Juan De Fuca Strait, where the city of Victoria is located. Finally, Zone E is the largest zone between Greater Vancouver and central at Vancouver Island containing the Gulf Island and inner islands.

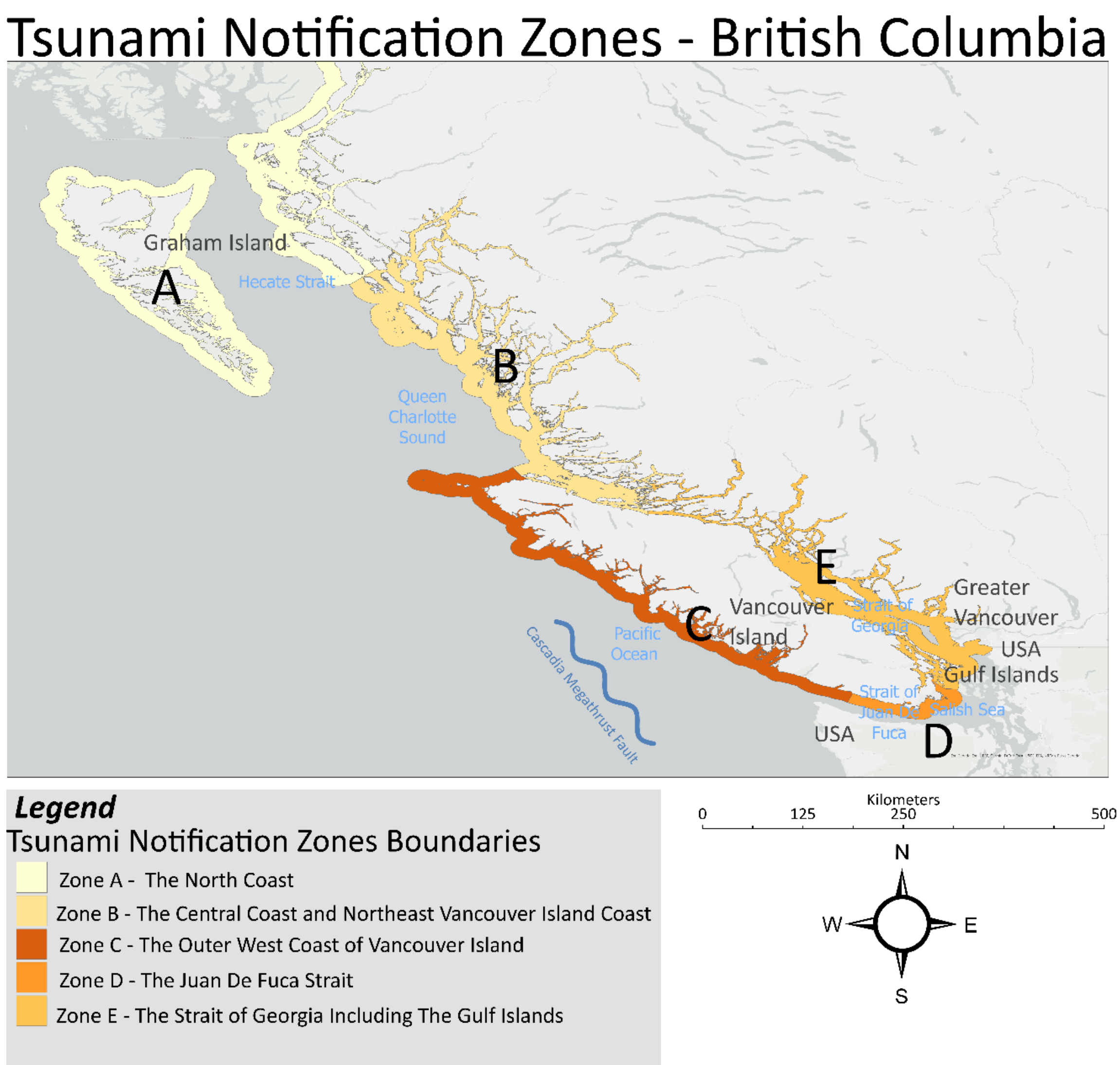

Figure 10- Tsunami notification zones information map:, 5 zones and their geographical details. (Data Source [35])

The tsunami notification zones receive alerts according to the alert system level, shown in Table 3. This is composed of 5 levels, possible threats, and recommended actions [107]. The most important levels to give attention to are ‘advisory’ and ‘warning’, as one implies a high probability of intense currents, while the other signifies potential land inundation. The suggested response for these significant alert levels is population evacuation and keeping distance from the coastline. Using literature review [22], [24], [88] information about the possible damages in Vancouver for the proposed scenarios and PGA data, it was possible to match the tsunami zones with these alert levels, as shown in Table 3, indicated by arrows . It was essential to match zones with different categories for the worst case of the Cascadia event because the RUSEMARIE model formulation is created relating different alert levels with the damage analyses. More details and explanation about this will be given in model Section 3.2.2. The geographical location, earthquake intensity, and tsunami megathrust play a critical role in defining each zone's threats and possible damages.

Table 3- Notifications alert levels, related threats, and proposed actions and integration with tsunami zones according to the proposed scenario. (Based on[36])

Alert Level	Threat	Action	
Cancellation	Tidal gauges show no wave activity	Confirm the safety of local areas	→ A
Information Statement	Minor waves at most	No action suggested	→ B
Warning	Flood wave possible	Full evacuation suggested	→ C
Advisory	Strong currents likely	Stay away from the shore	→ D
Watch	Danger level not yet known	Stay alert for more information	→ E

Infrastructural damage is another factor to consider when performing a ship damage analysis, as described in the literature review Section 2. Mainly because of earthquakes, ports and bridges are considered critical infrastructure elements. Depending on the proximity of vessels with these structures, the damage to vessels should be considered; for example, if a bridge collapse due to an earthquake and there is a vessel navigating under that bridge, there is a possibility for damage. In relation to ports and terminals, there is a probability of other structures collapsing, such as cranes breaking down. When vessels are close to such port or terminal structures when these collapse, resulting structural losses can turn a vessel not safe to navigate, and hence unable to be engaged in emergency response operations. The data relating to damage was provided by the SIREN project, where a model to analyze critical infrastructure was created; using data about peak ground acceleration, permanent ground displacement, the fragility of structures, and recovery hazard [19]. The detailed analysis calculation of damage probability was performed on berths and road segments using the Graph Model for Operational Resilience [80]. From the initial data set, it was possible to extract bridge data.

In the SIREN report the data was presented as damaged or undamaged for ports and passable and unpassable for roads and bridges. Besides that, most bridges encountered by maritime traffic are located in the Greater Vancouver area. More detailed information about damage bridges and ports damage can be found on SIREN report and paper[12]. In this research, as described above, the infrastructure damage will be used as a parameter for identifying trajectory points where a vessel is in risk of damage. If ports or bridges are classified as damaged/unpassable, and if a ship trajectory point is near that area, this specific point is considered to result in damage to that ship. In Figure 11 below, it is possible to see ports identified as damaged in red, while points highlighted in green represent undamaged conditions. Extrapolation was performed according to geographic features for ports locations where the damage analysis was missing. In summary, the damaged ports and bridges database includes 45% of ports being damaged and around 73% of the bridges, for the given Cascadia Earthquake scenario. Table 4 below shows the percentage for each region.

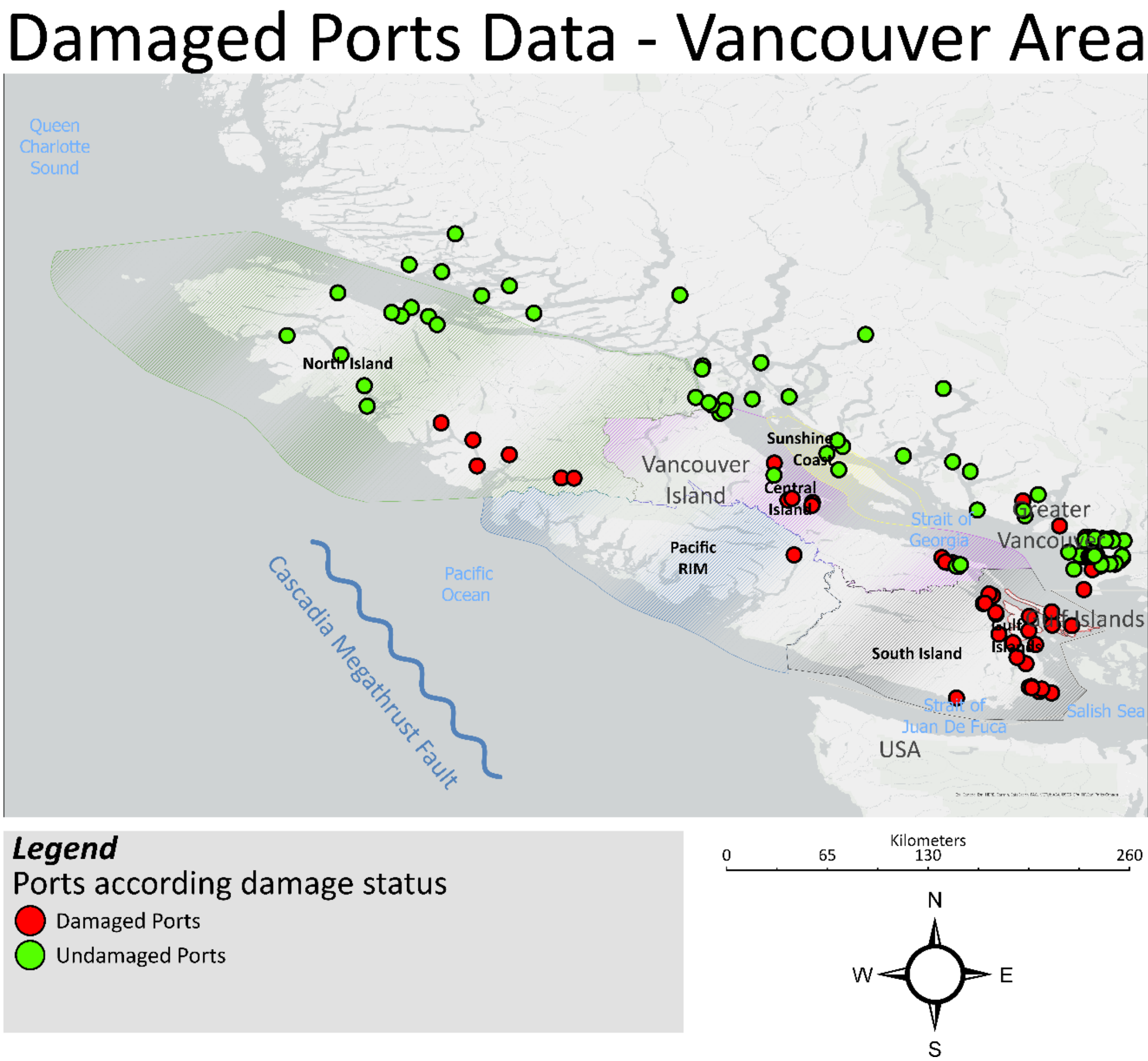

Figure 11- Data point information showing damaged and undamaged ports according to SIREN report studies. (Data Source [12]).

Table 4- Ports and bridges damage percentage for each region.(Based on [12])

Region Name	Ports Damage	Bridges Damage
Sunshine Coast	0%	no bridge near the sea route
South Island	100%	33%
Pacific RIM	100%	no bridge near the sea route
North Island	35%	no bridge near the sea route

Gulf Islands	100%	0%
Central Island	59%	100%
Greater Vancouver	25%	82%

Besides direct damage following the earthquake, the ensuing tsunami also has its own impacts. As described in the literature review in Section 2.2, tsunamis constitute two major dangers: waves and currents. In this thesis, a plausible worst-case scenario of the Cascadia Earthquake and tsunami is considered, so information and data associate with very strong currents were added to the RUSEMARIE model. In such a scenario, very strong currents are expected south of Vancouver island due to its geographical configuration, as well as its intermediate location between the open sea and coastal area. In addition, most ports located at bays and channel areas increase the probability of strong currents. Powerful currents may lead to ship damage, e.g. leading to ship capsizing or due to damage to ports and coastal structures, and the resulting debris being carried away. So, due to these current impacts for the south of Vancouver Island, more specifically the Tsunami zone D shown in Figure 10, this attribute information is added to the RUSEMARIE model for this zone.

There is research about the relationship between current speed and damage based on the most recent tsunami events, as described in Section 2.1 of the literature review. Due to this region's importance and vulnerability, some studies of currents were performed in this area, where currents in narrow channels could reach extreme values of around 17 m/s (33 knots) and 16 meters waves in small bays being the Cascadia scenario considered in this research [24], [46]. Hence, the dataset for currents used in this research was based on the report that studied the coastal flood inundation for this area, in which the area was split into 6 areas. The data was analysed according to different reference locations, with Table 5 providing summarized information according the report[24]. For Tsunami zone D, the RUSEMARIE model analyses the vessel location in relation to the 6 current areas, shown in Figure 12 and Table 5 below. The damage index performed by Lynet et al. inform when the currents are between 9-12 knots or 4.63-6.17 m/s [15], the damage observed for major docks, boats and large vessels off moorings is extreme damage, where more than 50% of docks and vessels will be damaged. So, comparing these numbers with the current velocity in the selected areas, 4 regions will experience severely damaged ports and also vessels in that area, as shown in Table 5. These regions are Esquimalt, Juan de Fuca Area, Sooke and Victoria. So, if vessel trajectory points are located in these current areas, they will be classified as damaged.

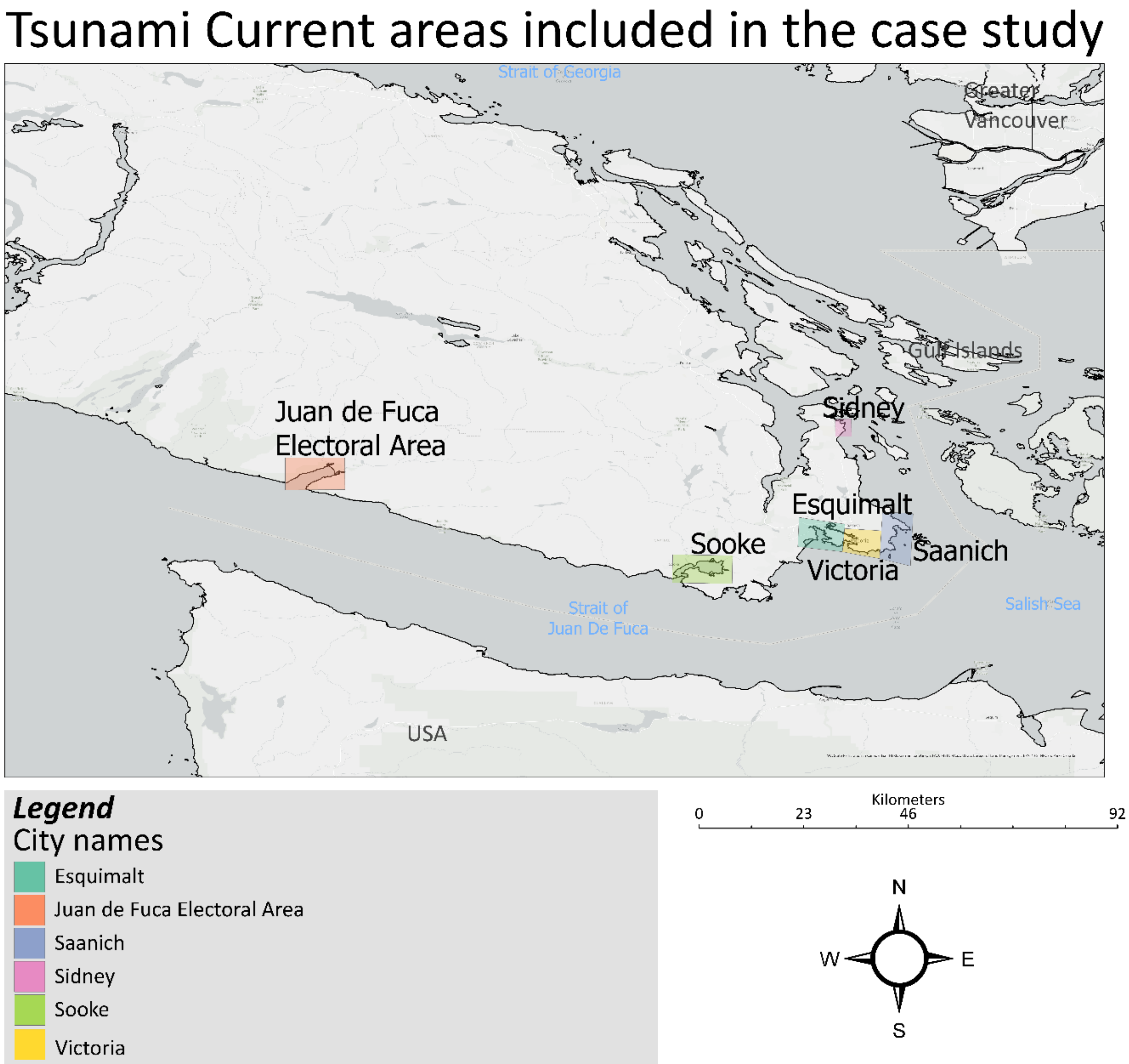

Figure 12- The 6 tsunami areas where the Cascadia currents can affect ships` availability. (Data Source [15])

Table 5- Area with currents from the Cascadia megathrust tsunami scenario, with information about water elevation, tsunami arrival time, and statistic information about wave crescent elevation and velocity.(Based on[15])

			Average		Upper Limit	
Area name	**Water elevation (m)**	**Tsunami arrival time (min)**	**Max wave crescent elevation (m)**	**Max current velocity (m/s)**	**Max wave crescent elevation (m)**	**Max current velocity (m/s)**
Esquimalt	6.85	75	8.85	9.25	11.02	12.37
Juan de Fuca Area	7.42	40	12.31	10.38	12.31	10.38
Saanich	3.57	90	5.7	1.34	6.32	1.96
Sidney	4.69	110	6.73	3.02	7.11	3.65
Sooke	7.13	60	6.24	6.82	7.46	8.96
Victoria	5.55	80	7.4	6.86	7.85	8.87

Besides currents, tsunamis create waves that can sink a ship depending on their intensity, encounter location, and sea depth, along with carrying ships to land and distorting structures depending on wave height (See Section 2.3). More details about how waves are included in this research are presented in the next section.

3.1.5 Vessels tsunami information

A tsunami is a natural event that raises concerns to the government, ship industry, and ship owners. Because of that, there are some safety guidelines suggesting what a ship's navigator should be aware of and what to do in the event of a tsunami, and instructions that the ship crew should follow, especially small vessels [65]–[69]. Usually, instructions are divided according to the location of the tsunami and the distance to the vessel. Local tsunamis are those with 10-30 minutes arrival time, while and distant tsunamis have a time of more than 3-4 hours before it reaches the vessel location. Another category of instructions will depend on the ship's location, whether it is positioned at sea or in port when the tsunami warning notifications are issued. The following diagrams summarize some details found in diverse guidelines, with shared information and important details. These guideline specifications guided the formulation of the proposed RUSEMARIE model, such as the safety depth for evacuation zone, the relation between local tsunamis, notification zones, and response actions. More details about model considerations will be described in Subsection 3.2.2, where the model is explained in detail.

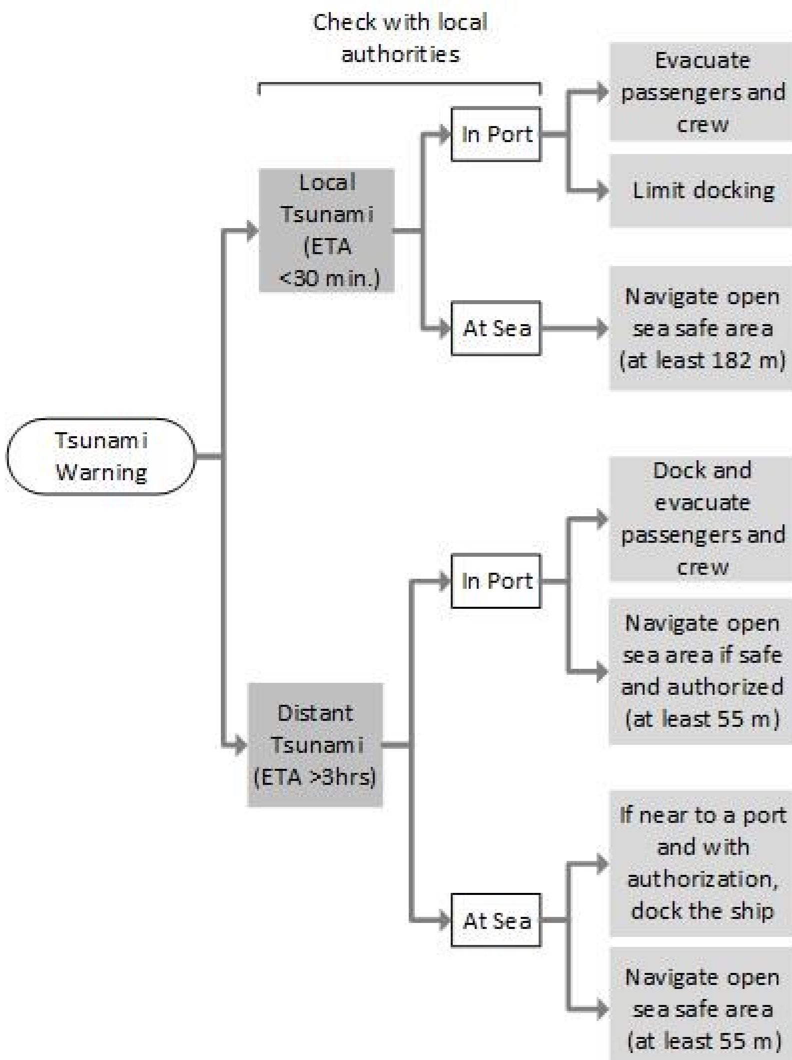

Figure 13- Summarized tsunami information from different navigation safety guidelines, with information for local and distant tsunamis.(Based on[39])

These guidelines suggest the safe depth for a waiting sea evacuation area, so the bathymetric data from the EMBC database has been collected for the British Columbia region [108]. Figure 14 shows the data used in the model according to the depth classes defined in the British Columbia Marine Ecological (BCME) classification report [109]. The legend on the map illustrates the classes from shallow to abyssal, where the depth range for shallow waters is between 0 and 20 m, while abyssal areas have depths greater than 1000 m. As observed in the map, the depth sections in this dataset are scattered, which means that there are different depths variations in the sea floor. The data is not precise and

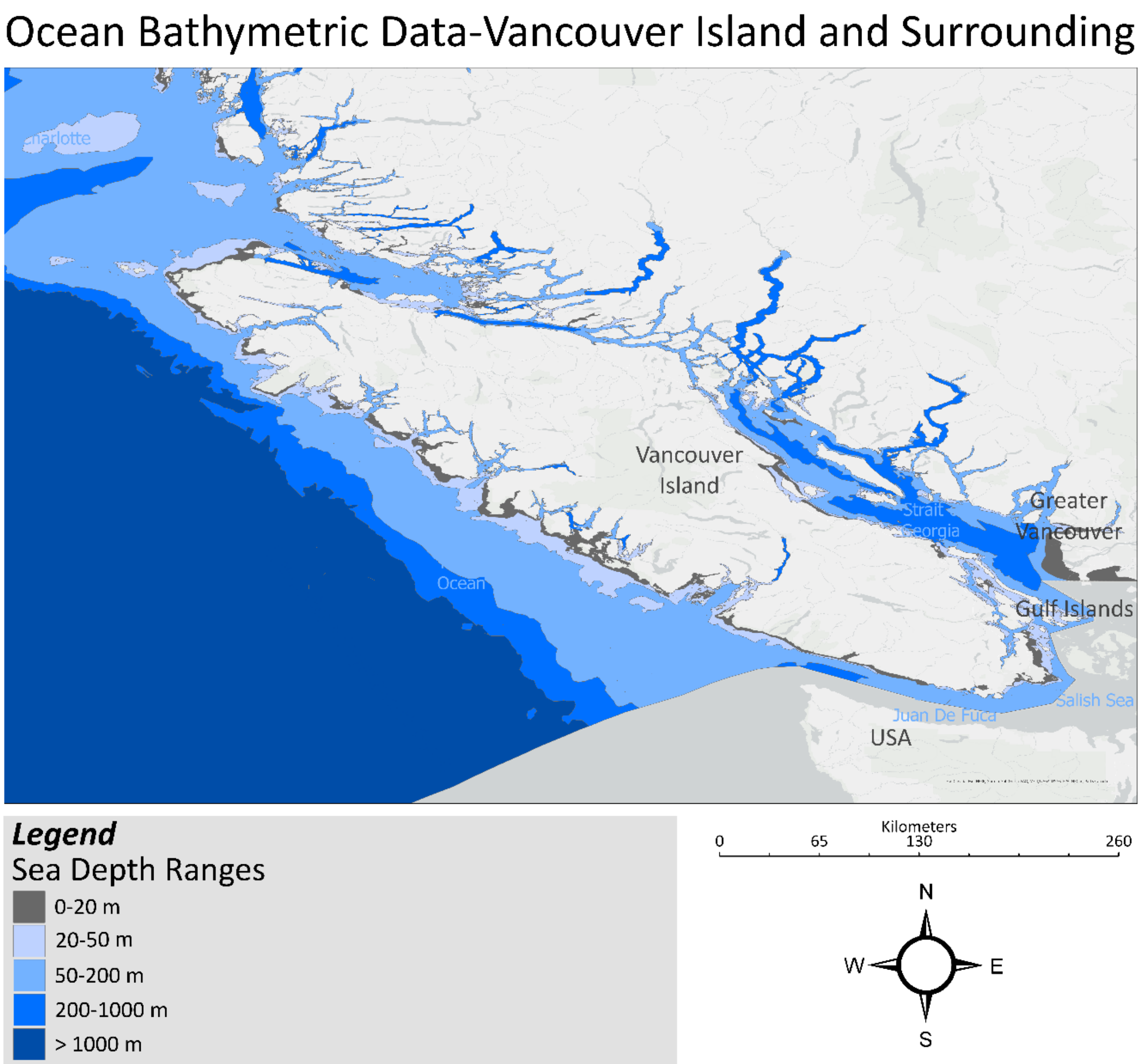

Figure 14- Bathymetric dataset with sea ranges between 0-100m for the Vancouver region. (Source Data [44])

the depth has non-uniform ranges, such as 0-20 m, 20- 50 m, 50-200 m, 200-1000 m and >1000m however these ranges classified according to ecological classifications defined by BCME.

The bathymetric data have two purposes in the model. First, as input data to analyze the depth areas which are safe for vessels to stay at during a tsunami event. Second, the information is used to calculate the tsunami arrival time, because the velocity of the tsunami wave depends on the depth of the sea area, consequently affecting the estimated time of arrival.

The first purpose is to analyze safe ship evacuation areas, as pointed out in the guidelines above. Some of them suggest 100 meters and others 100 fathom, that is 182 meters, as a safe depth for ships to stay in case of a local tsunami. The bathymetric ranges dataset that matches that safety range are 50-200m, 200m-1000m, and >1000m. As can be observed, the range 50-200m implies that this bathymetric area might be unsafe due to its ranges, so, making a conservative assumption to reduce the risk, only the other two ranges in the dataset were selected to be part of the safe area, as can be observed in Figure 15.

Another dataset used from the tsunami depth safe areas is the central polygon point. To be able to calculate the travel time to a safe area, the central point of the areas was selected as a reasonable option. Multiple factors can interfere with sea evacuation areas, such as multiple ships navigating to this area, safe aids to navigation (AtoN), possible floating debris from earthquakes, and narrow safe regions. Because of that, there is no clear definition of what point ships will consider to be a safe position to stop in these evacuation areas. Hence, the central points of each area are chosen to be the safe end location for travel time calculations, and these points will be adopted in the tool to calculate travel times from the ship position to the safe area. The black dots on the map of Figure 15 represent the central points of the safety regions' location. This dataset comprises 248 points.

The bathymetric data used contain ranges, so to calculate the tsunami velocity, the higher range (i.e. the greater water depth) is used in the formula below, as a conservative assumption. Table 6 below shows the velocity calculations considering the ranges. The deeper the ocean depth, the higher the tsunami velocity, while the shallower the ocean depth, the lower the tsunami velocity. So, each segment length in the tsunami path, which is a line for each overlayed depth area, will be divided by respective depth velocity resulting

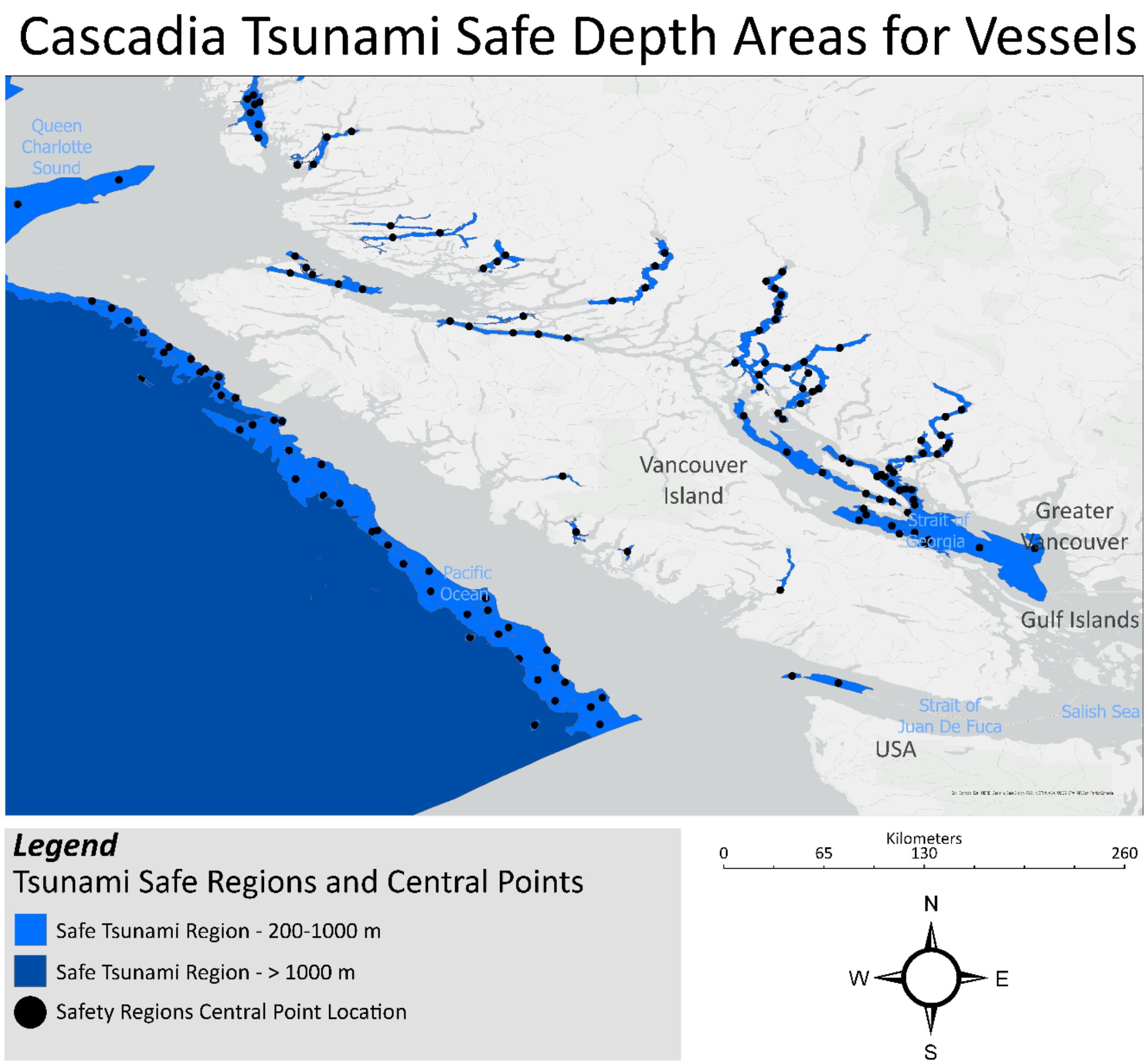

Figure 15- The 2 ranges of information that are part of safe tsunami regions, with depths bigger than 200 m and their central location. (Based on [44])

in an estimated arrival time [110]. The tsunami velocity formulation consist of the square route of the gravitational acceleration multiplied by depth, the physics and formulation development can be found at Stevenson work [111].

$$\text{Tsunami Velocity} = \sqrt{Gravity * Depth} \qquad \text{Tsunami arrival time} = \frac{Distance}{Tsunami\ Velocity}$$

Table 6- Information with the class depth information, their ranges, and the calculation for tsunami velocity(Data Source[44]).

Class	Depth range	Maximum Depth(m)	Velocity (m/s)
Shallow	0-20 m	20	14.00
Photic	20-50 m	50	22.14
Mid-depth	50-200 m	200	44.27
Deep	200-1000 m	1000	98.99
Abyssal	> 1000 m	1000	98.99

All the datasets and information presented above will be part of methodology development, applied in the models, and part of the implementation process to obtain answers to the research questions. That is laid out in the next sections.

3.2 Methods

This section discusses the methods used to process the data and provide quantitative insights into the system-level damage extent to maritime transportation assets due to an earthquake-tsunami event. Two developed models will be introduced and described in detail, as these comprise the most important aspects of the method. First, the processes and analyses to understand the daily ship patterns are presented in the Marine Vessel Movement (MVM) model section. Then, the RUSEMARIE model, which estimates the ship`s availability after an earthquake-tsunami event for a given ship location and contextual conditions, is explained. After that, the process of using these two models for the datasets in the studied area of Southern British Columbia is explained. Finally, the use of selected descriptive statistical techniques to obtain system-level aggregate insights into the damage to ships in the study area is described.

The Marine Vessel Movement model and the RUSEMARIE model are a type of spatial analysis and rely on Geographic Information Systems (GIS) techniques for their practical implementation. GIS software can be used to integrate data, develop, create, calculate, and analyze various functions related to spatial information, such as point coordinates, lines, polygons, and other spatial attributes. Because the primary datasets used for obtaining insights into the damage to ships in earthquake-tsunami events have strong spatial characteristics, and because the likelihood of ships being damaged is highly dependent on the spatial conditions, a spatial analysis tool is considered most suitable for this research. The two models were implemented and applied in this research using ArcGIS Pro, an advanced GIS software.

3.2.1 Marine vessel movement

The Marine Vessel Movement model's purpose is to generate ship data, specifically origin and destination ports, travel times, trajectories, paths, and routes. To study the possible damage to vessels, it is important to know their navigation patterns, so the MVM model has the function of generating these patterns in a quantitative format. Mobility data is the field that studies movement patterns for moving bodies such as animals, people, vehicles, and other motion sets. This field encompasses work addressing data collection and reconstruction, database configuration and mining, methods, uncertainties, and outputs visualization [96]. For the current research, because the use of the AIS data has a time field, the concepts and methods of spatial-temporal patterns were applied in the development of the model.

Different terminologies are used in the mobility data research area, sometimes applied interchangeably. In the current work, the terms are given the meanings illustrated in Table 7. An itinerary can be defined as a movement between two locations, i.e. going from A to B [102]. A route is a predefined way or course taken to get from an origin to a destination, a course to go between A and B. A track is a mark left by a person, animal, or vehicle in passing; this could be a point or line segment. In contrast, a path is a set of points to get from the origin to the destination following a route. Finally, the trajectory is a sequence of ordered positions with a spatial-time component for a specific itinerary.

Table 7- Terminology and illustration for movement research field that will be used in this research.

Terminology	Illustration
Itinerary	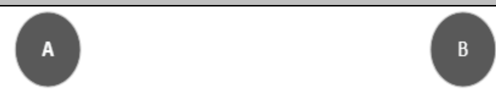
Route	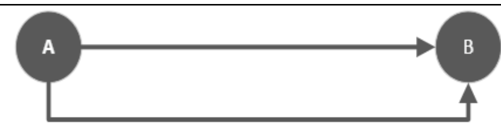
Track	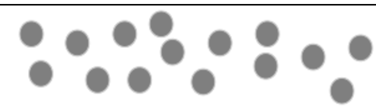
Path	
Trajectory	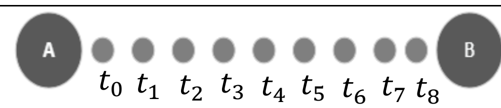

A spatial-temporal analysis studies the patterns of moving objects looking to extract their normal behavior [102]. There are several methods to study tracks and generate paths and trajectories: K-means, density-based, homogeneous groups of trajectories, classification approach, location-based structures, and other methods [96]. In the maritime traffic and AIS data literature, other methods were used, such as Grid-based analyses [112], density-based spatial clustering, spatial traffic statistics [113], traffic density analyses [114], automatic maritime routing through turning nodes generation [115], and sequential pattern mining [116]. In the current work, to develop the Marine Vessel Movement model, a combination of methods is applied for each phase of spatial-temporal patterns analysis. First, a dynamic threshold trajectory reconstruction method is used, followed by a homogenous group of trajectories (HGT) based on itinerary data, where this last tool is part of data mining. Similar work was done in [102] and [117].

The threshold trajectory reconstruction method consists of identifying trajectory start and end points. This is followed by time and distance threshold preparation, resulting in trajectory reconstruction, which means connecting points that belong to the same trajectory according to thresholds resulting in a path line. After the trajectory line reconstruction and origin and destination ports are identified, the information is clustered according to itineraries, generating homogenous groups of trajectories of which the median data is calculated. During this phase, the main outputs are median voyage time based on each itinerary, and a centreline path representing the route based on reconstructed trajectories. An advantage of these approaches is that there were well-studied and utilized in previous projects involving AIS data, and that their implementation is reasonably straightforward through the use of predefined tools in the ArcGIS software.

In the next paragraphs, more details are given about the MVM model and tools used. Figure 16 shows the flow and steps of the MVM, considering input data, processing, and output data. The model runs for each vessel, and the fleet is split into different files. The model starts with an analysis of vessel stop points. The tool 'Find Dwell Locations' [118] uses time and distance information to analyze when moving elements are in a stationary position, resulting in polygons. Once this analysis is performed, some outliers are removed: areas not near the coastline and those representing other ship movements. After that, the polygons are matched with the port point dataset (see Section 3.1.3), relating the stop areas with port information.

The second step in the MVM model is to define the start and end points in a trajectory, corresponding to the initial stage for an analysis of movement. A start point is defined as a point at which there is a change in velocity from 0 to a large number. An end point is the opposite, i.e. when the velocity data moves to 0. So, a trajectory is defined for each set of start and end points with a group ID (group identification number) for a sequential time stamp. As this project uses AIS data, the Speed Over Ground (SOG), and field information detailed in Subsection 3.1.2, it is utilized as a variable that sets the movement. However, as the AIS system also reports when ships are stationary, resulting in several sequential 0-values, the SOG parameter defined as a start condition is bigger than 0.1 and the end condition smaller than 0.1. Using the toolkit from ArcGIS with a tool named 'Detect Incidents' [119], the method described is applied to the AIS dataset.

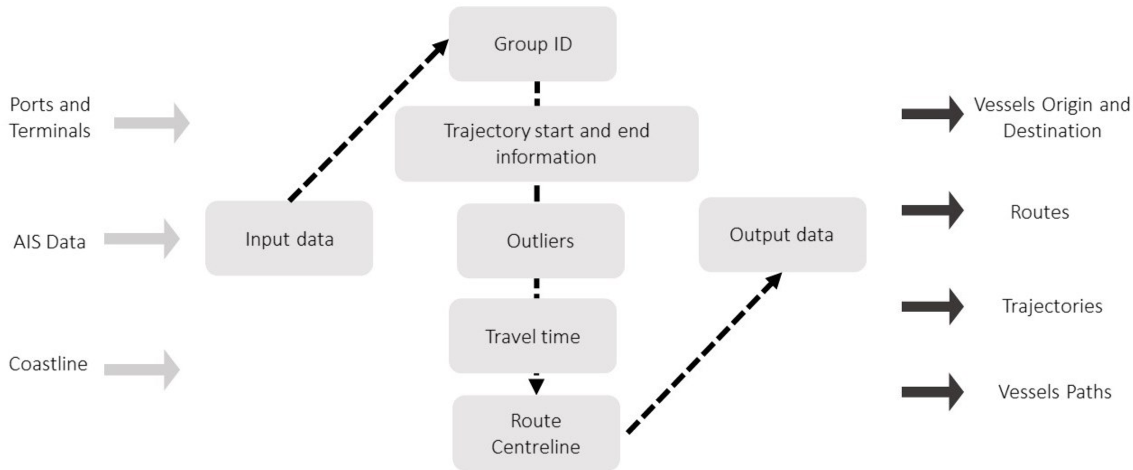

Figure 16- Marine Vessel Movement model with input, processing steps, and output data.

The next part of the method consists of reconstructing the tracks and turning them into lines according to the group ID, using the time and distance thresholds. The 'Reconstruct Tracks' [120] tool from ArcGIS automatically performs this analysis, generating a line. It uses time stamp information to analyze the time between two points, and according to the time threshold parameter, if there are points farther apart in time that this threshold, it splits the track into two different tracks. Moreover, in concurrency and using the same logic, it also analyses the distance between points and splits them if these do not comply with the distance threshold. After these time and distance analyses, the output data are lines with IDs. So, to finalize this step, an outlier detection procedure [121] is performed, to eliminate for example tracks with a small number of points that do not represent a full trajectory, tracks with short distances, tracks with short travel times, and tracks that are overlapping land spaces. In other words, a visual and data cleaning step is used to identify all tracks that differ from normal navigation patterns.

The fourth step is connecting the origin and destination port information with the reconstructed data information. This step will be done through joining two previous steps, the outputs from the dwell port polygons with the reconstructed paths. Using a spatial joining tool [122], if the start point of a path is at the same area as one of the dwell port polygons, the origin port feature will be added to path table data, with the same logic being applied for the destination port feature. So, the tracks data table contains the origin and destination ports, voyage time, mean SOG, and other trajectory details. The information can be clustered according to itineraries.

The next steps are based on groups of itineraries for each ship. The first step has a line representing the itinerary for each ship, and this process is made using a central feature tool [123]. This tool calculates the distance for each centroid for all the lines, and the line with the shortest cumulative distance is chosen as the centrally located feature. The mean travel time is calculated according to homogenous trajectories using the calculate field tool [124] from ArcGIS. The output file is a centreline for each itinerary for each ship, where the mean voyage time data is also brought together.

3.2.2 Earthquake-tsunami loss prediction model for marine vessels

Having presented the dataset pieces and MVM model for this study, now the main method of the research will be described. The RUSEMARIE (Earthquake- Tsunami loss prediction model for marine vessels) model aims to classify vessel trajectory points according to whether or not a vessel at that location is expected to be damaged due to an earthquake-tsunami event. This generated data will be used as a basis for answering all four research questions introduced in Section 1.

Risk research suggests that people tend to have a positive bias concerning emergency disasters due to common myths [125]. It is plausible that the public has the risk perception that ships will not be damaged in a Cascadia event, especially the large ones, assuming that all maritime assets will be available to support emergency response operations. Nevertheless, the 2011 Japan Earthquake showed that is not always the case, the Japanese also underpredict the possible earthquake-tsunami consequences.

During the literature review research, some tsunami ship safety guidelines were identified as described in Section 3.1.5, as well as literature related to the classification of observed vessel damages recorded following the Japan 2011 earthquake. That literature classifies following elements of ship damage: tonnage, situation during the tsunami, ship material, engine type, ship location categories, and damage types. Therefore, no specific method was identified to calculate ship damage considering the spatial relation. So, the developed RUSEMARIE model and framework were created specifically to answer the research questions, by merging the guidelines information with information about impacts and damages from earthquake-tsunami events, and the spatial position of the vessels. Hence, as this is a new approach, based on the best available but limited, evidence, appropriate caution about the results of the model application is warranted. As will be elaborated in Section 3.3 this will be done through a thorough strength-of-evidence assessment as recommended in state-of-the-art risk research for preparedness planning [126].

First, the normal voyage trajectory of the vessel was studied and analyzed using AIS data and the MVM, as well as some characteristics information such as size by tonnage, vessel type, origin, and destination ports. Then, information is extracted from the literature review about what types of damage earthquakes and tsunamis can present to vessels. Earthquakes can cause ground shaking and soil liquefaction, leading to the collapse of infrastructures. Port loading and unloading infrastructures and bridges are the land-based structures with proximity to vessels when these are docked or navigating under these structures, so that a possible consequence of an earthquake is being hit by the collapsing pieces. In contrast, tsunami damages are related to the waves and currents, according to research made by Muhari et al. [1] from data of the 21,000 vessels damaged, including small boats and fishing vessels, in the Japan 2011 earthquake-tsunami event, with collision, allision, sinking, stranding, and dragging the most frequently occurring reasons for damage. A collision occurs between vessels while in an allision, a vessel strikes one or more structures, and includes cases when vessels hit debris in the ocean. Such situations can lead to sinking, grounding, flooding, fire, or loss of some capability. So, the proposed RUSEMARIE model analyzes how close the ship is to these structures. Stranding occurs when a ship is trapped in a shallow body of water such as sand and rocks. Dragging is when a ship is carried to the land due to elevation of water and, in cases when a vessel is moored in a port, loosening of this mooring. Both the stranding and dragging damage types depend on wave size, velocity of currents, and depth of the ocean. In the model, the analysis are made whether a ships can navigate to a tsunami safe area, that is, to depth regions where stranding and dragging are avoided.

After identifying the damage types for each circumstance associating these with causes for them, the next step of the model is to identify and relate different levels of danger with damage types considering geographical attributes. For this phase, the tsunami zones summarized in Section 3.1.4 are utilized as a basis, as these zones already have alert and threat levels, according to topographical configuration, that were correlated for this specific Cascadia scenario. Therefore, the RUSEMARIE model was divided by zones and their relationship with the damage caused. In addition, it was developed using spatial analysis concepts and methods because earthquakes and tsunamis, especially the Cascadia scenario, have a huge impact on a large geographical area, with damages related to location-specific characteristics. Most of the damage causes have spatial and location components.

The RUSEMARIE tools execute a spatial analysis that results in a binary categorisation: ‘damaged’ and ‘not damaged’. Further descriptive statistics steps are performed on the complete resulting dataset, to improve the understanding of patterns emerging from the application of this model, answering the research questions of Section 1. Figure 17 shows the main steps of the RUSEMARIE model, without detailed specification of tsunami zone features. The earthquake-tsunami event is the initial condition. Then, the distance from the port and bridges are calculated, then the analysis of which ports and bridges are damaged is integrated. Then, for each zone, a different element is calculated considering the possible tsunami damage types. That is, if a ship point is in a safe area or if a vessel is able to move to a safe area within the available time window. In addition, vessel size is considered, recognizing that small vessels involve higher risks, analyses include currents in some specific areas, and the distance to the port. These can be the cause of different damage types as mentioned above, collision, allision, sinking, stranding, and dragging. In the next paragraphs, each procedure and tool will be described in detail.

The earthquake damage caused to vessels is the first step in the RUSEMARIE model, based on the infrastructure collapse given the direct earthquake impacts. In this step, first, the distance of the points of a ship trajectory to the locations of ports is calculated using the ArcGIS tool named ‘Near’ [127]. If the points are within a 1 km parameter range, these are retained for further analysis, i.e. to check if this port is considered damaged, as obtained from the data description(Section 3.14). If a vessel trajectory point is within the specified parameter range and if the port is damaged, that point will be given the status ‘damaged’.

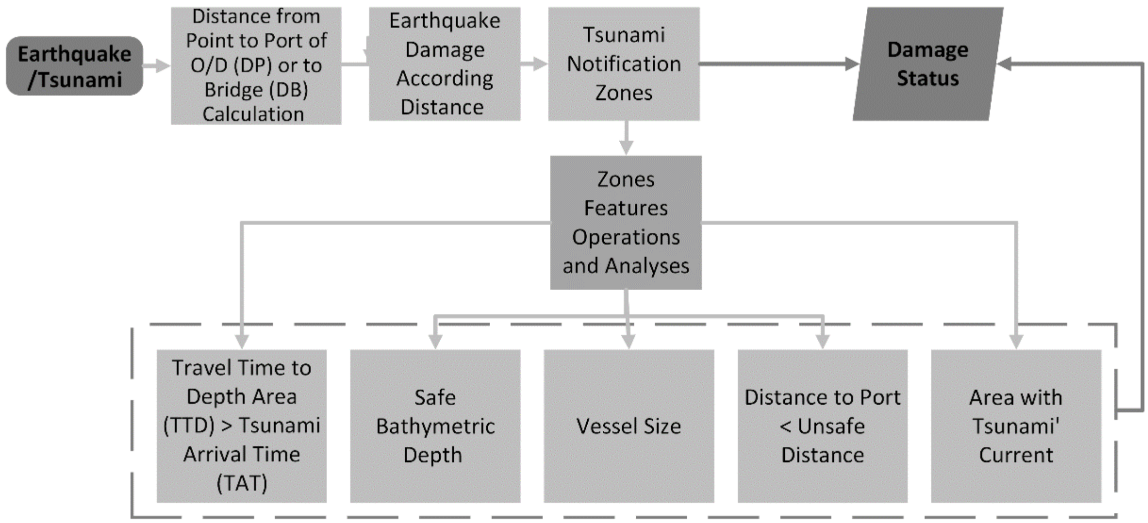

Figure 17- A overview of the RUSEMARIE processing steps triggered by an earthquake-tsunami event.

Thus, a conservative assumption is made that if a ship is close to a port subject to direct earthquake damage, the vessel will also be damaged. In the other case, where the vessel trajectory point is within the 1 km distance range, but if there is no damage to the port, that point receives the status 'not damaged'. This logic is applied to all vessel trajectories, for all ports.

In the same way, the bridge's distance is analyzed for a distance range of 500 meters. The distance parameters for bridges and ports are different because bridges are horizontal structures that ships navigate under, while most port structures have some vertical component, such as cranes, and ships navigate near, for example, berths. Similarly as before, points within the 500 m range are considered as 'damaged' if the bridge damaged in the earthquake, and 'not damaged' if the bridge is not. Following these steps, points classified as 'not damaged' are further analyzed from the perspective of possible damage due to tsunami.

In the RUSEMARIE model, tsunami waves are generated at exactly the same time that the earthquake occurs. However, because a tsunami is initiated at a location offshore, specifically the Cascadia scenario as described in Section 2.1, it takes some time for the waves to reach vessels in maritime and coastal areas, and hence before the related damages can occur. This also gives vessels the possibility to reach a location of safety, depending on their initial location and the time before a tsunami reaches them. Using the treats levels described in Section 3.1.4, the different tsunami zones present a different threat level for the Cascadia scenario. So, to determine the location of each point in relation to the tsunami zone, the ArcGIS tool named ‘Near’ is used. This tool measures the distance between the features, in this case, zone and point, and adds a column at the point table with the closest zone. In other words, each point receives a zone classification according to its proximity.

Due to its geographical location and distance from the Cascadia tsunami, zones A and B have a low threat level description as tidal gauges showing no wave activity. Thus, no abnormal wave or current formation are expected in this zone. In the analysis, if a vessel trajectory point is in this zone, it receives the status of ‘no damage’. Trajectory points associated with another zone receive a status ‘continue next step'. This step is performed using the classification made in the previous step and the calculating field tool.

Tsunami zone E has the treat alert information ‘danger level not yet known’, with an associated suggested action of staying alert for more details. This zone is located between Vancouver Island and Greater Vancouver. Vancouver Island is a geological barrier which smooths the tsunami waves, although due to its many bays, straits, and enclosed areas, the currents influence the safety of navigation. Due to its boundaries with zone D and indeterminate danger level and recommended actions as obtained from tsunami navigation guidelines described in Section 3.1.5, a cautious approach is considered in the analysis for this zone. Hence, in this zone, two features are calculated: the ocean's depth, and whether ships can navigate to safe areas before the tsunami arrives at the vessel location.

For the depth calculation, the data from Figure 15 were used if the points were located within the safety tsunami areas, using the ‘Near’ tool in ArcGIS. Where the depth range exceeds 200 m, the vessel trajectory point receives the status ‘no damage’, but if it is located in an area with a water depth of less than 200 m, they receive the status ‘next step’. For region E, the next step is calculating the tsunami estimated arrival time (TAT) and travel time to a safe area (TTD).

These two estimated times use the same model builder tool called ‘cost path’ [128] as basis for their calculation. This tool calculates the minimum path from a start to an end location using raster distance information, resulting in a line with corresponding length and geographic information. Furthermore, this tool uses coastline information as a barrier to avoid lines intersecting with land areas. For the TTD, the start location is the considered vessel trajectory point, and the end location is a central point in the safety tsunami area, see Figure 15. After the ‘cost path’ tool generates the line information, the estimated travel time is calculated using the average ship velocity, which is derived from the SOG data. As the RUSEMARIE model runs differently for ferries and tug-barge combinations, the SOG parameter used in the calculation differs. The average SOG for tugs is 10.1 km/h (i.e. 5.4 knots), and for ferries 20.37 km/h (i.e. 11 knots) according to AIS data. Figure 18 below shows the processing steps and data used.

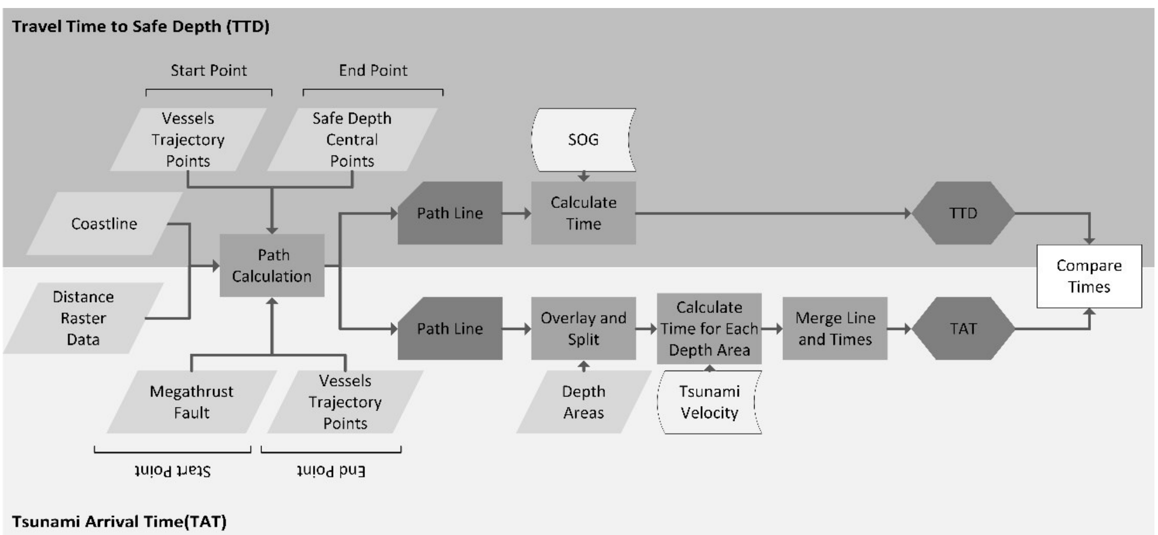

Figure 18- RUSEMAREI detailed information for estimating travel time to safe areas and tsunami arrival time.

For the TAT, the start location is the Cascadia Megathrust Fault line, shown in Figure 18, and the end location is the considered point of the given vessel’s trajectory. After the ‘cost path’ tool generates the line information, the line is overlaid for each depth region which the line intersects, and its length is split, generating several segments per depth area, depending of the location. For each segment, the length is divided by the depth maximum velocity data presented in the Table 16. The maximum velocity is based on the formula $\sqrt{gravity * depth}$, as explained in Section 3.1.5. Then, to calculate the final arrival time, the time associated with each segment of a specific line is summed up. The summarized tsunami arrival time expression can be founded below. To validate this approach, the TAT time as computed above is compared with results of another study [24]. For the purposes of the current analysis, the RUSEMARIE tsunami arrival time is considered close enough to the ones from this report, which relies on more detailed tsunami estimation models.

After the TTD and TAT calculation, the start point at TTD and end point at TAT for a given vessel trajectory point, are compared. As the analysis is made for several points along the path, and because the final analysis of the damage probability consider all results for each trajectory point, this relatively simple static time calculation of travel time to the safety tsunami areas is considered reasonable. If a ship at a given location has enough time to navigate to a safe area before the tsunami arrives, the point is labeled as 'no damage'. However, if the tsunami arrives before the vessel has time to navigate to a safe depth area, the point is labelled as 'damaged', which corresponds to the condition that TTD exceeds TAT.

Tsunami zone D is considered an intermediary zone between the worst zone and the low damage zone, between zones C and E. This zone has a strong current threat status, with associated safety recommendations to avoid the shore. Because of the significant influence of the current feature in this Tsunami zone D, the vessel size will be considered a factor in the analysis. This step follows the structure of safety guidelines suggested by governments, especially for small vessels, as outlined in Subsection 3.1.5. The conditioning and processing in this zone D are different according to vessel size. For ships with tonnage less than 300 tonnes, the distance to the port contributes to damage because of the high likelihood of stranding damage type due to tsunami currents. The distance calculation uses the same procedure as the earthquake distance to the port, as explained above, at earthquake damage related to port proximity, with the same parameters. So, if less than 1 km from a port, it will be damaged; if not, move to the next step, which analyzes if the small vessels are away from the port but in areas where strong currents might happen. Using the data about currents from Figure 12 and Table 5 and the background information of Section 2.2.2, if a small ship is located in any of these areas, they are assigned the status 'damaged.' The analysis uses the ArcGIS tool 'Near,' similar to the port distance step described earlier. If a small vessel is not located in areas with a dangerous current, the same procedure as for zone E is applied, depth and time calculations. For ships above 300 tonnes, navigating in this zone D, only the depth and the TTD and TAT values are calculated, following the same steps as explained above for zone E, and also resulting in ‘damaged’ or ‘not damaged’ status for each point.

Zone C is the final tsunami zone in the RUSEMARIE model. It represents the highest danger zone as its geographic location is the closest to the Cascadia megathrust fault line, with the tsunami wave of a Cascadia Earthquake expected to arrive between 15 to 30 minutes. The treat level is rated as ‘flood wave possible’ and the suggested government action is ‘full evacuation’. As suggested in the navigation safety guidelines for tsunami events, when a local wave occurs there is not much time for action, such as navigating the vessel to a safe depth area. The likelihood of extensive damage to a vessel is high in this zone, and consequently, fewer analyses are performed for vessels located in this area. The safety location for a ship it is on a safety depth area. No matter the water depth, near to a port the damage is taken as certain to occur, due the intensity and proximity of the tsunami leading to collision, allision, sinking, stranding and dragging, as described in the literature review Section 2.2. Thus, in zone C, if a point of a ship trajectory is near a port, 1 km range, it will be labeled as ‘damaged’, and when it is located in an area where the depth is not safe, less than 200 meters depth, it will also be considered ‘damaged’. The calculation for these two analyses uses the same logic described in the paragraphs above for other zones, see the analysis is done for zones E and D. The ‘damaged’ and ‘not damaged’ categorization is made using the following logic showed on Figure 19.

Figure 19 shows a diagram which contains further details about the logic contained in the RUSEMARIE model. It starts with the earthquake damage analyses, and then moves on to the categorization of vessel trajectory points to tsunami zones, with their respective damage calculations leading to a classification as ‘damaged’ or ‘not damaged’. At a high level, RUSEMARIE is a taxonomical model categorizing data points according to geographical and other information, leading to an output table where all vessel trajectory points are categorized as either ‘damaged’ or ‘not damaged’. This resulting table is subsequently used to generate summary and descriptive statistics, relating these with maps representations, and answering the research questions introduced in Section 1.2.

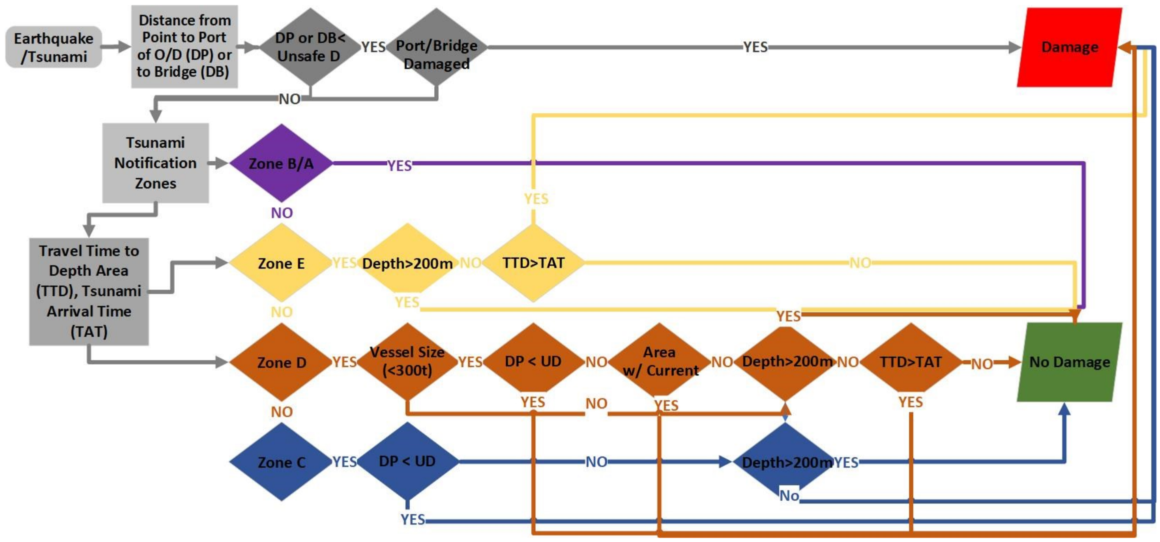

Figure 19- RUSEMARIE model structure with processing procedures, with the tsunami phase split in zones corresponding to Figure 10.

In the next sections, a summary description of the application of the method is presented, with especially Sections 3.1 and 3.2.2 containing some further details about the practical implementation of the RUSEMARIE model to the considered case study of the Cascadia earthquake-tsunami disaster.

3.2.3 Research implementation and processing

The MVM model and RUSEMARIE model are developed to support the investigation of ship damage due to earthquake-tsunami events. This section provides further details about how these two models are applied together as part of the methodology, including the implementation and processing of information. Figure 20 shows a schematic overview of the methods, including the input dataset, models, and outputs. It exemplifies the data and methods described in the previous sections and provides further details about the implementation to a specific case study.

As mentioned in previous sections, the model is developed and implemented using GIS software, in particular ArcGIS version 1.2. This computer software is used to process the information through the model builder, a geoprocessing model. The model builder on ArcGIS is a programming language that uses visual workflow to build models and geoprocessing data thought pre-building tools. Some of the tool of either model run using a parallel processing factor, decreasing operating time and improving computation capabilities. During the development and implementation of each tool, several tests were performed for each vessel group sample, barges, and ferries. In addition, this was performed with different parameters, so the most suitable and reasonable values were chosen in the implementation phase.

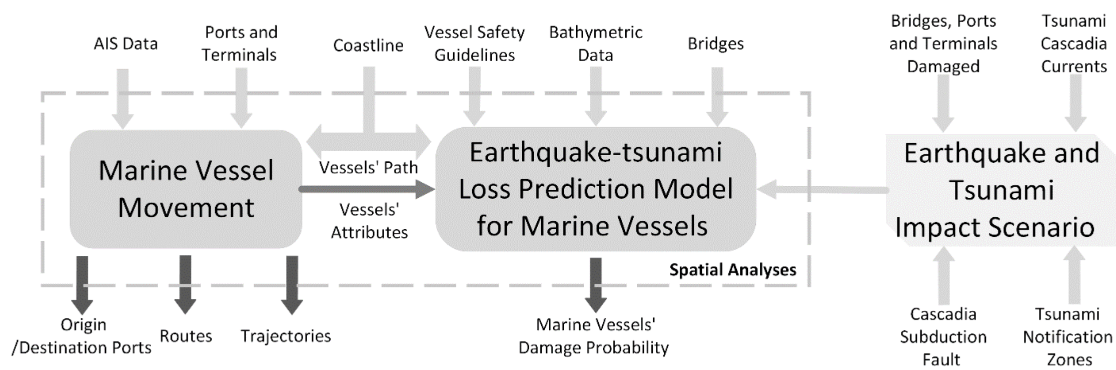

Figure 20- A overview of the research methodology, including information about input datasets, models, scenarios information, and output information.

The first step of the implementation of this research starts with splitting the AIS database sample file into separate files according to the chosen fleet described in Section 3.1. Then, for each vessel file the MVM is applied, generating paths and average voyage times. These files were merged into two files: one for tug-barges combinations and another one for ferries. These files contain ship descriptive information, origin and destination port, line spatial information, average travel time, and mean SOG. Then, to perform the analyses of RUSEMARIE, the tool 'Generate Points Along Line' is utilized, generating points along lines each 500 meters, with these parameters chosen after some experimental testing using values ranging from 100 to 1000 m. In other words, creating points using this parameter resulted in the best line pattern representation and application in the RUSEMARIE model, considering the limitations of reasonable processing time. Then, using the scenario dataset described in Section 3.1.4, the RUSEMARIE analyses were performed for each point for both files. After each point is given a 'damaged' or 'not damaged' characterization, some descriptive analyses were performed using MS Excel. These will be described in Section

3.2.4 below, and follow the calculation and categorization of damage probabilities into ranges. The descriptive analysis probabilities were merged with the line's information obtained from the MVM, so maps and regions analyses can be generated using ArcGIS, and graphs and tables using Excel.

3.2.4 Summary statistics and presentation

This section outlines the techniques applied for obtaining summary statistics and presentation of the results, which support summarizing the output of the RUSEMARIE model, providing information to answer the research questions. After the ROSEMARIE results are generated for the vessel trajectory data for tug-barge combinations and ferries, the information concerning 'damaged' and 'not damaged' is available for each trajectory point, as explained above.

Summary statistics are constructed to support risk-informed disaster preparedness planning, i.e. with the view to better understand the risks and to provide support information for decision-makers and stakeholders. The following summary statistics were derived: ship damage probability, relation between ship size and type and damage probabilities, analyses of the factors contributing to whether vessels are damaged or not, overlay of damage probability ranges and routes, grid analyses sea areas in terms of the probability of vessel damage, and ship capacity reduction for different regions in British Columbia.

First, a table with a summarized number containing 'not damaged' and 'damaged' points is generated for each vessel, along with a total number of points for the trajectory for all the routes for given vessel. Then, the ship damage probability is calculated for each ship, by comparing the total route points with the total points categorized as 'damaged', independent of the route. The damage probability is calculated independent of the route, using all damage points of a vessel combining for example damage points of route X and Y. The reason is that there is no specific and exact information about when the earthquake and tsunami will happen, i.e., there is no way to know what position on the ship's route a vessel would be at when an earthquake occurs. To better represent the results, and to support a risk assessment, the probabilities are divided into categories according to Table

8, starting at 0-5% damage probability, until 95-100% damage probability, represented using different color damage scales. The data is represented using a pie chart graph made using MS Excel. This information will structure the answer to the first research question: How many ships will be available to support humanitarian supply chain operations in Vancouver Island coastal area?

Table 8- Color scale information with probability and damage levels.

Color	Damage Probability	Risk damage levels
Dark Green	0%-5%	No damage
Light Green	5%-25%	Low
Yellow	25%-50%	Medium -Low
Orange	50%-75%	High-Medium
Light Red	75%-95%	High
Dark Red	95%-100%	Damage

As detailed in previous sections, the ship's analyses were made for tug-barges combinations and ferries. To better identify patterns in the data, the ships were further divided into 6 groups. Each type of vessel was divided into 3 categories: small, medium, and large, so that more specific insights in damage patterns can be obtained. The ferries were divided according to their size capacity, accounting for the length and breadth dimensions. For tug-barges combinations, as these consist of two different marine assets which are connected, the size categorization is based on the tug's gross registered tonnage, because the tug size is related to bollard pull and, consequently, to barge size and carrying capacity. These results were also represented using a pie chart graph made using Excel software. The information obtained in this way will be utilized to answer the second research question: What is the relation between ships groups sizes and damage probability considering Vancouver maritime logistic operations?

Table 9- Ferries size classification details.

Group	Vessels size capacity (container)
Small Ferries	<40
Medium Ferries	40-100
Large Ferries	>100

Table 10- Tugs-barges size classification details.

Group	Gross Registered Tonnage (Tonnes)
Small Tug-Barge combination	<100
Medium Tug-Barge combination	100-200
Large Tug-Barge combination	>200

The third research question focuses on obtaining insights in what are the hazardous sea areas or routes for a ship to navigate on in case of a tsunami in a Cascadia earthquake-tsunami scenario. To obtain an answer to this question, a route damage analyses is performed. This means that the damage probability was calculated for each ship in each route, by comparing the number of points categorized as 'damaged' in that route with the total number of points on that route. This information was also obtained for the 6 vessel type and size presented in Table 9 and Table 10, and matched with the spatial information about the vessel routes. The analysis is performed using ArcGIS software and the results are represented by maps. First, all ships are shown together, following which several maps are created for each ship group, as detailed above, resulting in a total of 7 generated maps.

The second set of analyses performed to support answering this research question is based on a grid analysis. The study region was divided into grids of size 15x15 km, using the ArcGIS tool 'Generate Grid from Area' [129], resulting in 1976 grids as shown in

Figure 21. With this analysis, the damage information is shown in grid cells, focusing on sea areas instead of vessel routes. As summary statistics information, the frequency of points will be presented in a map, by counting the number of points in a grid, using the ArcGIS ‘Spatial Join’ tool. In addition, the hazard level for different sea areas is calculated by the dividing the number of points categorized as ‘damaged’ in a given grid by the total number of points in that grid, independent of the routes or number of ships in the area. The maps showing the information are prepared using ArcGIS and use the damage probability scale presented in Table 8. A map is produced only for ferries and another one for tug-barge combinations.

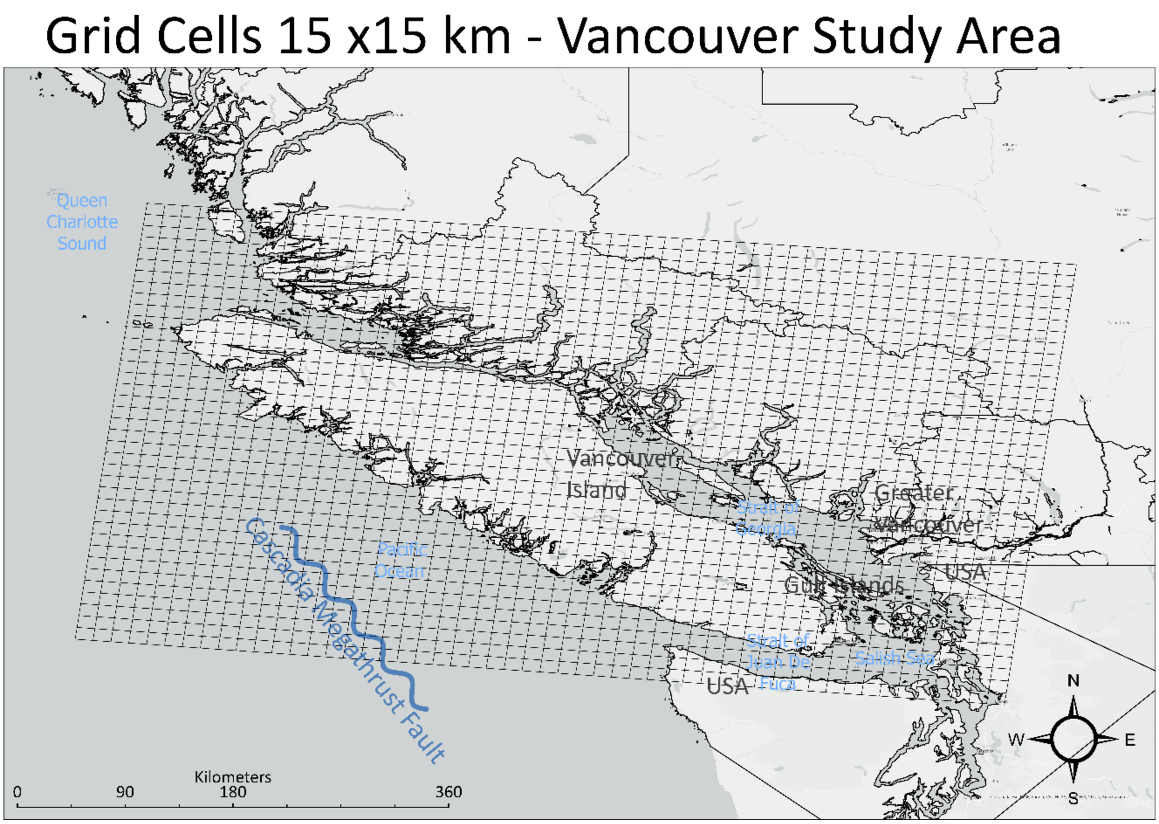

Figure 21- Grid with 15x15 km in the case study area, that will be used to show ship damage probabilities for these grids.

The final part of the analysis of the results addresses the relation between the regions elaborated in Section 3.1.1, and the damage probability for the vessel routes, as explained in this section's second paragraph. The aim of this analysis is to obtain information to answer the fourth research question, i.e. which regions of Vancouver will likely be exposed to a reduced ship capacity for emergency logistics deliveries due to ships not being available in the immediate disaster response phase. For this analysis, a comparison is made between the number of ships servicing these regions before the earthquake-tsunami event and the number of ships which are expected to remain operational to service these regions, considering the damage probability and the fact that some ships will not be available. Hence, to perform this analysis, the routes damage scale will also be taken into account, i.e. an analysis is made of the ship damage probability on routes connected with a specific region of British Columbia, using the data of Figure 3. These analyses are also performed using the ArcGIS 'summary information' tool [130], and presented as a map in the results section.

3.2.5 Models risk uncertainties analyses

The results of the investigation about ship damage in an earthquake-tsunami disaster are intended to be used in a risk assessment and risk management context, as pointed out at the introduction. Acknowledging that the state of risk research literature stresses the importance of relying on the best available evidence and to be transparent about uncertainties, a state-of-the-art strength of evidence analysis method is used to study these elements [131]. The critical evidence level technique is a method used in state-of-the-art risk analyses, aiming to systematically analyze the limitations of each aspect underlying the analysis, by combining the strength of evidence with the sensitivity of the model or analysis step with respect to the analysis outcome [132]. Thus, this technique gives systematic insights into the limitations of the analysis. Instead of providing selected qualitative impressions about the limitations as commonly done in many risk analyses and research, it is a structured way to recognize the strengths and weaknesses underlying the analysis and its results. It aims to provide comprehensive and consistent insights into the extent to which various aspects of risk analysis can be relied upon. This assessment of the criticality of the various evidence aspects can also be used as a basis for making a second-stage risk analysis, where the initial risk analysis results (the first stage risk analysis) are interpreted alongside the evidence assessment, and final judgments about risks are made

[133] Finally, the evidence criticality assessment can provide a sound basis for discussions about future work.

The evidence criticality matrix shows the criticality level for each evidence aspect underlying the analysis. This matrix includes the data and model processes applied in the methods used in the analysis. Referring to Section 2, examples of such data and model processes include the Marine Vessel Movement model, the RUSEMARIE model, and the considered earthquake-tsunami scenario. The evidence criticality matrix aims to support answering the following questions:

- What is evidence with low and high criticality?
- How good it is the study considering the critical evidence and their justifications?
- How much can the study be relied on for risk-informed decision-making and developing emergency preparedness and mitigation plans?

In sum, this evidence criticality matrix approach is used to understand the overall limitations of the results of the risk analysis.

The critical evidence matrix (Figure 11) is composed of the strength of evidence and its implications for the results, i.e. the sensitivity of the results to a specific aspect of the analysis process. The assessments are performed for each evidence element considering four levels of criticality. The evidence criticality level helps to identify important aspects of the system, i.e. data and parts of the models that significantly affect the results, but about which there is only weak evidence available. Low criticality evidence elements, represented by number 4, have a strong strength of knowledge and low implication in the results. On the other hand, high criticality evidence elements, represented by number 1, have a low strength of knowledge and high implication in the results. The intermediate levels consist of medium-high (2) and medium-low criticality (3), along with their respective ratings of strength of evidence and implications for the results.

The horizontal component of the critical evidence matrix is the strength of evidence, which consists of an analysis of each piece of evidence and its overall strength. This gives a general idea about how good the evidence elements are. Four evidence type categories are considered in this evidence strength. Data is the first category, which analyses the availability, reliability, and generalization of parameters, variables, and all

Table 11- Critical evidence matrix created to analyse the data empirical implication and the strength of the evidence.

Empirical Implication /importance	Weak	Medium	Strong
High	1	2	2
Medium	2	3	3
Low	3	3	4

Strength of Knowledge/Evidence

types of data sets. The second category is model processes, represented by calculations, GIS tools, and other computation methods, which are considered in terms of accuracy and prediction. Assumptions, the next category, indicate simplifications and generalizations made by the analyst in the application of data sets or model processes. Finally, in the fourth category, literature-based expert judgments concern the available level of information for decisions concerning the model design, and accounts for the references and other sources.

All these categories together support the final overall judgment related to the level of knowledge for a given aspect of the evidence, which are classified as weak (indicated in red), medium (indicated in amber), and strong (indicated in green). These four categories are rated by the analyst and are accompanied by a justification that describes the reason for using this data or model process, and sometimes how it was utilized in the research. More details about the categories and their definition are given in Appendix 3. The results of the evidence strength for the methods underlying the analyses will be presented in Section 4.4, with further details available in Appendix 5.

In this research, the importance/implication is defined as a qualitative empirical analysis of the elements and their observed degree of impacts on the results. During the creation and testing of the models developed in Section 3.2, tests and model checks were performed to observe what effect the use of different data, parameters, variables, and calculations have on each model's results. These tests and model checks provided a basis for the judgment about the importance of a given analysis aspect.

The importance table has one category and a justification for each evidence element. Moreover, its analysis outcomes are divided into three importance levels. Low importance (indicated in green) means that they only weakly affect the results and do not contribute significantly to bias the results. The data is not part of the main calculation (variable), it is used to prepare the data and in pre-model calculations, such as cleaning raw data, selecting information, importing data, joining tables, matching data sets, and categorizing results. The medium importance level (indicated in amber) means that the associated evidence element has a medium effect on the results, indirectly contributing to biases in the results. The data is not part of the main calculation (variable), but supports the main data or model step. It does not contribute directly to the final results but is a step before the main calculation. Finally, the high implication level (indicated in red) means that the analysis aspect strongly affects the results, contributing to bias and deviation of the results. The data is part of the main calculation (variable) or model step that contributes directly to the final results. The justification column is additional information to understand how much the results would change if the data or model process utilized is different. The importance table information cane be found on Appendix 3 and the results for the implication analysis on Appendix 6.

3.3 Methodology summary

Natural disasters affect coastal communities and the maritime transportation system in British Columbia. No earlier analysis of the impacts of earthquake and tsunami events on vessels is known to have been performed in this study area. This qualitative approach was exploratory because this project focuses on emergency preparedness risk management. This study uses a mix of positivism and interpretivism as underlying research philosophies to examine the data about the earthquake-tsunami event and to develop quantitative models to understand ship damage. The input data set was presented using study area details, earthquake and tsunami impacts, and details about ships.

The two models presented use geographical information methodology. The MVM model produces ship data such as origin and destination ports, travel times, trajectories, path, and route from the AIS database. This information is used in the RUSEMARIE model, which analyses the possibility of damage to a ship in case of an Earthquake-tsunami event using a threat geographical analysis. The purpose of this was to present the data and the methods that support the research questions, which aim asses ship damage and its consequences, providing a risk assessment approach. In the next chapter, the results generated by these tools will be presented, relating them to the research questions.

Chapter 4
Results

Estimating if a ship will be damaged and understanding the effects of earthquake-tsunami events on the availability of the fleet is essential for developing an emergency preparedness and response logistic plan for coastal communities. This study aims to understand, investigate, and analyze the extent to which marine vessels can be expected to be damaged in British Columbia following a major disaster. Based on the day-to-day operational patterns, a new methodology is proposed to estimate the probability of a vessel being damaged by a natural disaster. The methods use the Marine Vessel Movement (MVM) model and the RUSEMARIE model. These utilize GIS techniques, with results providing a basis for answering the four research questions provided in Section 1.2. This study uses a quantitative modeling approach to estimate the damage risk for different vessel groups and tsunami zone levels. To support quantification, it also applies a qualitative design to establish a knowledge base for the possible availability of ships in case of an earthquake-tsunami event.

The results chapter summarizes the main findings and observations using maps, tables, and graphs from outputs from the above-mentioned models. The demographic information related to ships and ports is presented first, followed by the results from the MVM model, in particular the vessel routes in the area. These intermediate results are presented in Sections 4.1 and 4.2. Then, using the routes in the RUSEMARIE model, the ship damage results are outlined, with the research questions answered in Section 4.3. Thereafter, uncertainties associated with the research outcomes are provided. The final Section presents a summary of the most important findings.

4.1 Vessels and ports in the case study

This analysis was performed using a group of 57 vessels selected according to the study case scenario information described in Section 3.1.1. The two ship types, composed of ferries and tugs-barges, were divided into 6 groups, as mentioned in Section 3.2.4. These groups' names and their features are presented in Table 12. Medium ferries have the more significant count of vessels, with ships comprising 40-100 containers capability. In comparison, small tug-barge combinations comprise the smallest group, with less than 100 tonnes of tug-pulling capability.

Table 12- Count of research vessels group categories

Vessel Group	Vessel Count	Size
Small Ferries	10	<40 containers
Medium Ferries	14	40-100 containers
Large Ferries	11	>100 containers
Small Tug-Barge Combination	4	<100 tonnes
Medium Tug-Barge Combination	11	100-200 tonnes
Large Tug-Barge Combination	7	>200 tonnes

Table 13 presents a picture of the vessel's length, breadth, and draught descriptive statistics to better understand the vessel group features according to size. Small ferries' average length is 69.69 meters, medium ferries are 123.15 meters, and large ferries are 149 meters. Although the tug-barges combination has average length groups ranging between 16.78 meters to 36.47 meters. The breadth of all six groups ranges from 6.25 meters to 27.38 meters, while draughts range from 2.64 meters to 5.36 meters.

Table 13- The six vessel groups and their size descriptive details

	Length (m)		**Breadth (m)**		**Draught (m)**	
Vessel Group	**μ**	**σ**	**μ**	**σ**	**μ**	**σ**
Small Ferries	68.69	17.30	17.23	1.94	3.62	0.93
Medium Ferries	123.15	22.81	23.89	2.21	5.26	1.21
Large Ferries	149.00	13.05	27.38	1.30	5.36	0.60

Small Tug-Barge Combination	16.78	2.27	6.25	0.19	2.64	0.21
Medium Tug-Barge Combination	23.57	1.82	7.15	0.86	3.78	0.50
Large Tug-Barge Combination	36.47	4.16	9.87	1.35	4.47	0.93

Combining the navigation and port damage information from Section 3.1.4, it is possible to examine the relation between port types versus damage, giving a better picture of the study case background information. The graph in Figure 22 shows this data, where it is possible to observe that the tugs-barges combination port type has a higher ports count, and most of them are undamaged. On the other hand, the ferry ports category contains more damaged ports than undamaged ones.

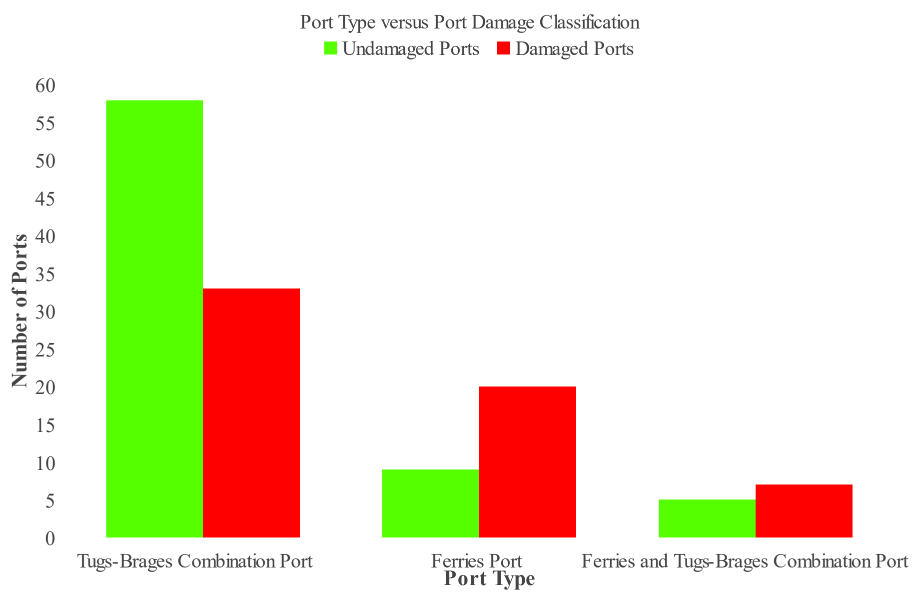

Figure 22- Descriptive data about the port type and their damage

The relation between damaged ports and terminals information with the tsunami zones for the studied Cascadia scenario is performed, with results shown in Figure 23. This illustrates an overview of port numbers in each region and the association with damage evidence. There are 99 ports located in Zone E, and 43 of these are damaged. While zone B has only 10 ports, none are damaged; whereas conversely, all the 10 ports in zone D are damaged. Finally, Zone C port consists of 11 ports, with 7 being damaged. These geographic distributions provide indications into the RUSEMARIE model, giving a better picture of the studied case scenario.

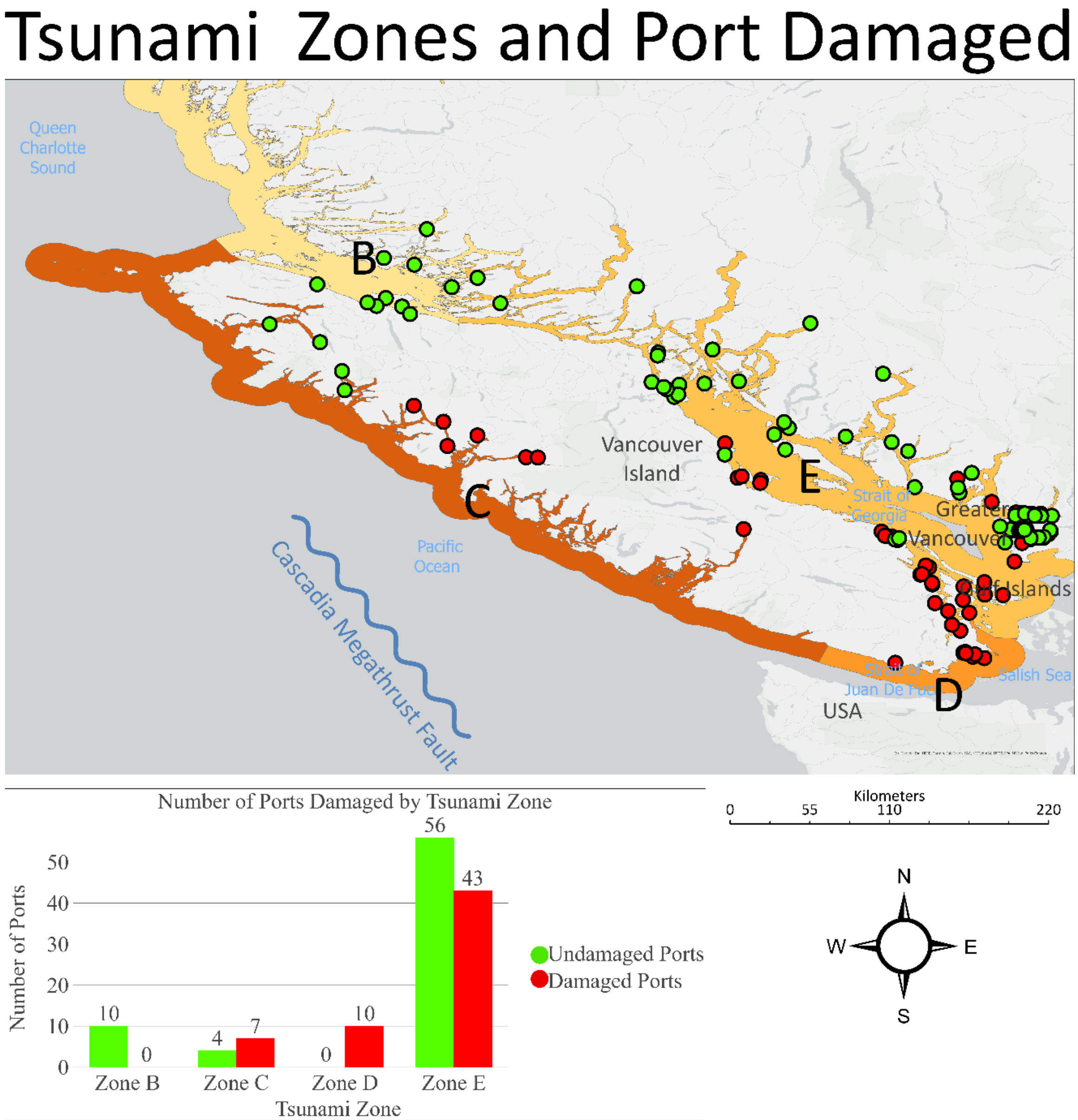

Figure 23- Data analyses of damaged port numbers according to each zone for the studies Cascadia scenario

4.2 Marine vessel movement

This section summarizes the main findings of the MVM model and lays down background information about vessels and port operations. These results are not directly related to the research questions but give a more comprehensive picture of navigation patterns, forming intermediate results. In addition, the dataset of final routes generated using the MVM model is used as input information for the RUSEMARIE model to identify the damage of ships according to their routes.

The following subsections will introduce an overview of AIS data, show outcomes of port usage according to the origin and destination details, and their relation with the Tsunami zones and Vancouver regions information. Moreover, the following section compresses the identified itineraries and routes according to vessel groups.

4.2.1 AIS descriptive

This subsection describes selected AIS sample dataset descriptive information to contextualize the point distribution of vessel movements in the area. The AIS sample data in Section 3.1.2 is represented in Figures 24 and 25. In total, 4,255,615 analyzed points, including 2,385,429 from ferries, and 1,870,186 from tug-barges. Figure 24 illustrates the point density for ferries according to the grids in 1,976 total grids. Of these, 1,776 contain no points, whereas 200 contain points. There are 6 ranges, the denser grid close to the Gulf Islands area and the less dense distributed along the Strait of Georgia and Strait of Juan de Fuca. It is also possible to observe denser points near some coastal areas, bigger than 22,164. By examining the data, it is found that it matches with port locations due to a significant number of points representing vessels being moored, anchored, or docked, i.e. vessels not engaged in navigation.

Figure 25 represents the density of the tug-barges also points in grid format, with 1,976 grids with 1,433 no points and 543 grids with different range densities. They are spread around the studied area, with the denser grids located south of the Strait of Georgia and Greater Vancouver. Most of the tug-barges docking locations are at Fraser River in the Greater Vancouver area

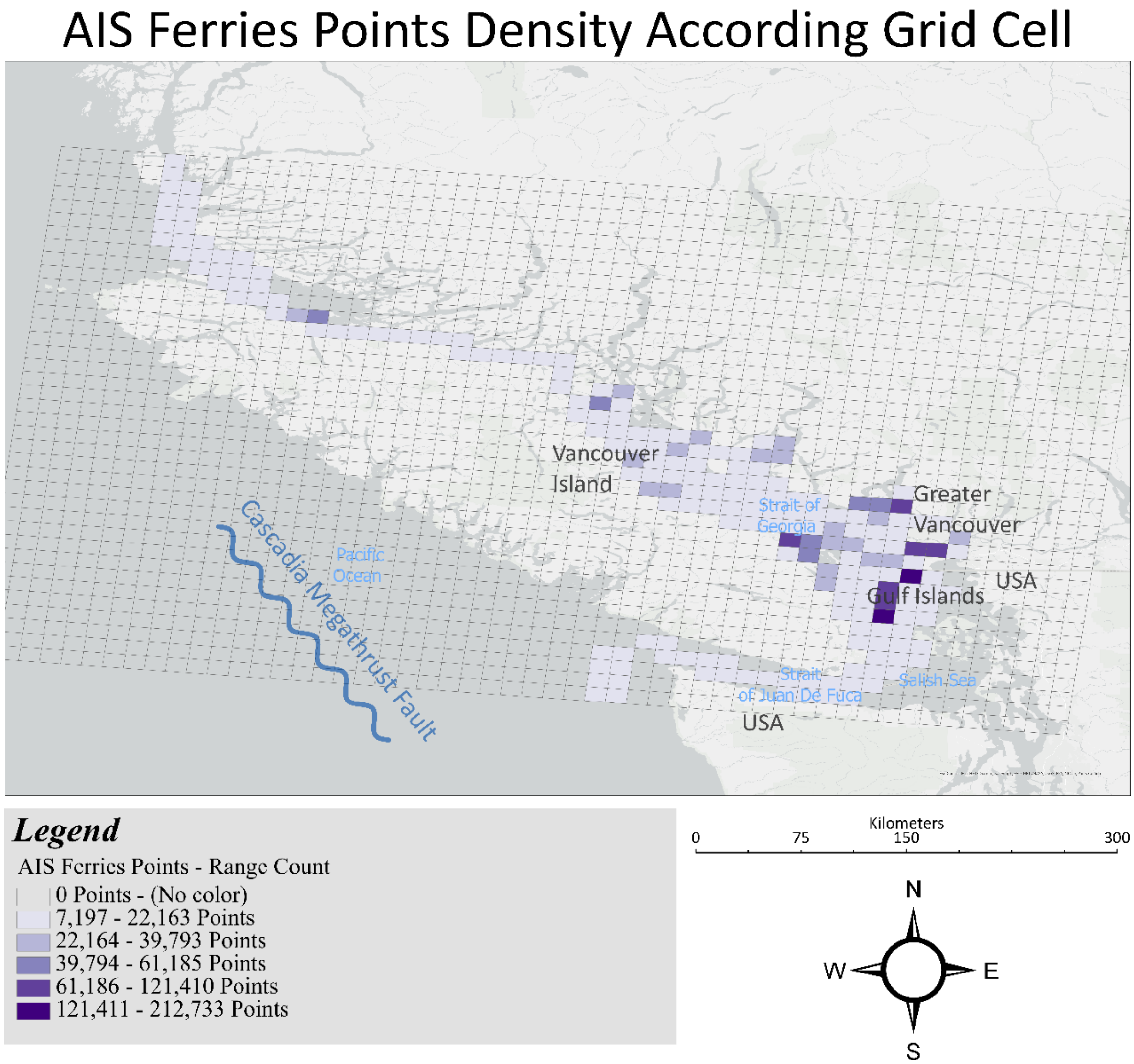

Figure 24- 15x15 km grids used to analyze the density of the AIS sample ferries points used in the research

These two figures illustrate two main issues. First, tug-barges have more points distributed around the studied area than ferries. Second, observing the ranges density of ferries is larger than tug-barges despite the same process step that generated natural breaks in data ranges for both maps. Hence, tug-barges reach a larger area but have less dense grids, whereas ferries navigate almost inclusively in the Strait of Georgia but with more dense grids.

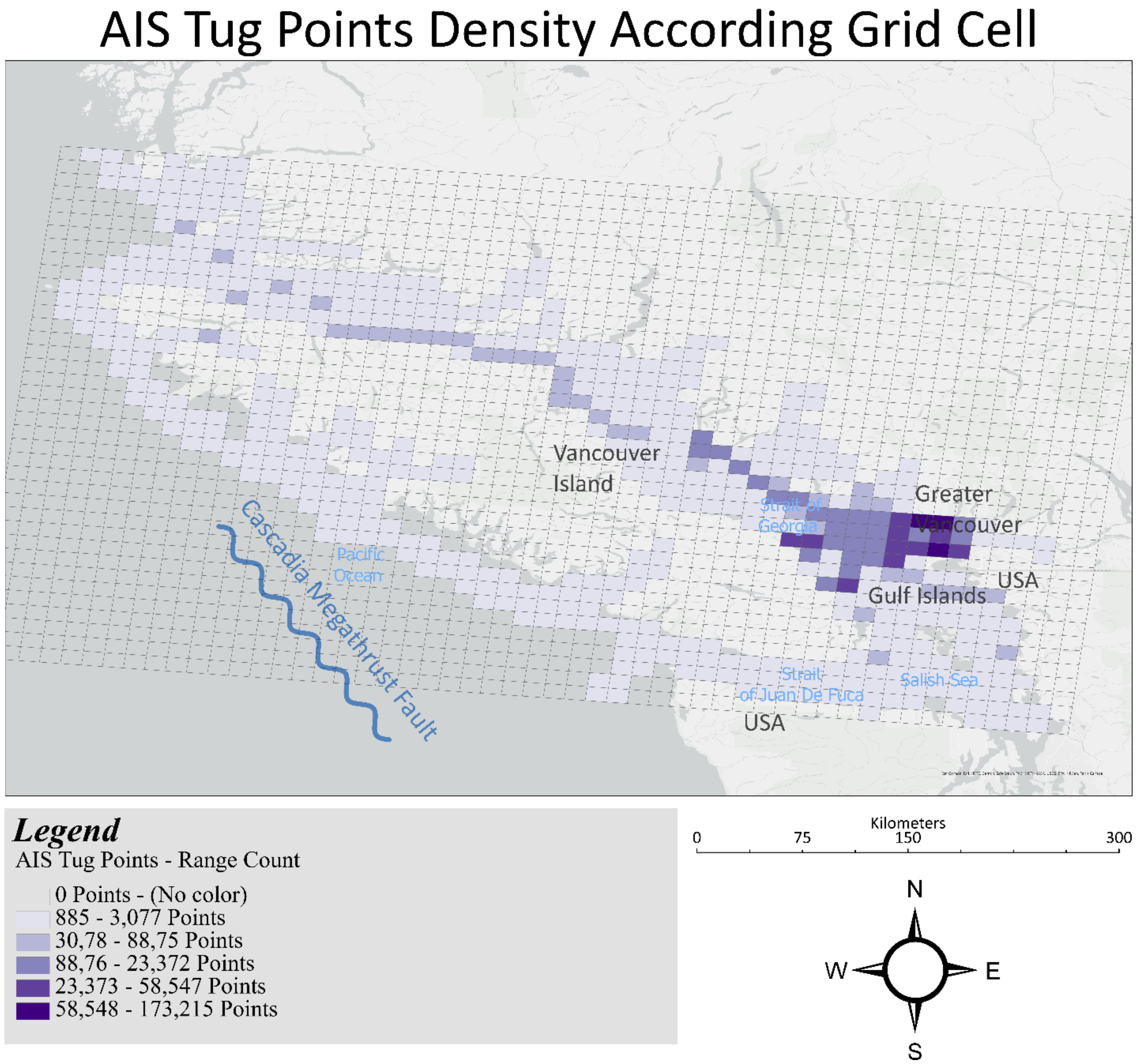

Figure 25- 15x15 km grids used to analyze the density of the AIS sample tug points used in the research.

Using the time stamp information from each point, it was also possible to analyze the points' time information from 2018, as represented in Figure 26. Ferries had more registered points during the Fall, especially in December, with almost 300,000 points. In comparison, January and February had less than half of the occurrences. Tug-barges also have almost the same patterns, but the difference is in July with fewer points compared with the same month for ferries.

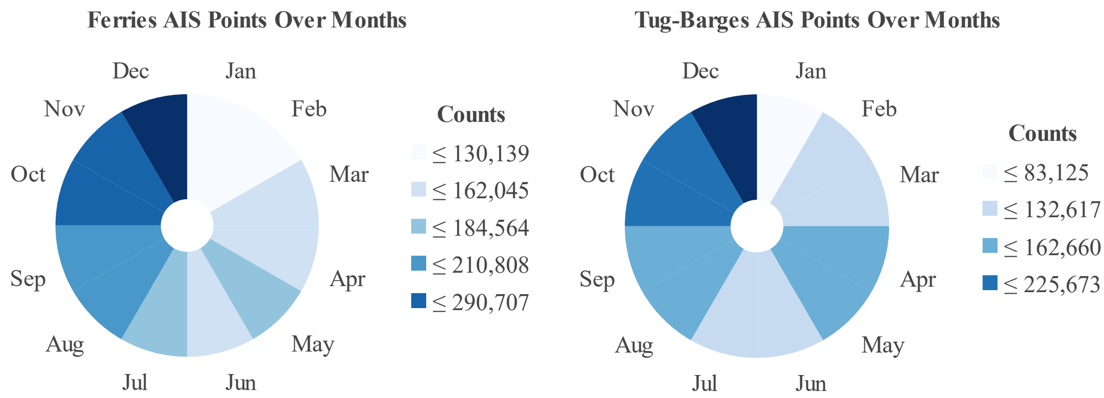

Figure 26 - Ferries and Tugs-barges summary point count for each month during 2018

4.2.2 Origin and destination ports

Based on the trajectory start and end points and the matching process with the ports and terminals information described in Section 3.2.1 and zone and region routes distribution, it was possible to identify the usage according to vessel numbers originating or departing from a specific port and the number of routes. This information is shown in Figure 27, where the usage is represented in the map where taller bars represent the most used ports, i.e. the pink origin and purple destination. Greater Vancouver has more origin ports, South Island has more destinations, and Gulf Island has a taller bar with a balance of ships arriving and departing.

In addition, the graph at the bottom of Figure 27 shows route ranges for port count according to origin and destination information. There are 11 ports not being used as origin for any of the routes, which means that these only appear as destinations. On the other hand, there are 58 ports not being used as a destination but only as an origin. The highlighted port count is that there are 52 ports used as origin and connected with 2 to 5 routes and 25 destination ports in the same connection route range. In addition, only 7 ports have more than 40 routes connecting as origin, and 9 as destination. This indicates the importance of a few ports in terms of the high number of routes departing or arriving at this small group of ports. These are located at South Island, Gulf Islands, and in the Greater Vancouver area.

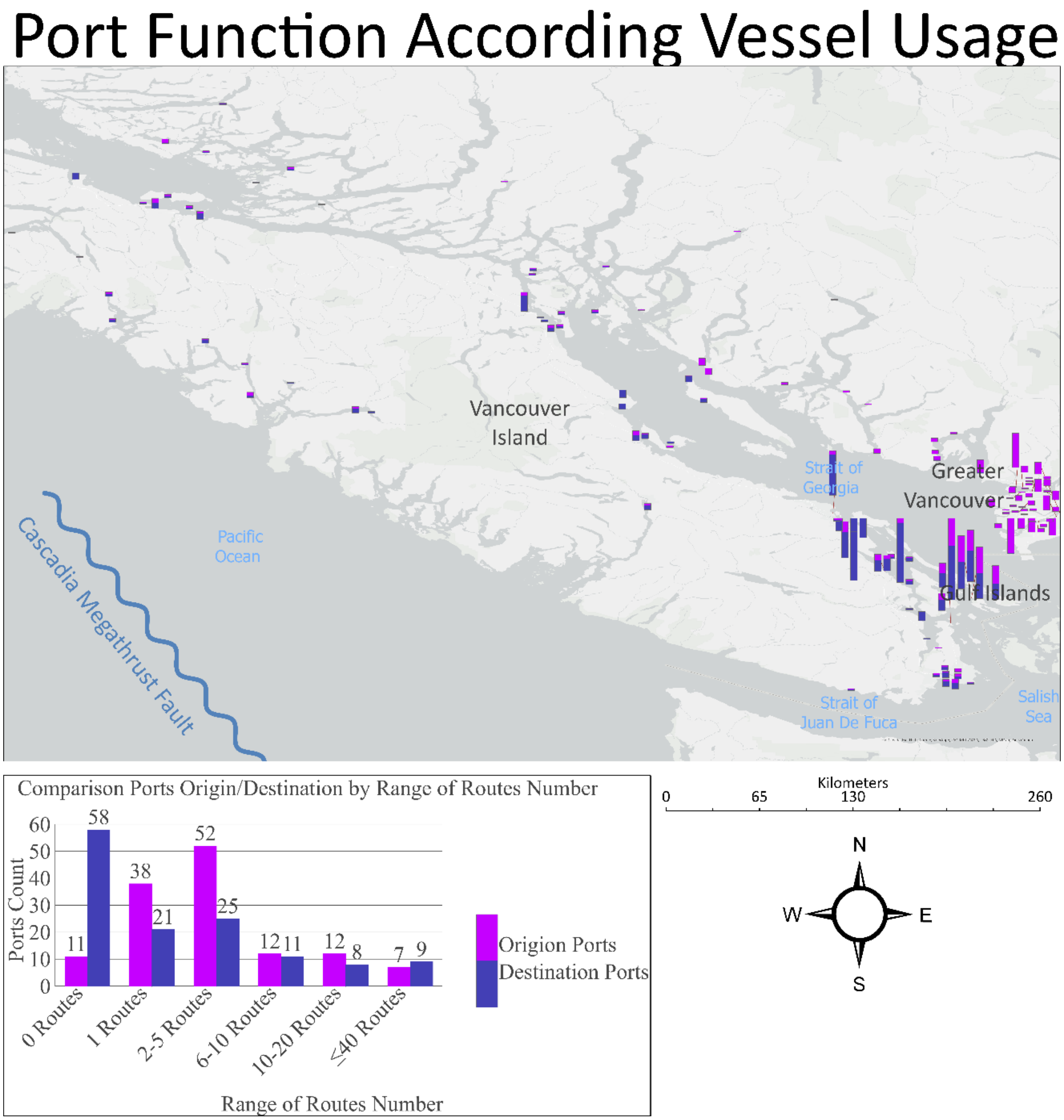

Figure 27 - Ports location and usage by ships, showing in purple origin and blue destination information and aiming to provide an overview of the most and less used ports. A graph was added at the bottom showing route range numbers with origin and destination ports

Based on the route information, matching port origin and destination with the Tsunami zone data, it was possible to analyze which zones contain more navigation activity, as can be observed in Figure 28. There are more than 471 routes with origin and destination in Zone E; the second most used originated in zone E and navigated to zone D with more than 71 routes. All zones have routes starting and ending in their zones. In addition, Zone E has more routes for both origin and destination and also is connected with all zones for both origin and destination.

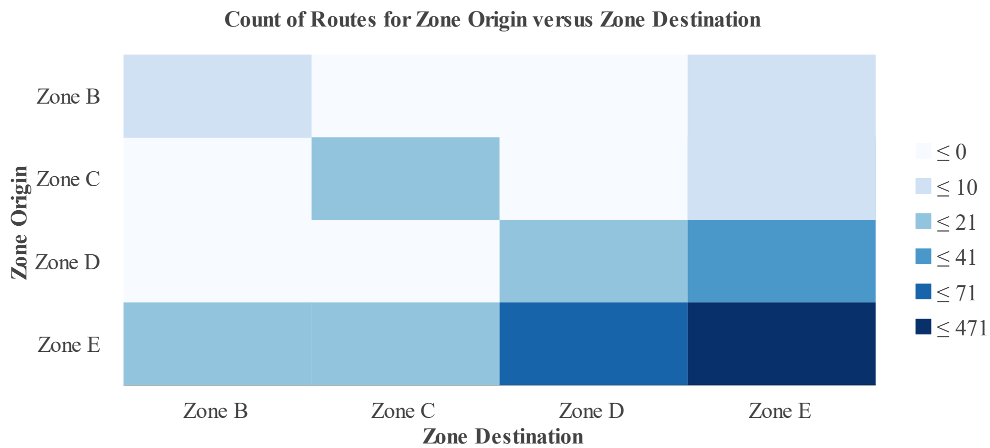

Figure 28- Analyses of the routes count between tsunami zones

The same analysis described above was also performed for the 6 studied zones and Greater Vancouver, as shown in Figure 29. Most routes start at the Greater Vancouver area and end at Central Island, with a total of more than 159. With more than 109 routes, the Greater Vancouver area connects with South Island, and with the same range Gulf Island with itself. In addition, Greater Vancouver is the origin region that connects with all other 6 regions with a different number of routes.

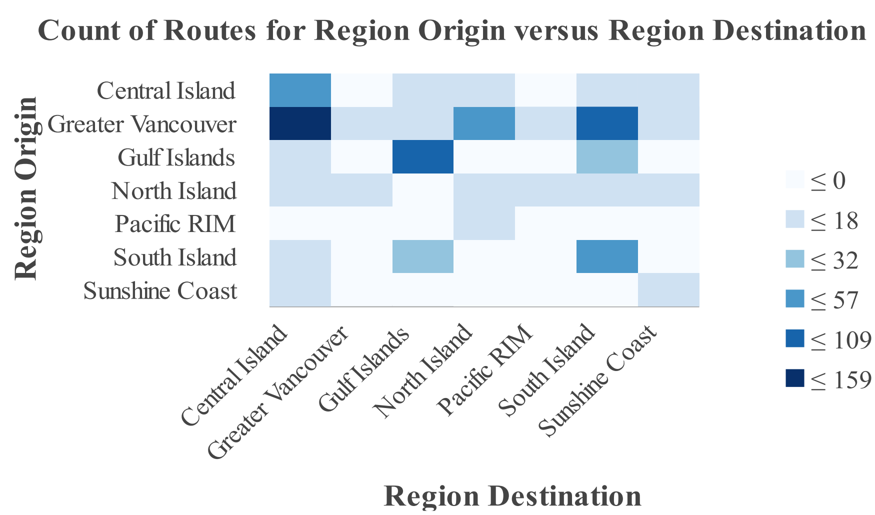

Figure 29 - Analyses of the routes count between regions

4.2.3 Itinerary and routes

This section analyses the results from the 57 studied vessels that resulted in 672 unique paths. In total, 329 itineraries were analyzed according to the 6 vessel type groups and the 4 tsunami zones. Figure 30 illustrates the distribution of routes according to the vessel groups. Medium-sized tug-barges totalize 217 routes, being the larger count, with in second place medium ferries with 169 routes. On the other hand, large ferries represent a smaller group with 47 routes.

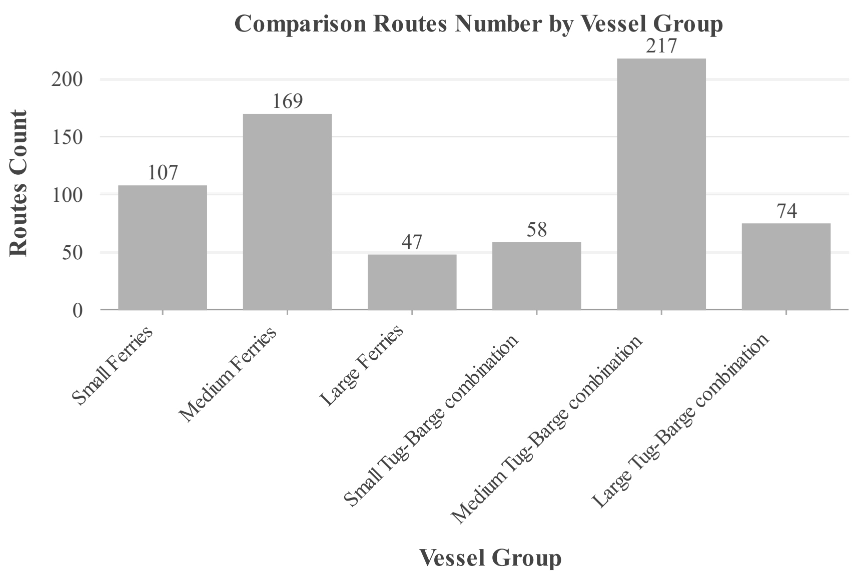

Figure 30 – Number of routes by vessel group.

Analyzing the 672 found routes according to the itinerary means independent of specific vessel routes. In total, 329 itineraries are most utilized and composed of one route navigated by one vessel. In comparison, 33 itineraries have 5 to 7 routes composing them, and 5 itineraries contain 8 to 11 grouped routes.

The navigation patterns of the vessel groups for the combinations of the origin and destination zones are presented below in Figure 32. Medium vessel types operated at zone E, being the medium ferries also mostly operating between Zone E and D. The only vessel type that operates between Zone C and Zone E combination is medium tug-barges.

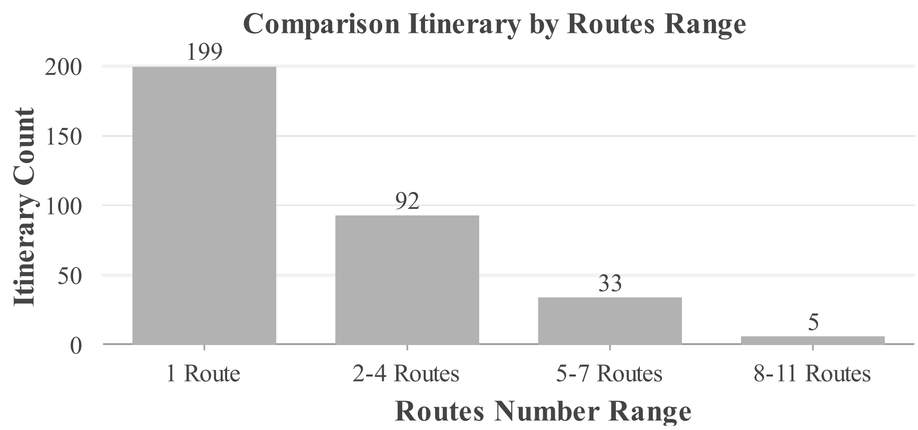

Figure 31- This graph informs route ranges compared with itinerary count

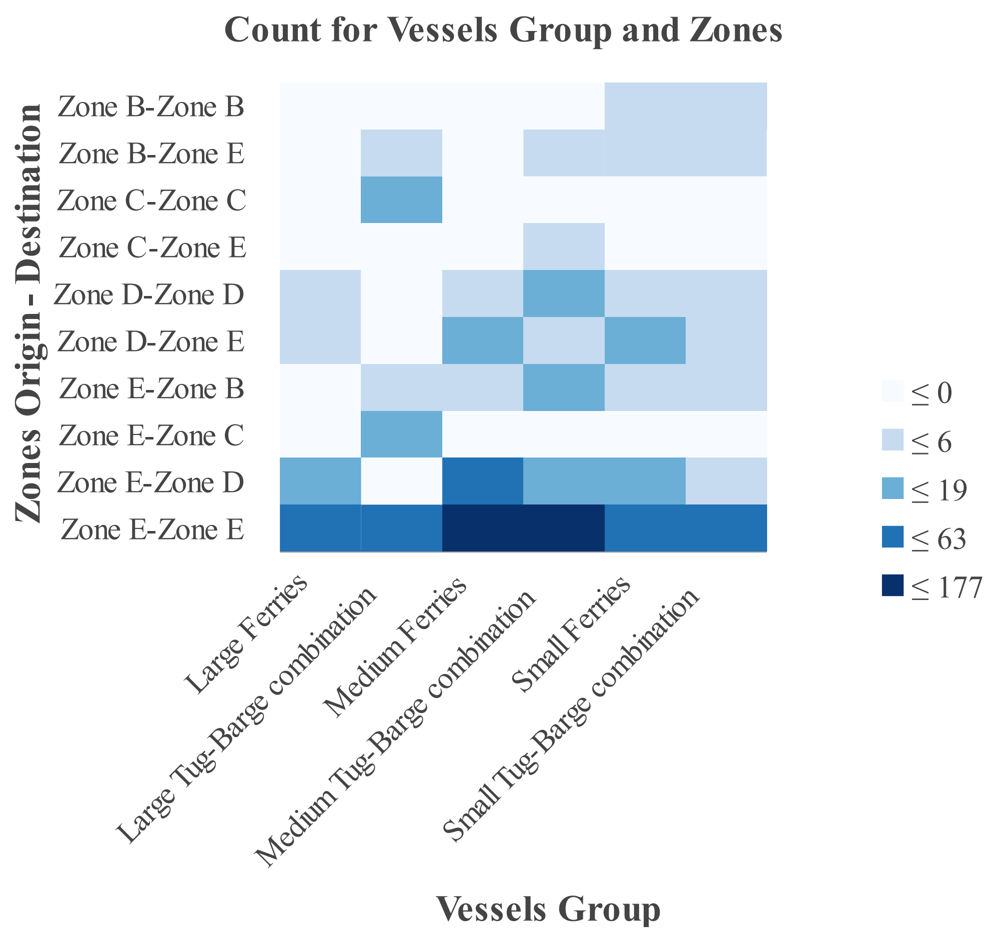

Figure 32 - Comparing each vessel group with the location of the origin and destination ports according to the zones

In the final step of the AIS analyses, the central routes were created to represent the navigation patterns of the studied vessel. Figure 33 shows ferries routes where small and medium ferries navigate in the Strait of Georgia, while large ferries patterns are concentrated South of Vancouver, including the Gulf Islands. Figure 34 shows tug-barges routes where small and medium tugs mostly travel at the Strait of Georgia, while large tugs navigate in the open sea on the Pacific Ocean. Due to their power; they are also called ocean tugs.

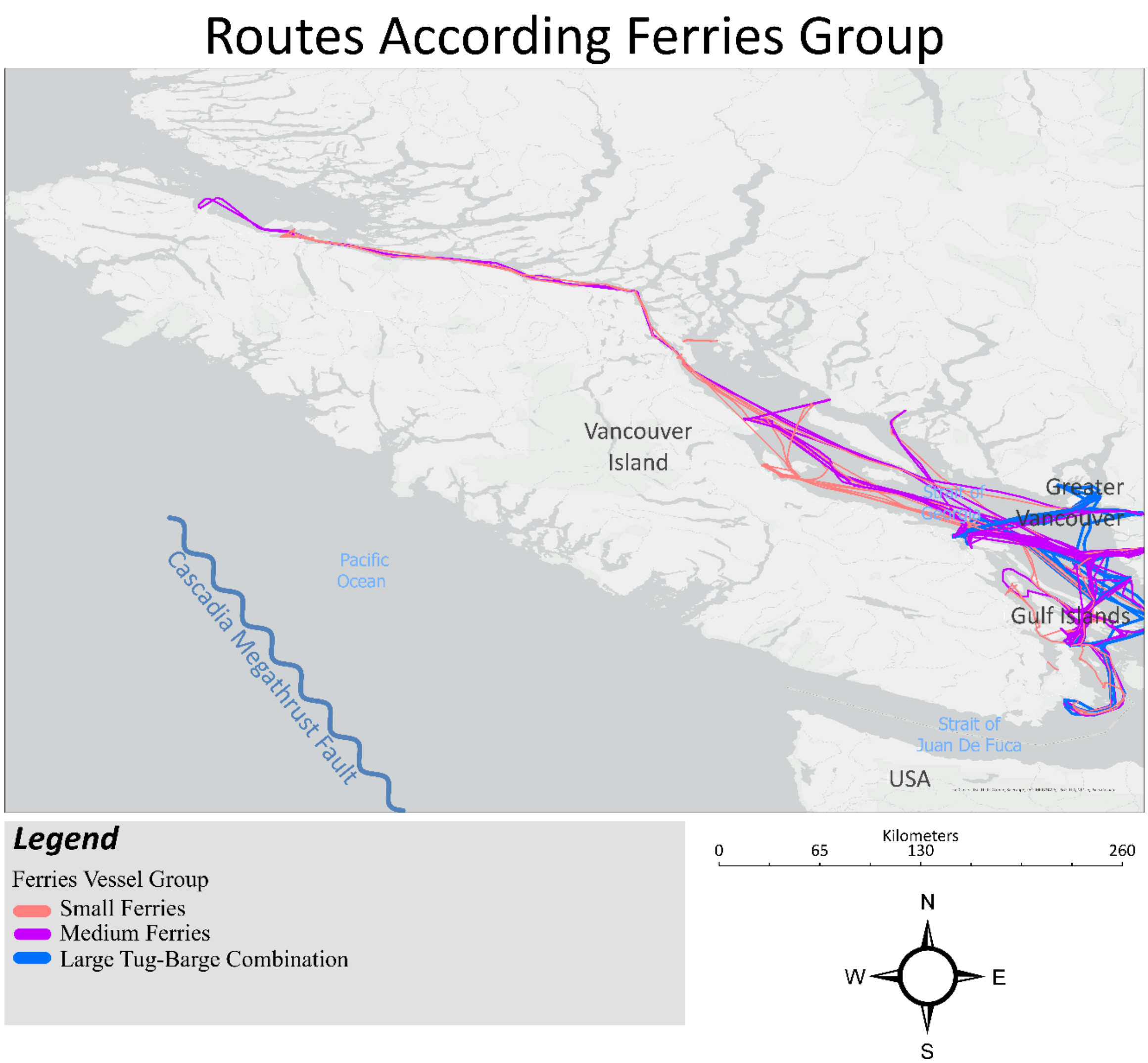

Figure 33 - The centreline path from ferries generated for each vessel according to their routes in a specific itinerary

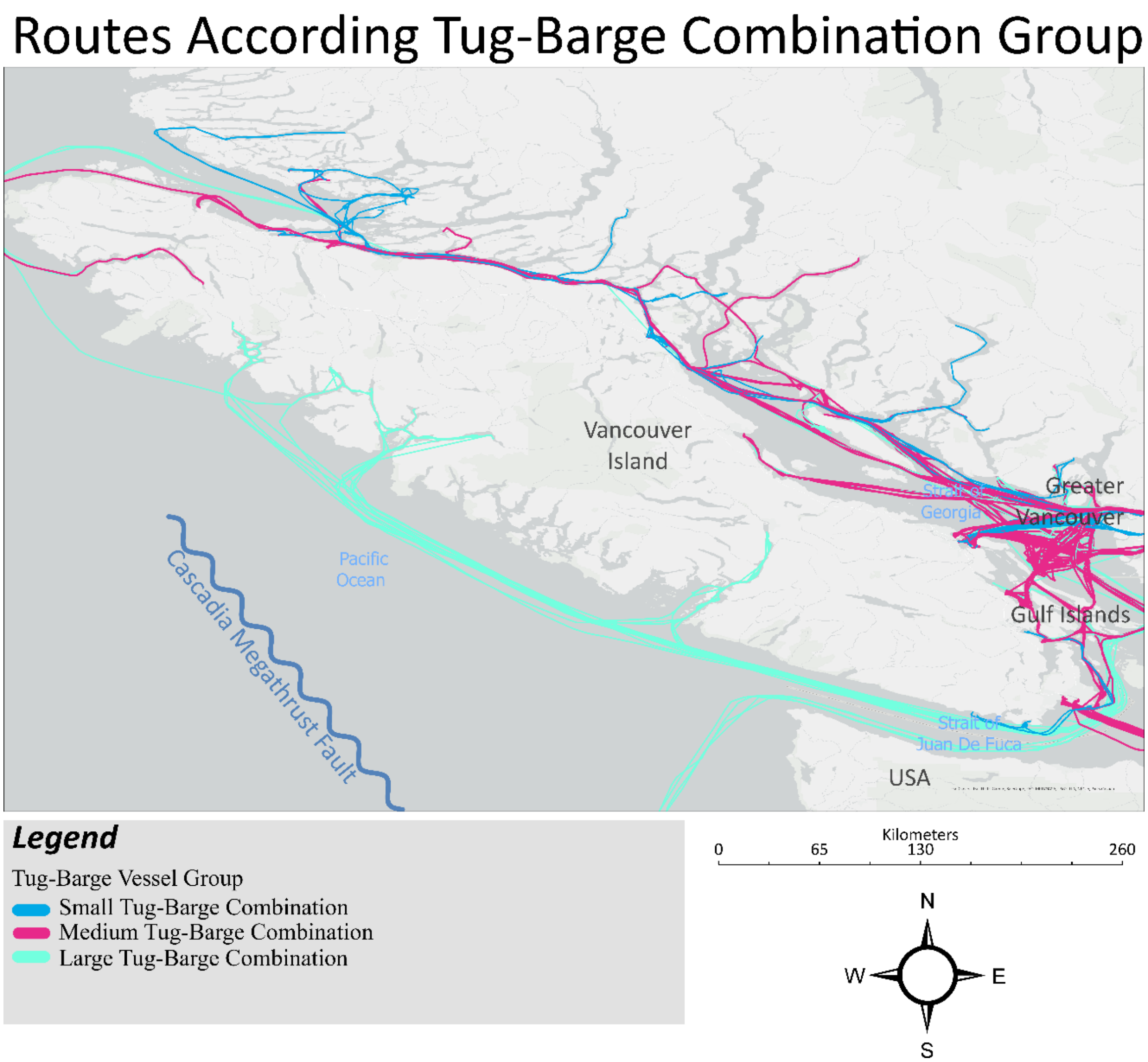

Figure 34 - The centreline path from tug-barges generated for each vessel according to their routes in a specific itinerary

4.3 RUSEMARIE model results

The following sections provide the results and information necessary to answer the research questions, aimed to understand, investigate, and analyze the damaged marine vessels. This is done using the developed RUSEMARIE model and the centerline paths obtained from the MVM model, applying it to the studied case. The Cascadia worst-case scenario for British Columbia was used in the RUSEMARIE model to answer the four research questions.

This section illustrates the results of the model procedures. First, the output of the RUSEMARIE model is presented, followed by descriptive statistics analyses. The damage probability results are first provided on the entire vessel population level, followed by results for the different ship type groups, answering RQ1 and RQ2. Then, the damage probability according to grid cells and routes are mapped out, supporting RQ3. An analysis of damage according to Tsunami zones and Vancouver regions is thereafter presented, answering RQ4. This section represents the qualitative aspect of the research. Then the critical evidence results are described, comprising the qualitative analyses component of this study. A summary of the main findings is presented in Section 4.5.

Figure 35 and 36 shows the outcome of the RUSEMARIE model, where 111,141 points from 672 trajectories were analyzed according to the model variables, resulting in damage or no damage status. As described in Section 4.2, the ferry data are concentrated between Vancouver Island and Greater Vancouver, illustrated in Figure 35. The damage points are concentrated South of Vancouver Island and around the Gulf Islands. While tug-barges combination points data, Figure 36, are distributed around the studied region, also having damage points south of Vancouver Island. In addition, there are a considerable number of damage points facing the Pacific Ocean, located in open sea areas. There are 26,425 ferries points, with 11,924 of them assessed as damaged and 84,716 tug-barges points, with 47,143 assessed as damaged. The following subsections will present statistical results derived from these points-based results.

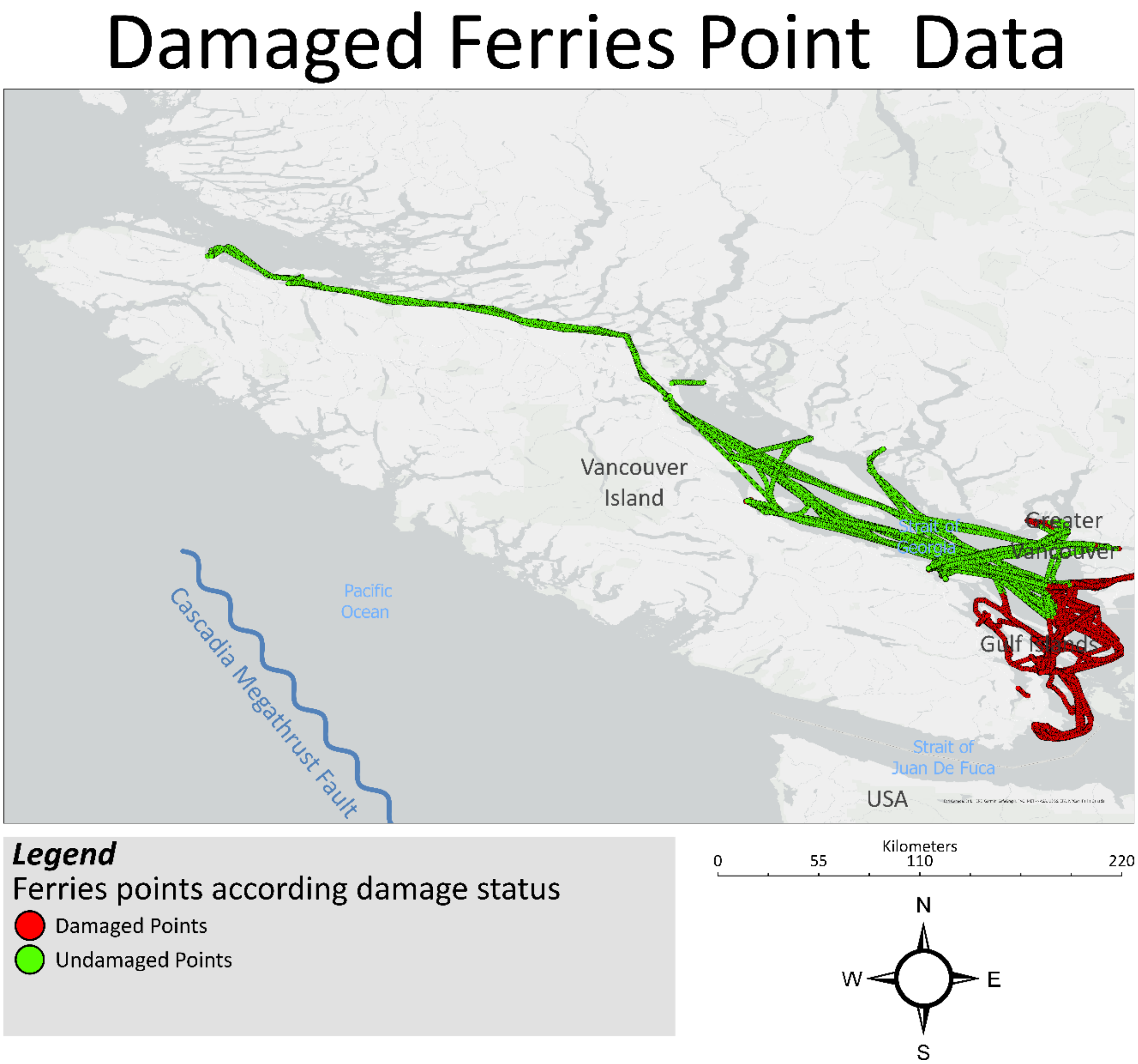

Figure 35 – Ferries points from the centreline generated each 500m applied to the RUSEMARIE model, resulting in assessment of damage status of points

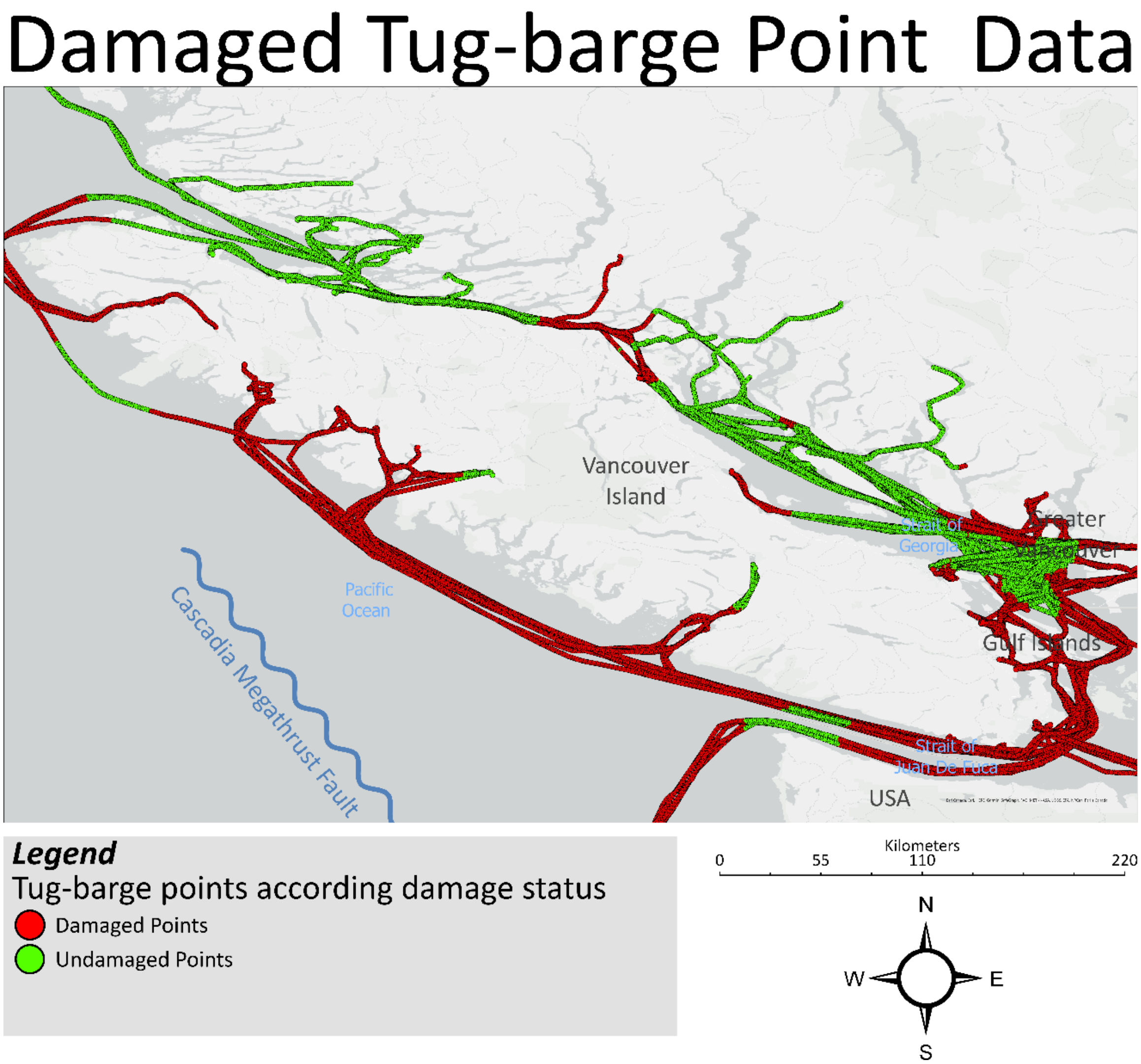

Figure 36 - Tug-barges points from the centreline generated each 500m applied to the RUSEMARIE model, resulting in assessment of damage status of points

4.3.1 Ship availability probability by group

This subsection provides vessel probability damage analyses of the results of the damage points resulting from the RUSEMARIE model, presented in Figure 35 and 36. The vessel damage probability results are independent of the routes; in other words, these consider all damage points of a specific ship no matter the route. All the damage points were normalized, i.e. divided by the total number of points being performed for each ship. This information is used as a basis to answer the first research question: How many ships will be available to support humanitarian supply chain operations in Vancouver Island coastal area? Appendix 4 presents a summary table with all 57 vessels' damages probabilities.

Figure 37 presents the summary information of all ship damage probabilities, for different probability ranges. As can be observed, there are 6 ships with a damage probability between 0-5%, with only 1 ship having a 0% probability of being damaged. The 25-50 % damage probability range has the larger proportion with 22 ships, followed by 50-70% damage probability range, which includes 14 ships. The highest damage probability range, 95-100%, contains 8 ships, whereas there are 7 vessels with 100% damage probability. The expected number of unavailable ships according to the minimum and maximum probabilities scales is According to the minimum and maximum probabilities scales, the expected number of unavailable ships ranges from 23 ships for the minimum probability scale to 34 ships for the maximum probability scale of unavailable vessels.

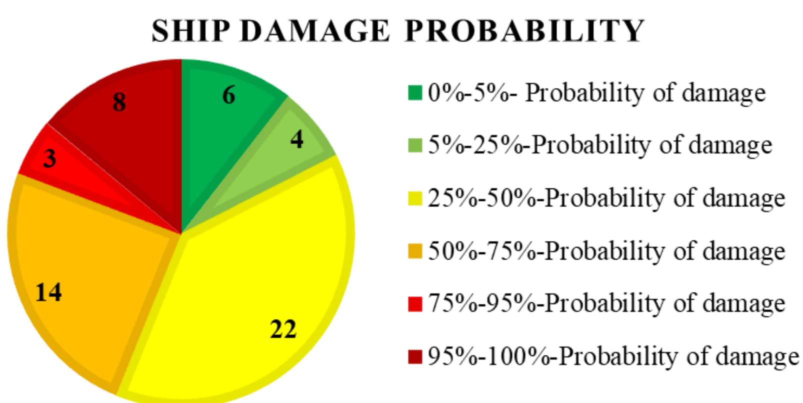

Figure 37 - Pie chart of all vessel damage results according to 6 damage probability ranges

To better understand the damage probability and the possible impacts on different vessel groups, the damage probabilities were divided into vessel group types for ferries and tug-barges combinations, with results presented in Figures 38 and 39, respectively. Using this information as a basis, the second research question can be answered: What is the relation between ships groups sizes and damage probability considering Vancouver Island maritime logistic operations? Small ferries have the same count of vessel damage in the 25-50% and 95-100% damage probability ranges, medium ferries' have a larger damage count in the 25-50% range, and large ferries also have a larger count in the same damage probability range. For the tug-barges combination, small tug damage probability ranges are between 5-50%, medium tugs' larger damage probability count is 25-50%, and large ferries' larger count range is 50-75%. Comparing ferries and tugs figures and information, it can be seen that ferries probability damage results are more spread between the 6 ranges while tug-barges were concentrated in a few damage probability ranges.

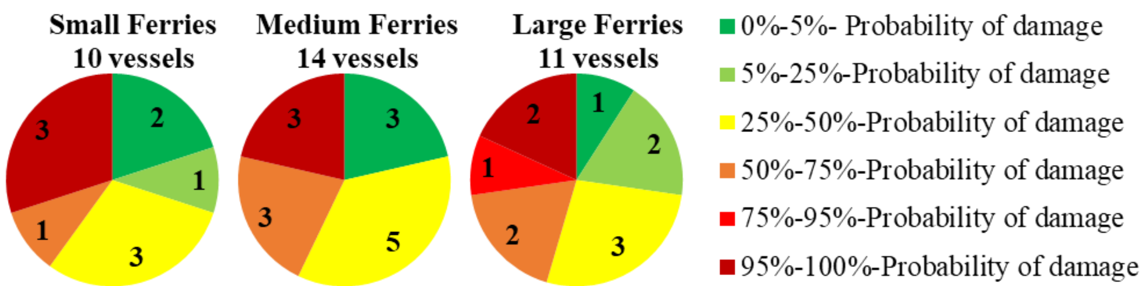

Figure 38 - Pie chart for ferries vessels damage results by group according to 6 damage probability ranges

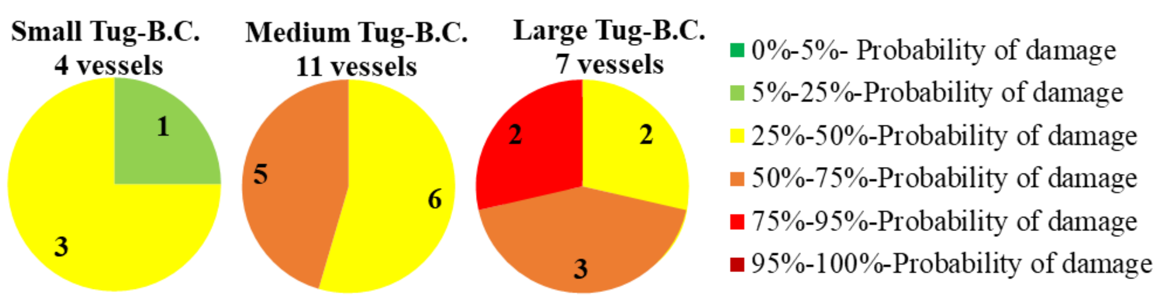

Figure 39 - Pie chart for tug-barges combination vessels damage results by group according to 6 damage probability ranges

As vessel groups for ferries and tugs have different sizes, an analysis of proportionality and damage probability is proposed in Figure 40. There are only ferries-type vessels for the 0-5% damage probability range, and 5-25% small tug-barges are a larger proportion. The 25-50% probability damage range has all vessel groups, with the small tug-barges combinations being the largest, followed by medium barges. The 50-75% damage range has medium and large tug barges with more expressive proportions. The 75-95% range has only large ferries and tugs but tugs with a bigger proportion. In the last range, 95-100%, there is only the ferries group, with small ferries being the larger group.

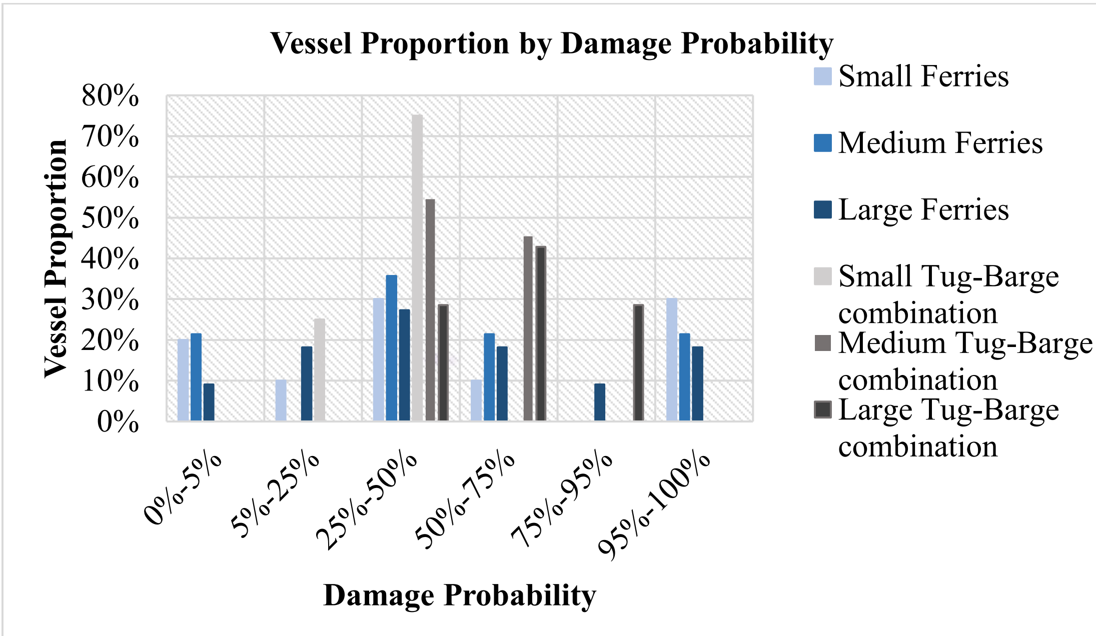

Figure 40 - Comparison between damage probability levels and vessel groups

4.3.4 Maps of dangerous navigational areas

This subsection will present the point's damage probability according to the grid cells shown in Section 3.2.4. These analyses are useful to identify dangerous areas independent of ship type analyses. They support the answer to the third research question: Which regions of Vancouver Island will likely be exposed to a reduced ship capacity for emergency logistics deliveries due to ships not being available in the immediate disaster response phase? The 1,976 grid cells were overlaid with damage points from RUSEMARIE results presented in Figures 35 and 36. It was possible to identify 1,539 empty cells, that is, no data; cells with points but no damage, totalizing 167 cells. Then, for the cells with damage points, comprising 270 cells, the damage probability was calculated and classified according to the 6 damage ranges. Figure 41 is the representation of the processing for all studied fleets. There are 4 cells with a damage range of 0-5%, 15 with 5-25%, 11 with 25-50%, 10 with 50-75%, 18 with 75-95%, and 212 with 95-100%. Most of the grids with high damage probability are concentrated between Vancouver Island and the North of Greater Vancouver. Identifying sea evacuation from the grids is an interesting finding to be discussed later.

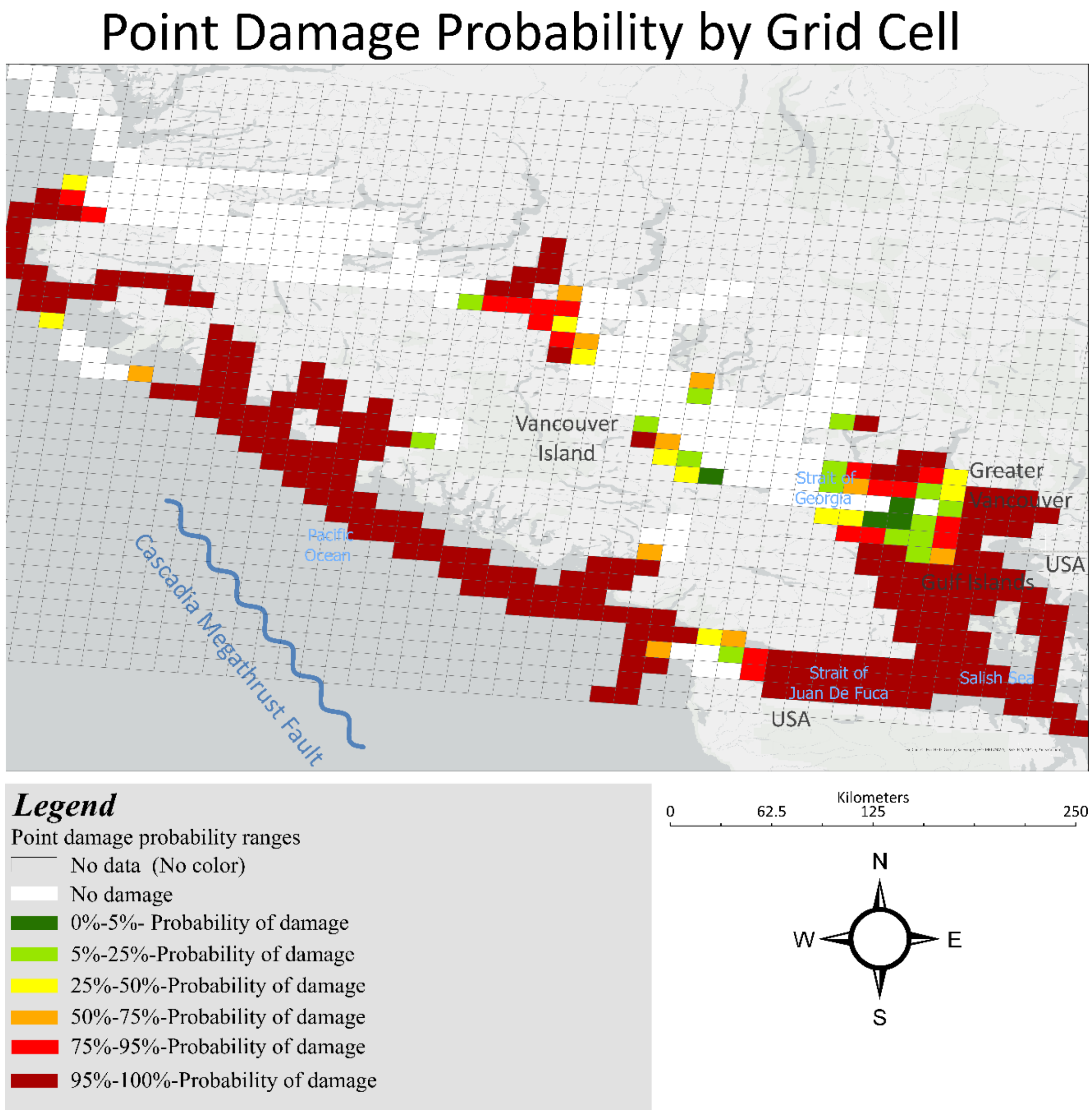

Figure 41 - Damage probability of all points from Figure 35 and 36, analyzed by each grid cell, showing the areas with higher damage probability

Using Figures 42 and 43, it is possible to identify the dangerous and evacuation/safe areas according to the ferries and tug types and their navigation patterns. Ferries with dangerous grid cells, with 95-100% damage probability, are around the Gulf Island and South of Vancouver Island. It is possible to observe some grids to be used as evacuation areas, where no damage or at least 5-25% damage probability were identified, being them really close to damaged ones. Using the depth map, shown in Figure 14, and comparing that with Figure 41, this grid can likely be considered safe due to the depth of these sea areas. Tug-barges follow the same analyses for this Gulf Island region. However, looking at the Pacific Ocean area and the damage grids in Figure 43, there are also some evacuation areas, especially at the beginning of the Strait of Juan De Fuca and North of Vancouver Island facing the Pacific Ocean. These results are important and can help support developing vessel safety guidelines for emergency preparedness.

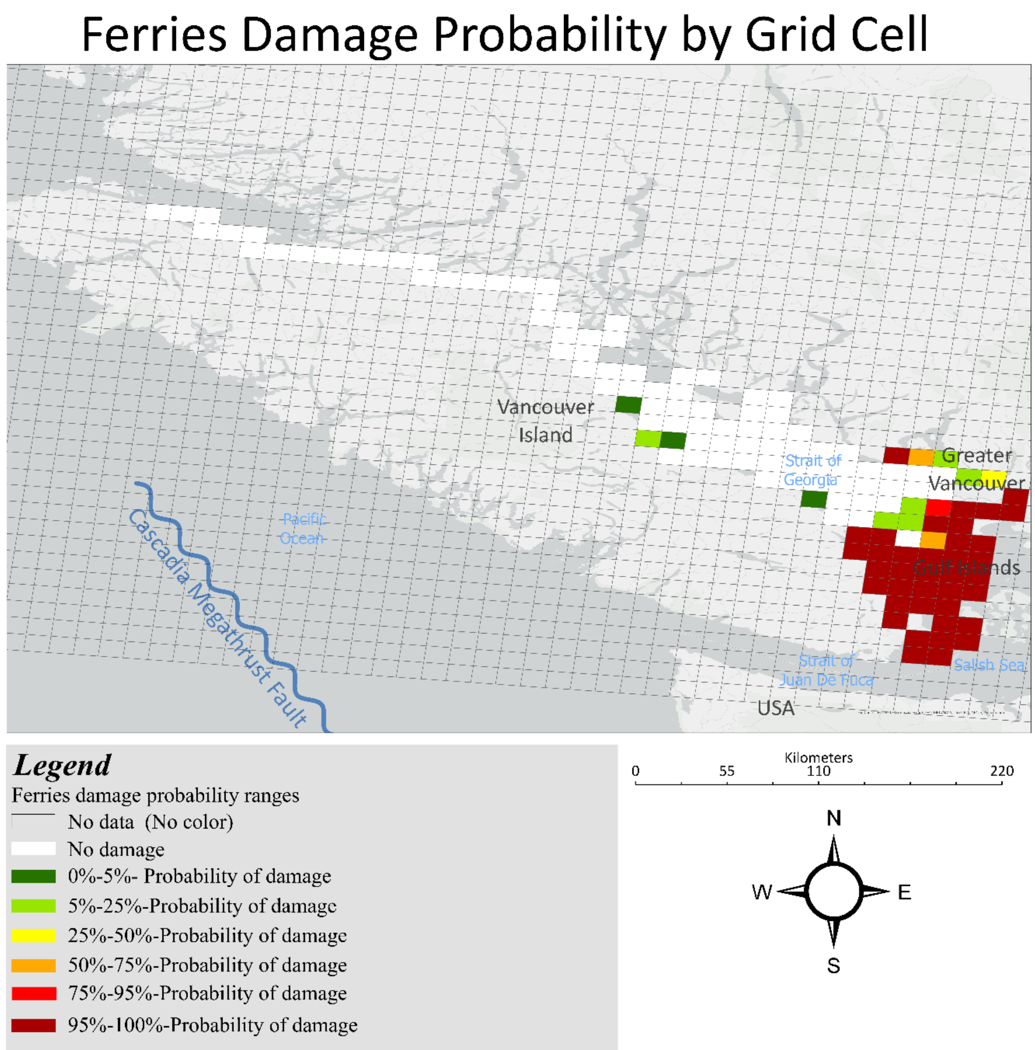

Figure 42 - Damage probability of ferries points from Figure 35, analyzed by each grid cell, showing the areas with higher damage probability

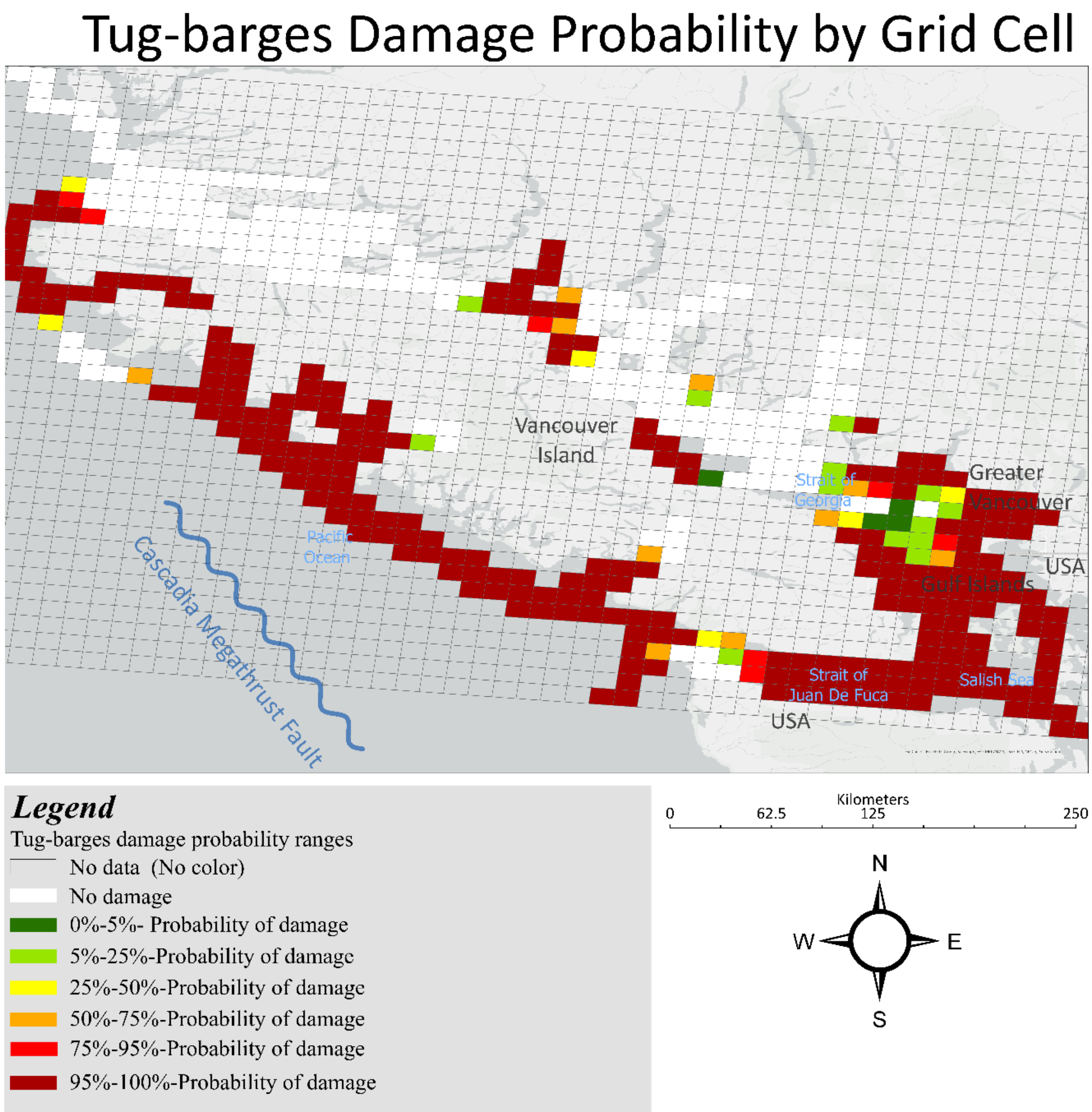

Figure 43 -Damage probability of tug-barges points from Figure 36, analyzed by each grid cell, showing the areas of higher damage probability

4.3.3 Routes and ships availability maps

The last two sections present the damage according to each vessel and grid cell. However, here, the damage analyses are performed for each route presented in Section 4.2.4; i.e. the damage probability calculation is specific for each vessel's route. The damage probability calculation considers damage points on that route by the total number of points, and then groups the information according to the 6 probability ranges. The analyses of routes will establish the information to the third research question: Which regions of Vancouver Island will likely be exposed to a reduced ship capacity for emergency logistics deliveries due to ships not being available in the immediate disaster response phase? Figure 44 shows the damage for all the vessel fleets, where the routes with highest damage probabilities, with values higher than 75%, are located in the Pacific Ocean and South of

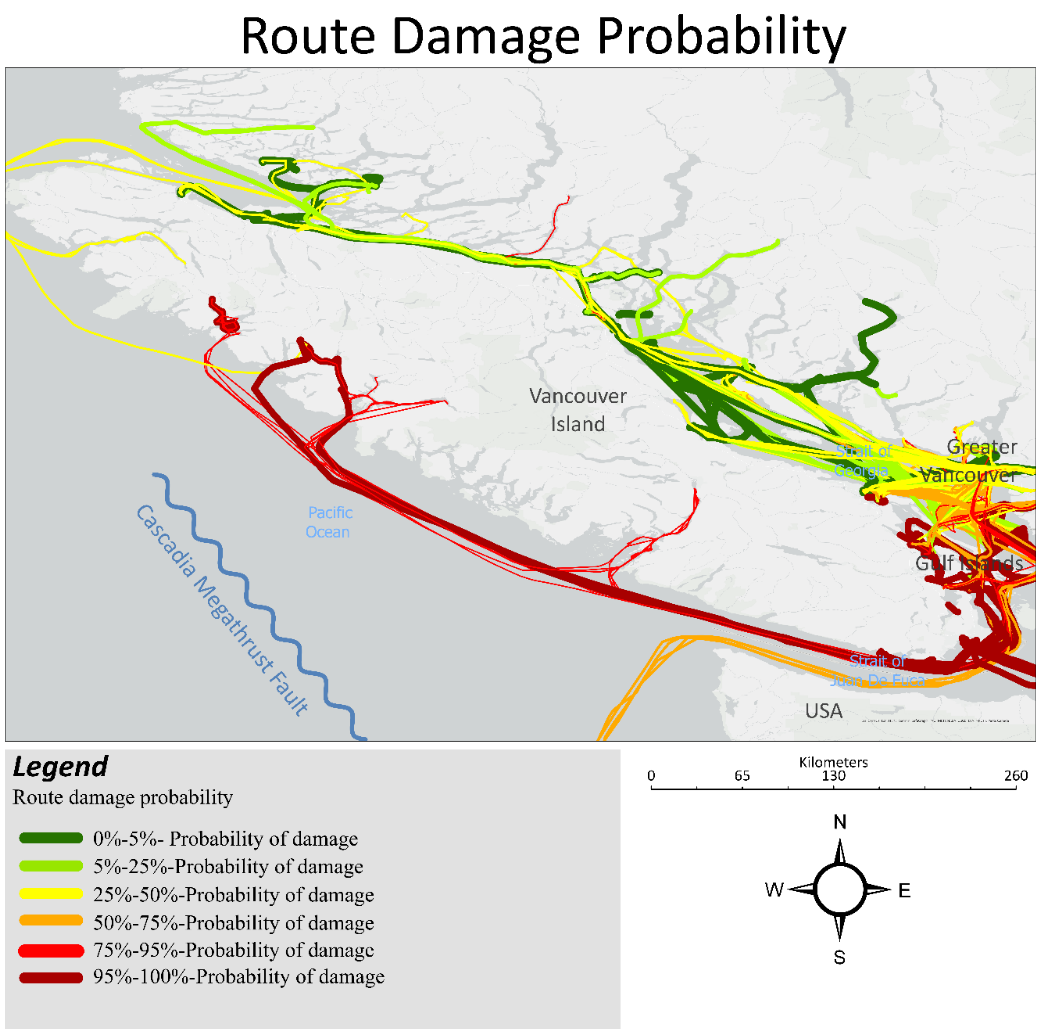

Figure 44- Damage probability ranges according to points damage probability calculation in each path

Vancouver Island. On the other hand, the safety routes, with less than 50% damage probability are located North of the Strait of Georgia.

Using these data and splitting the information according to the 6 vessel groups, it is possible to investigate whether vessel type and size make a difference in route damage. Figures 45 to 50 show data according to vessel groups. Small ferries that navigate around Gulf Island have a high damage probability, similar to medium and large ferries. The biggest difference is that small ferries are safer, navigating Greater Vancouver and Vancouver Island upper at Central Island region. The small tug-barges vessels have low damage probabilities if they navigate in the Strait of Georgia, while medium and large tugs will have more damaged routes, especially south and west. Particularly large tugs with longer routes, sometimes starting in a less damaged area and navigating to dangerous areas. As there are more damage points on these long routes, this leads to a route with a higher than 75% probability of damage. Alternatively, if routes have fewer damage points, even though part of the route is in a dangerous area, this can lead to lower ranges of damage probability, such as the 25-50% range.

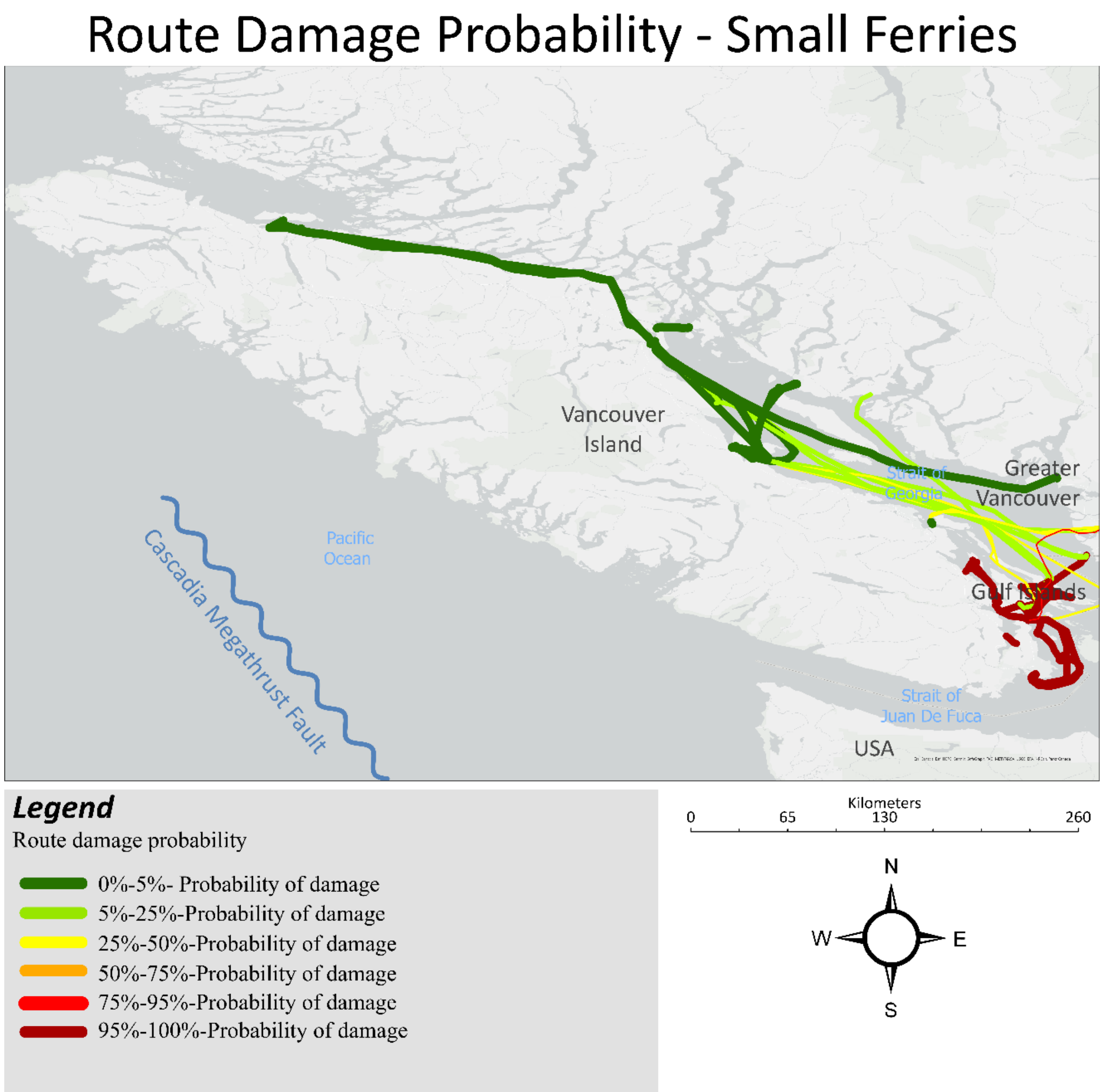

Figure 45 -Damage probability ranges according to small ferry points damage probability calculation in each path

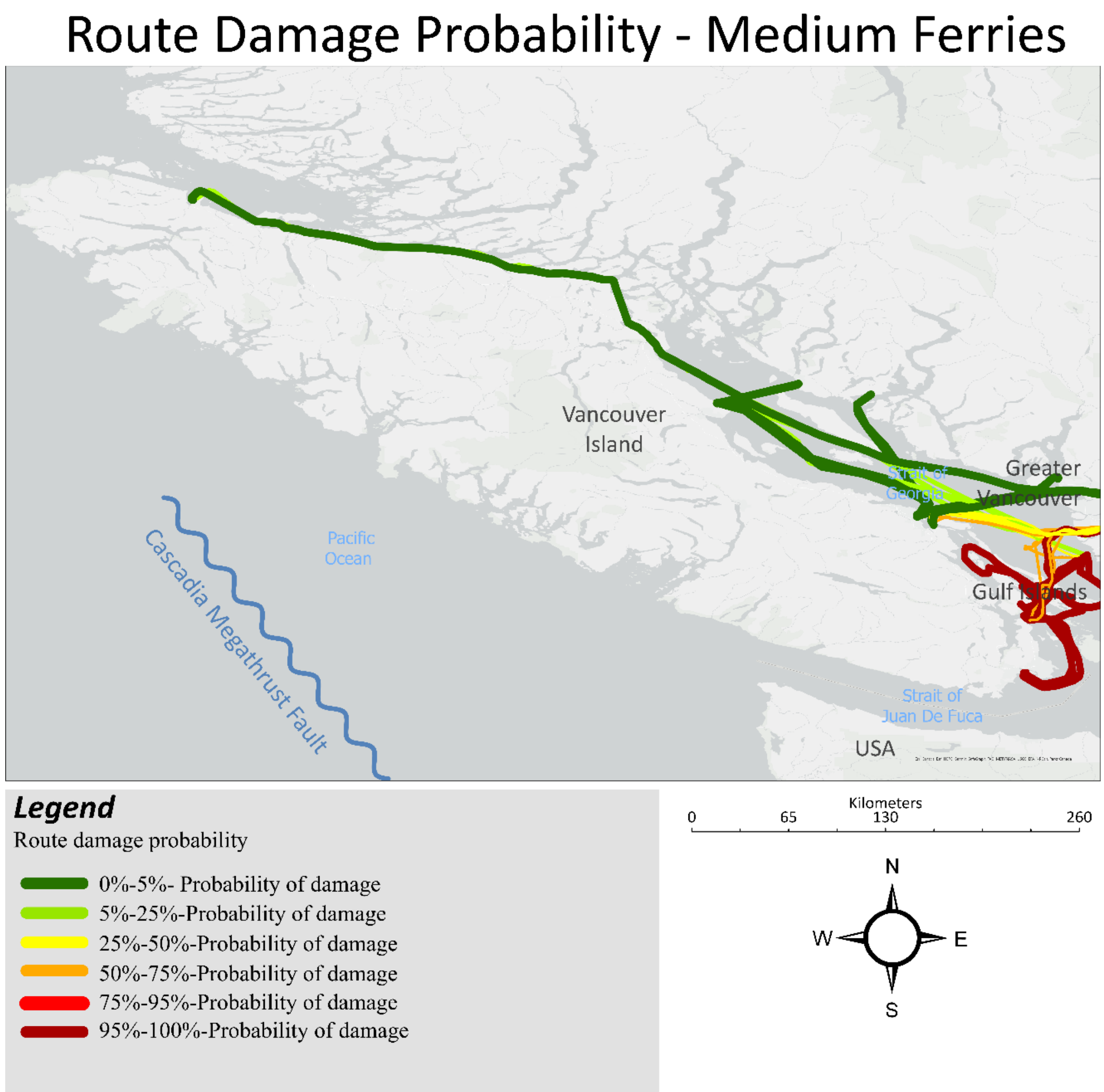

Figure 46 - Damage probability ranges according to medium ferry points damage probability calculation in each path

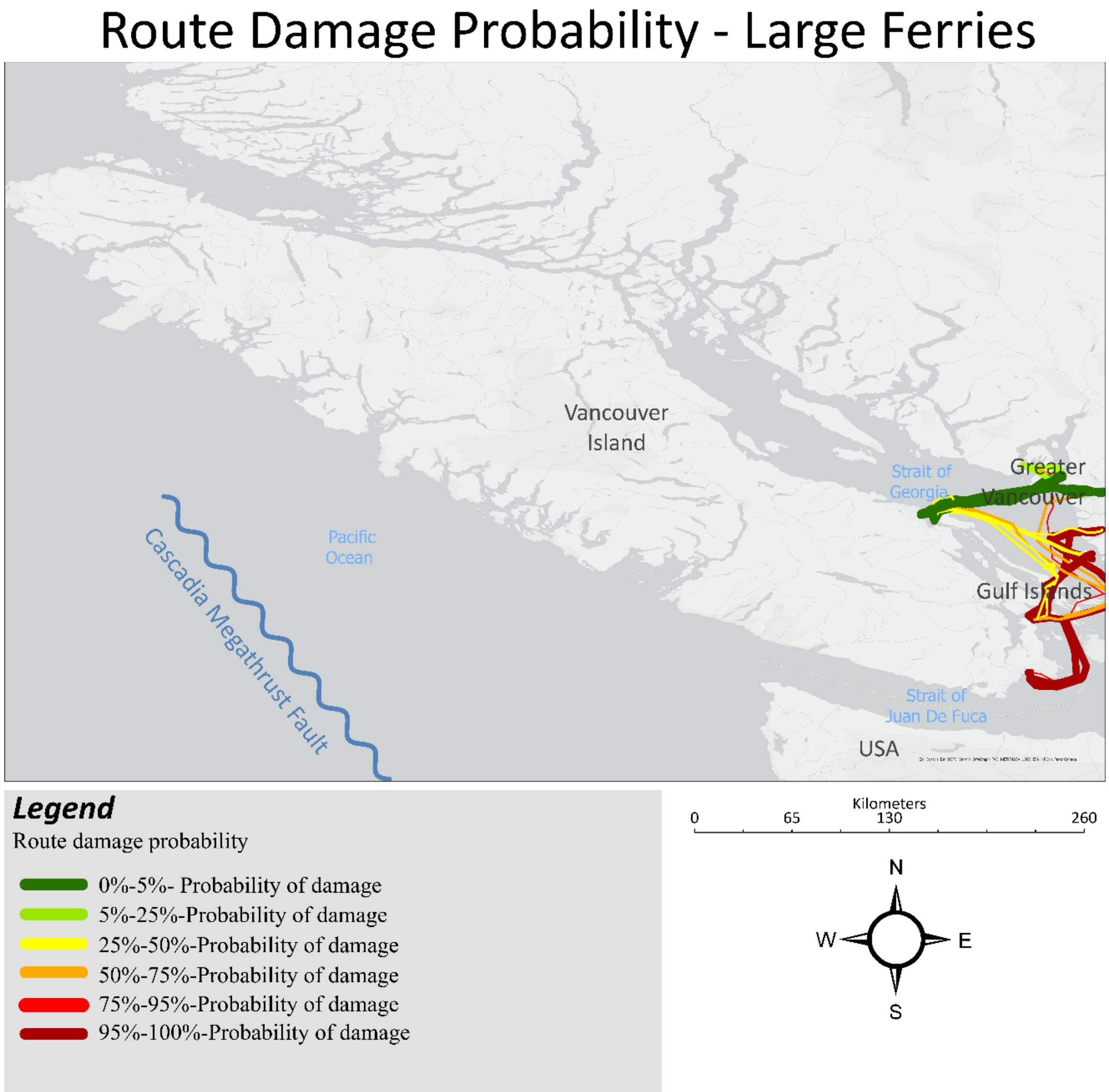

Figure 47 - Damage probability ranges according to large ferry points damage probability calculation in each path

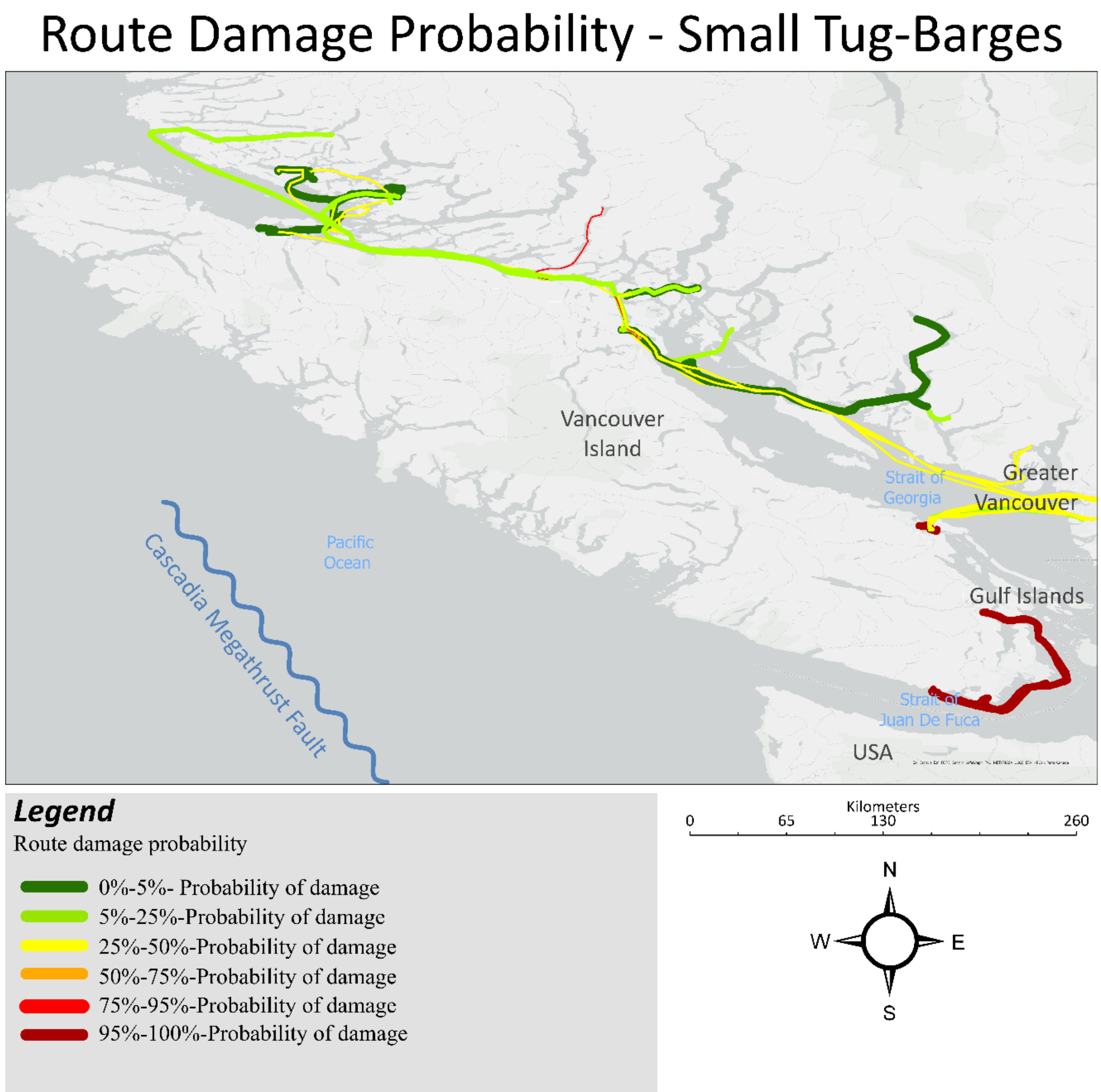

Figure 48 - Damage probability ranges according to small tug-barges points damage probability calculation in each path

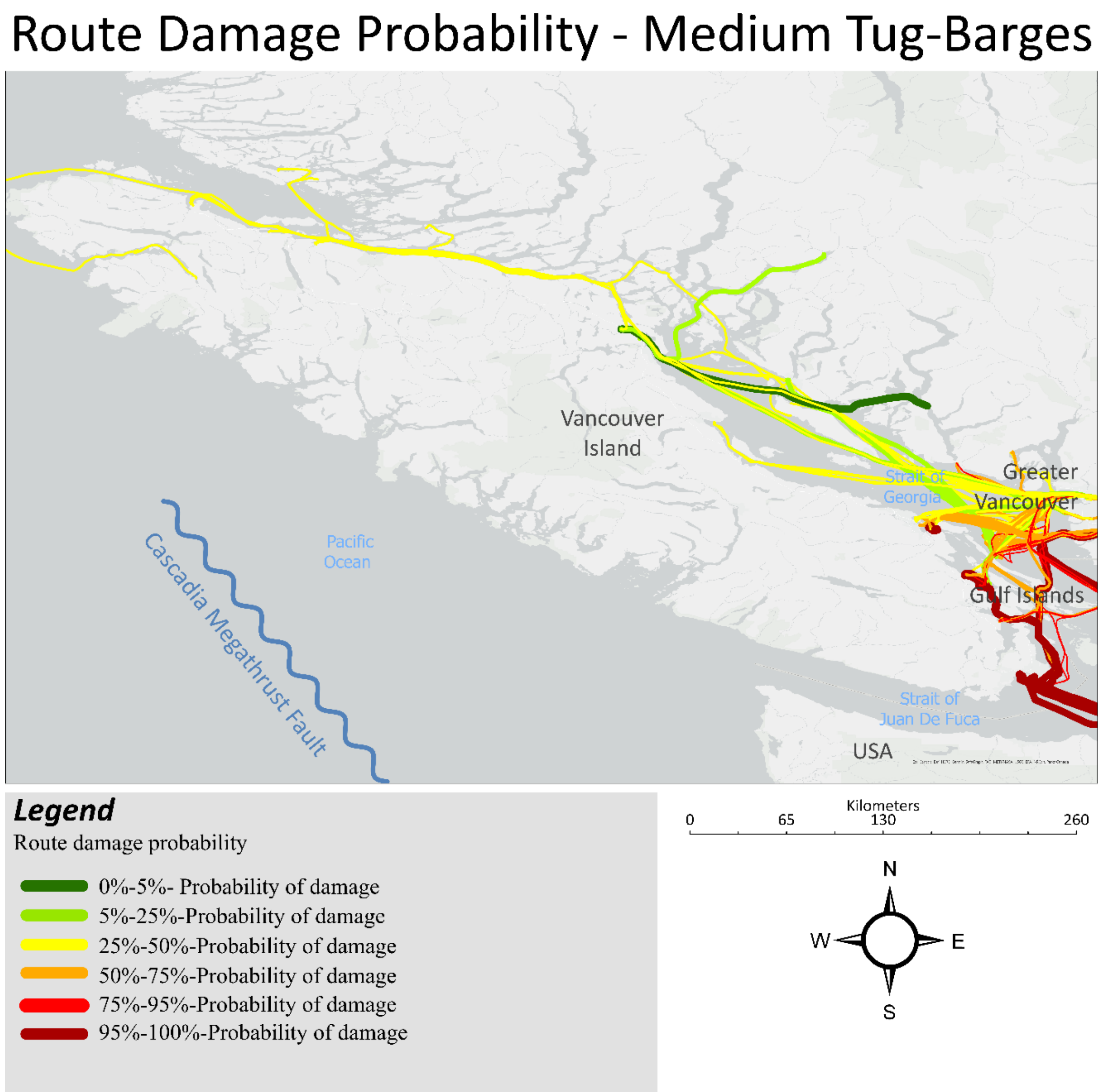

Figure 49 - Damage probability ranges according to medium tug-barges points damage probability calculation in each path

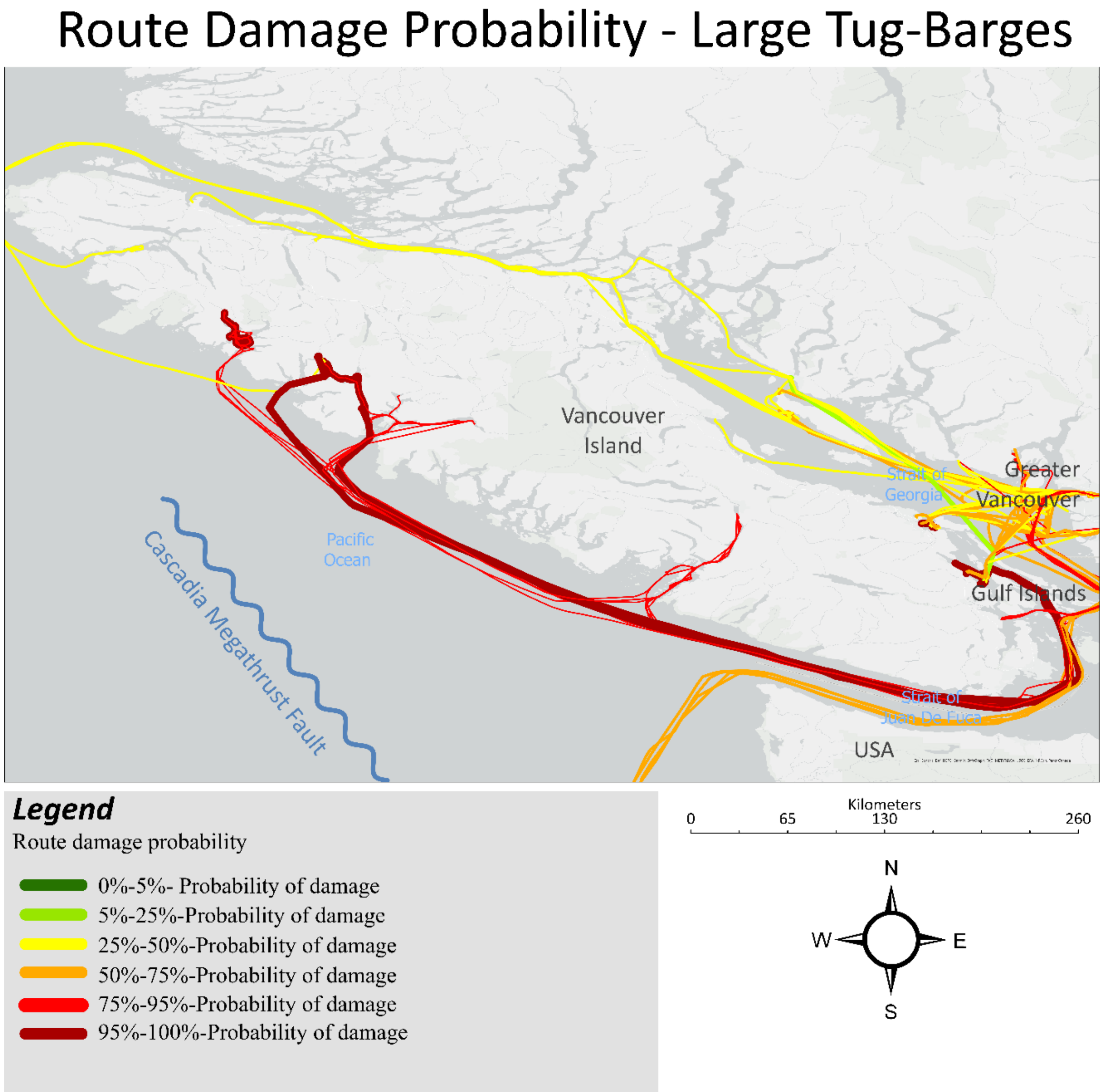

Figure 50 - Damage probability ranges according to large tug-barges points damage probability calculation in each path

4.3.5 Vancouver Island communities and ship availability

Coastal communities are impacted by a reduced ship availability, especially in emergency response situations, whereas this transportation mode is important to support humanitarian logistics. It was possible to compare standard operation data (Sections 4.2.2 and 4.2.3) and damage information using the ship (Section 4.3.1) and route (Section 4.3.3) damage probability data, matched with tsunami zones and regions, to assess the reduction of navigation capacity. This information helps create a context for the fourth research question: Which regions of Vancouver Island will likely be exposed to a reduced ship capacity for emergency logistics deliveries due to ships not being available in the immediate disaster response phase? The range of damage probabilities higher than 75%, higher than 95%, and equal to 100% was used in the analyses considering the different damage probability levels each one imposes on the navigation.

Table 14 shows the number of vessels that navigate in each zone and the reduced proportions according to the 3 damage ranges. Zone E has more ships navigating with an average of 15% reduced capacity in all 3 damage probability ranges. Zone D, with fewer vessels than zone E, presents a significant reduction of the vessel, especially at 100% damage range with fewer than 21% ships. There is no capability reduction in zone B, but zone C with only 3 vessels, has a possible reduction of ship number, considering the 75% damage probability.

Table 14- Number of ships navigating according to tsunami zones and damage probability bigger than 75% decrease proportions

		Ship Damage Probability		
Zones	**Ship Count**	**>75%**	**>95%**	**100%**
Zone E	57	19%	14%	12%
Zone D	28	29%	25%	21%
Zone B	12	0%	0%	0%
Zone C	3	33%	0%	0%

The same analyses of Table 14 were made for regions on Vancouver Island instead of zones and are presented in Table 15. Greater Vancouver has a higher ship count, being the region where ships depart and having a connection on land with other areas; it will not be the focus of the analyses. South Island is the region with more ships and has a reduced ship capacity by an average of 32%. Gulf Island, with fewer ships, is estimated to have a reduction of at least 50% of the vessels normally servicing the area. North Island is the region with proportionally lowest reduction at the 75% damage probability level. In addition, Central Island did not present any reduction in ship capability.

Table 15 - Number of ships navigating according to regions and damage probability bigger than 75% decrease proportions

		Ship Damage Probability		
Region	**Ship Count**	**>75%**	**>95%**	**100%**
Gulf Islands	10	70%	60%	50%
Pacific RIM	2	50%	0%	0%
Sunshine Coast	2	50%	0%	0%
South Island	27	41%	30%	26%
Greater Vancouver	53	15%	9%	8%
North Island	10	10%	0%	0%
Central Island	23	0%	0%	0%

The reduction capability analysis is also performed at the routes between zones and regions; with calculation results presented in Tables 16 and 17, respectively. Examining the navigation between the Tsunami zones table, some zones have no capacity reduction. Considering vessels departing and arriving in zone D, all 19 routes have a 100% damage probability. The navigation between zone D and Zone E also can be highlighted with a reduction of 80% of routes.

There are several combinations of regions, but by examining the ones with higher route count or damage impact, it some information can be highlighted. The navigation between Greater Vancouver and Central Island, which consists of 159 routes, will have almost no damage. However, the second-highest count, with 109 routes between Greater Vancouver and South Island, has at least a 12% route reduction, considering the 100% damage probability estimate. Besides that, considering the connection between Gulf Island

and itself, South Island, and Greater Vancouver, these combinations' reduction capability is 100% for all damage probability ranges.

Table 16 - Count of routes according to zone combinations compared with route damage probability greater than 75% reduction proportions

		Route Damage Probability		
Zones	**Routes Count**	**>75%**	**>95%**	**100%**
Zone E-Zone E	471	42%	35%	35%
Zone E-Zone D	71	86%	73%	65%
Zone D-Zone E	41	80%	80%	80%
Zone E-Zone B	21	0%	0%	0%
Zone D-Zone D	19	100%	100%	100%
Zone E-Zone C	17	88%	6%	0%
Zone C-Zone C	10	100%	50%	50%
Zone B-Zone E	10	0%	0%	0%
Zone B-Zone B	8	0%	0%	0%
Zone C-Zone E	4	75%	25%	0%

Table 17 - Count of routes according to region combinations compared with route damage probability greater than 75% reduction proportions

		Route Damage Probability		
Region	**Routes Count**	**>75%**	**>95%**	**100%**
Greater Vancouver-Central Island	159	1%	0%	0%
Greater Vancouver-South Island	109	55%	17%	12%
Gulf Islands-Gulf Islands	90	100%	100%	100%

Central Island-Central Island	57	54%	54%	54%
South Island-South Island	46	96%	96%	96%
Greater Vancouver-North Island	42	21%	0%	0%
Gulf Islands-South Island	32	100%	100%	100%
South Island-Gulf Islands	32	100%	100%	100%
Greater Vancouver-Gulf Islands	18	100%	100%	100%
North Island-North Island	17	47%	29%	29%
Greater Vancouver-Greater Vancouver	16	6%	6%	6%
South Island-Central Island	11	0%	0%	0%
Central Island-South Island	8	0%	0%	0%
Greater Vancouver-Sunshine Coast	7	0%	0%	0%
Central Island-Gulf Islands	4	100%	0%	0%
Greater Vancouver-Pacific RIM	3	0%	0%	0%
North Island-Central Island	3	0%	0%	0%
Central Island-North Island	3	33%	0%	0%
North Island-Greater Vancouver	3	33%	33%	0%
North Island-Pacific RIM	2	0%	0%	0%
North Island-South Island	2	100%	50%	0%
Pacific RIM-North Island	1	100%	0%	0%
Central Island-Sunshine Coast	1	100%	0%	0%
Gulf Islands-Central Island	1	0%	0%	0%
North Island-Sunshine Coast	1	0%	0%	0%
Sunshine Coast-Central Island	1	0%	0%	0%
Sunshine Coast-Sunshine Coast	1	0%	0%	0%
Central Island-Greater Vancouver	1	0%	0%	0%
Central Island-Pacific RIM	1	100%	0%	0%

4.4 Data analyses for risk uncertainties

Understanding the limitations and uncertainties of this research, focusing on models and scenario information is a relevant part of this research because it improves risk assessment information. In the following paragraphs, the results of the strength of evidence and importance analysis will be presented, as outlined in Section 3.2.5. First, the summary results of analyses performed for the strength of evidence and importance analysis are represented in Table 18. The complete analyses can be found in Appendix 5 and 6.

Observing the information in Table 18 for strength of evidence, for the MVM model 19 evidence elements were identified, with the analysis indicating that 68% of the evidence is strong, and that there is no weak evidence underlying this MVM model. For the RUSEMARIE model, 57% of the evidence is considered having medium strength, and 56% is also medium for the scenario. Inspecting the importance of the evidence, 42% of the evidence underlying the MVM model is low, whereas the RUSEMARIE model has a more spread out distribution, with 37% of the evidence in high importance. For the Scenario data, 44% of the evidence is considered of high importance. More substantial insights of the criticality of the evidence underlying the analysis can be found when looking at the critical matrix of each studied part.

Table 18- Strength of Evidence and Empirical Importance summary analyses information for the 3 main aspects of the research

	Levels	MVM	RUSEMARIE	Scenario
Evidence Count		19	30	9
Strength of Knowledge/Evidence	Strong	68%	27%	33%
	Medium	32%	57%	56%
	Weak	0%	17%	11%
Empirical Implication /importance	Low	42%	33%	22%
	Medium	37%	30%	33%
	High	21%	37%	44%

Table 19 shows the criticality of the MVM model for each piece of evidence. There are 5 pieces of evidence with low importance and strong knowledge, shown in the green cell, with no evidence classified in the high-weak cell, depicted in red. The cells with most evidence is yellow, with 6 pieces classified as medium importance but strong knowledge. Together, this indicates that the MVM is a reasonable model with overall relatively strong data and good assumptions underlying the information processing. More details about the terms and analyses of the following tables 19, 20 and 21 can be found on appendix 5 and 6.

Table 19 - MVM model evidence critical analyses, according to Importance versus Strength of evidence, of the 19 pieces of evidence

Empirical Implication /importance	Weak	Medium	Strong
High		M17,M19	M1,M4
Medium		M13	M2, M8, M10,M14,M15,M18
Low		M3,M7,M11	M5,M6,M9, M12,M16

Strength of Knowledge/Evidence

Table 20 shows the RUSEMARIE model's criticality, where 30 pieces of evidence were analyzed, consisting of data and processing information. There are 4 evidence elements classified as having high importance and low strength, indicated in red, while 5 evidence elements are considered having low-strong evidence, indicated in the green cell. The column with medium strength for the 3 levels of importance presented almost the same number of evidence, namely 5 to 6 elements. This setup indicates that the model is reasonable to provide insights in the likely damage of vessels navigating in the area, but that it would benefit from improved evidence, especially those aspects indicated in the red cells. That can the overall strength of knowledge and give more confidence in the results.

Table 20 -RUSEMARIE model evidence critical analyses, according to Importance versus Strength of evidence, of the 30 pieces of evidence

Empirical Implication /importance	Weak	Medium	Strong
High	R5,R7,R18, R22	R1,R14,R25, R26,R28,R30	R3
Mediu m	R21	R8,R11,R13, R16,R1,R20	R2,R29
Low		R10,R19, R23,R24,R27	R4,R6,R9, R12,R15

Strength of Knowledge/Evidence

For the scenario information, the criticality analyses are presented in Table 21, where 9 pieces of evidence were assessed. High importance and weak knowledge resulted only in one element: tsunami wave velocity calculation. The other evidence is evenly spread at medium to strong knowledge for diverse levels of importance. The criticality analysis indicates that a reasonable scenario is applied in the analysis, whereas it is possible to improve some evidence.

Table 21 - The Cascadia Scenario evidence critical analyses, according to Importance versus Strength of evidence, of the 9 pieces of evidence

Empirical Implication /importance	Weak	Medium	Strong
High	I9	I4,I7	I2
Medium		I1,I8	I5
Low		I6	I3

Strength of Knowledge/Evidence

4.5 Results summary

The research objective is to analyze the ship navigation information, and make inferences about their relationships with Earthquake-Tsunami damage elements. Understanding the studied fleet and their characteristics and port data was essential to support achieving the research objective. Using the AIS information and MVM model, it was possible to assess the navigation patterns. Ferries' vessels navigate the same set of routes several times depending on the itinerary and navigate the same route more than once a day. The navigation is restricted to greater Vancouver along the Straight of Georgia. In comparison, the tug-barges navigation area is all around Vancouver Island, with several routes for the same ship.

From the RUSEMARIE results presented above, it was possible to estimate the number of damaged vessels. Considering 95-100% damage probability, it is plausible that 8 ships will almost certainly not be available to support emergency logistics. Analyzing the damage probabilities for the 6 vessel groups, considering the 95-100% information, small ferries are most affected by Earthquake-Tsunami Cascadia event. Examining the maps in Figures 41 and 44, the area around Gulf Island and the area facing the Pacific Ocean has more damage points. Besides that, the routes connecting these areas and vessels navigating along these routes are more likely to be damaged. In the zones and regions affected studies, Zone D was identified as the most affected, and regions of South Island and Gulf Island had a high probability of having reduced capacity for emergency logistics.

The identification of critical evidence and the uncertainties associated with the models were assessed. The MVM model and scenario data have less critical evidence, while the RUSEMARIE model has some weak but critical evidence. In the next section, the relation between the model critically with the results will be discussed. Besides that, the implications of the results for emergency logistics will be outlined, followed by research limitations and uncertainties. Finally, future research involving humanitarian logistics, making use of and further advancing the here presented work, will be laid out.

Chapter 5
Discussion

Predicting whether a ship will be damaged and understanding the effects of earthquake-tsunami events on fleet availability are critical components of developing a strategy for coastal emergency response logistics and for disaster preparedness risk management. This research aims to comprehend, explore, and analyze the damaged maritime vessels in British Columbia following a Cascadia megathrust catastrophic event. A novel approach for estimating the likelihood of a vessel being damaged by a natural disaster is offered based on day-to-day operation patterns. The methodologies employ the Marine Vessel Movement (MVM) model and the RUSEMARIE model, both of which employ geospatial techniques to various datasets, to obtain information organized around the research questions. The probability of damage for different vessel groups and tsunami zone levels is estimated using a quantitative modeling technique in this work.

This chapter will present the main interpretations of the results and consider further implications. It is divided into 4 sections, starting with an interpretation of the findings mainly in the context of emergency response, followed by an assessment of uncertainties associated with the analyses, and limitations section considering the studied scenario. Then, the results of the maritime damage estimation are considered from the perspective of future research directions. Finally, a brief summary of the discussion is given.

5.1 Inferences of vessel availability estimation

The main research goal was to evaluate ship navigation data and draw conclusions about their connection with earthquake-tsunami impacts. The following topics will be interpreted in the following paragraphs, considering the disaster preparedness and emergency logistics context. Ferries travel the same set of routes several times following a regular schedule, while tug-barges have multiple paths for the same ship. So, using their routes, the RUSEMARIE model statistics point out that considering the 95-100% damage probability, it is fair to assume that 8 ships will almost certainly be unavailable to assist emergency logistics, with small vessels most impacted. The region surrounding Gulf Island

and confronting the Pacific Ocean correspond to the area with most points identified as being damaged, and the routes that link these regions are more likely to be harmed. Zone D is the most impacted, and areas of South Island and Gulf Island have a high probability of decreased emergency operations capacity.

Coastal communities rely on ships to receive supplies, especially in natural disasters, where they become more vulnerable, as described in the literature review Section 2.5. In several natural disasters, ships have been used to support emergency logistics, as described in Section 2.6. In the Great Japan Earthquake of 2011, ferries were used for emergency logistics, delivering and transporting first responders' supplies [3]. Hence, estimating the number of ships available can be important for preparedness planning in disaster preparedness risk management, as knowing how many transportation resources will be available to support coastal communities can inform mitigation options. This research suggests that the available fleet will be reduced at least 5%, considering the 95-100% damage as vessels being almost certainly damaged. However, it is plausible that there will be more vessels out of commission in an earthquake-tsunami event, as there is a relatively large probability of damage for a larger group of vessels.

During the disaster preparedness phase, it is important to have a reasonable understanding of the availability of resources, so that alternative plans and mitigation options can be devised. Knowing that some routes and ports will be damaged helps identify alternatives. So, to supply communities located in the North region and RIM region out to the Pacific Ocean, vessels should navigate to the Strait of Georgia until they reach a safe area in the North region. Another alternative is to deliver the supplies to the Central region by ship and the remainder of the journey by truck to the most affected areas, or to concentrate the air delivery to isolated areas.

Using the gridded information of damage probability, decision-makers, such as captains and the government administrators, can create better guidelines to inform safety measures for ships. More specifically, the grid information helps identify marine evacuation areas where a vessel should navigate to when a tsunami warning is issued. The sizes of ships play an important role in navigational safety, especially for large tugs that navigate in dangerous areas in an earthquake-tsunami event. For shipping companies, having awareness of the alignment of their operational routes and areas with the area-based damage information by vessel groups, can be instrumental to include appropriate safety procedures in their safety management systems, for instance related to route planning and communications, and companies could even account for the dangers of earthquake-tsunami events in making investment decisions when purchasing new vessels or tugs. Ocean tugs operating off the coast of Vancouver Island in the Pacific Ocean and small ferries operating in the South region are the most affected ship sizes; so that especially companies operating those ship types in those areas would be well-advised to develop reasonable mitigation options.

The RUSEMARIE results provide unprecedented information to support disaster preparedness and emergency response planning organizations and decision-makers. However, the criticality of the model indicates that the model, while based on the best available evidence, is associated with some uncertainty. Hence, the model would benefit from further improvement, and the uncertainties should be appropriately considered when using the results in a risk assessment context. Considering these uncertainties, this research suggests a reassessed damage probability graph in Figure 51. In this, the number of damaged vessels with 95-100% damage probability was reduced from 8 to 5 and distributed to less than 50% probability ranges. According to the minimum and maximum probabilities scales, the reassessed expected number of unavailable ships ranges from 20 ships for the minimum probability scale to 31 ships for the maximum probability scale of unavailable vessels, a decrease of 3 vessels in both minimum and maximum if compared with the original unavailable vessel information. This reassessed graph is more suitable for the research aim of understanding, evaluating, and estimating the damage to ships. The graph will better inform decision-makers with a more reliable assessment to consider a better disaster risk management approach.

By comparing the damage information results of this research with previous studies, it is possible to highlight that ship size is a factor. In the work by Suppasri et al., the damage of small vessels was studied, and this research also suggests that small ferries are the most impacted [55]. However, in the current work, depending on the navigation patterns, medium and large ferries and large tug-barges can also have a high probability of damage. This finding is significant in point out that not only small vessels are likely to be damaged. Moreover, considering that other emergency response logistics operations utilized large ferry ships averaging 10,000 gross tonnage due to limited resources such as port facilities and fuel [3], these estimations related to size indicate that ship location during the event plays an important role in damage, especially for large-size ones located in tsunami-vulnerable areas. Hence, the unavailability of medium to large ferries should also be considered during emergency planning.

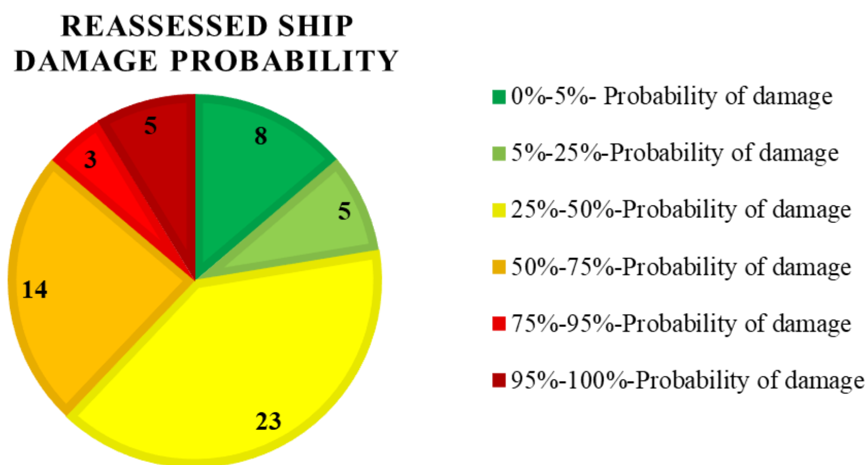

Figure 51- *Reassessed pie chart of all vessel damage due to RUSEMARIE model critical analyses results*

This research has contributed to the disaster preparedness and emergency response risk management field, proposing a model that helps estimate ship damage for events for which no historic data is directly available. The RUSEMARIE model would benefit from further improvement, but it is an appropriate assessment tool for emergency planning, indicating the availability of logistics resources. Using this information, it is possible to come up with mitigation plans and other complementary emergency plans.

5.2 Ship damage uncertainties and limitations

The last section examined the criticality of the models and scenario information. Here, the uncertainties and limitations will be discussed more broadly, focusing on the wider research context. There are some important limitations to the presented work which deserve to be mentioned, such as the scenario selection, the vessel fleet and type, the port damage, and the evidence for the tsunami currents.

British Columbia is the studied area, and the Cascadia megathrust worst-case scenario was selected as a basis for the case study due to the likely huge impact of the tsunami. This scenario was used in the proposed new methodology, RUSEMARIE, to estimate the probability of a vessel being damaged. However, to better understand the RUSEMARIE model's weakness and to better understand the vessel damage estimation and implications to communities, the RUSEMARIE model should be applied to other scenarios. The literature review pointed out the northern and central segments of the Cascadia zone as being other areas where an earthquake epicenter may be located, which could result in different damage estimates and provide more information for disaster risk management [22]. Hence, applying the RUSEMARIE model considering only one scenario is a limitation for the results for the studied ships.

Due to previous use in other natural disaster emergency logistics, ferries and tug-barges combination is chosen as the scope of the current study. Nevertheless, using more ship types or a bigger fleet could give more insights into the damage to the fleet available for humanitarian logistics. In the MVM and RUSEMARIE models, only 57 ships were studied, limiting the inferences of navigation patterns and damage to these two types. Other research studies on earthquake-tsunami damage include fishing vessels, recreational boats, and other vessel types [1]. While it is reasonable to focus on the commercial shipping operations providing logistics services to the island communities under normal conditions, focusing the research on only two ship types reflects only a small sample of the entire fleet in the area, possibly leading to biased results. Therefore, extending the research to other ship types could give more insights about damage and response options to emergency logistics decision-makers.

The damage resulting from proximity with structures, such as ports and bridges, is one of the uncertainties of the RUSEMARIE model. There is a lack of literature on calculations on port structural damage resulting from earthquakes, and further ensuing ship damage. These elements are associated with some uncertainty in the RUSEMARIE model, but as these account for a relatively small share of the trajectories, it is reasonable to conclude that the model and its results are plausible. Nevertheless, having more dedicated research relating historic earthquakes and possible future earthquake scenarios with structural damages in ports and ships, would be a meaningful direction for future work.

Tsunami currents data and vessel damage were studied in the wake of the Great Japan 2011 Earthquake and other disasters [44]. For this research, the detailed current information for the Cascadia scenario was available only for the area South of Vancouver Island, specifically zone D. Hence, this was a limitation for the other regions, especially zone C facing the Pacific Ocean, where there is no land smoothing wave impact and loss of areas susceptible to tsunami currents. Understanding the Cascadia tsunami and current information for Tofino, Port Alberni, and Ucluelet at zone C is crucial. So, knowing the current velocity and strength in most bays, straits, and rivers around Vancouver Island would enhance the results and reduce uncertainties about the results.

Despite the limitations highlighted in this section, this research provided a reasonable understanding of the damage to ships in the event of a Cascadia megathrust earthquake-tsunami event. The results give a broad picture of a number of salient issues on the vessel and fleet level, distinguishing different marine and coastal areas. These can be used by emergency planners to develop strategies related to improved preparedness and response for humanitarian logistics, and to define guidelines for vessel companies and operators to anticipate and use during the earthquake-tsunami events.

5.3 Future research directions

This study proposed a new framework for earthquake-tsunami loss prediction for marine vessels that can be used to estimate the damage probability of vessels, identify dangerous areas and sea evacuation areas, the possible impacts on navigation, and influences on communities. However, the proposed RUSEMARIE tool is a dense combination of elements such as tsunami zones, infrastructure damage information, depth data, vessel travel time, tsunami arrival time, and currents in different areas. Further studies focusing on some elements will be beneficial to determine the vessels' availability and damage more accurately. Future research should focus on gathering more data about port infrastructure damage and the vessel impacts. In addition, future work could be dedicated to gather more data and information relating to the Cascadia megathrust scenario and the estimation of current data for other regions around Vancouver Island, especially for the areas west of the island and the areas facing the Pacific Ocean. This could be done by performing more ocean wave simulations about the Cascadia tsunami scenario, and applying the data to existing current prediction models to generate current velocities in various bays and narrows. Using more elements, more reliable data, and updating some calculations can improve the RUSEMARIE model's accuracy and give more insights to decision-makers.

Feature research could also focus on applying the approach developed in this study, especially the RUSEMARIE model, to other scenarios and areas where earthquake-tsunami occurrences happen. Furthermore, it would be interesting to use the past Great Japan earthquake-tsunami scenario of 2011, and comparing the estimation results with the empirically obtained damage information of that disaster [34]. This application could be an important step in validating the proposed damage estimation model.

The method used for the RUSEMARIE model which consists in using spatiotemporal points interpreted by a GIS-layered classification model to interpret those points in a way, could be used for different problems. Considering the maritime context, it could be used to classify wind and heat exposure on ships, ship movement violations of speed restrictions in marine protected areas, oil spl possibility according to navigation patterns, and others ship-related fields. This could also be applied outside of the maritime context, such as with the exposure of cars to pollution levels in cities. In a sense, this approach could be applied to a wider set of problems, which could also use an approach like the one proposed to get statistical insights into spatiotemporal data.

A study of the multi-modal distribution of relief supplies for Vancouver Island and the surrounding island is being made using ships [134]. In this context, using ship availability information as obtained from the current research could be an opportunity to better understand the impacts of ships' emergency delivery to affected coastal communities. The vessel damage probability information could also be used in other research by applying the ship availability information to humanitarian network distribution models to assess the emergency supply capacity of the maritime system. This information will help decision-makers and policymakers to understand the implications of such catastrophic events better, improve emergency response plans and develop ways to mitigate the ships not being available to support supply delivery to islands, enhancing the overall risk management of operations related to earthquake-tsunami events.

5.4 Discussion summary

Many coastal communities rely on ships to receive supplies, especially in natural disasters. In several natural disasters, ships have supported emergency logistics, such as the Great Japan Earthquake of 2011. Estimating the number of ships available helps in the planning phase of emergencies. Research suggests a reduction of the fleet by at least 5%, considering that these will sustain damage with 95-100% probability. It is plausible that a considerably larger share of the fleet would be damaged. In addition, the damage grid allows decision-makers to develop better ship safety measures and ship sea evacuation regions. Vessels should travel to the Strait of Georgia until the safe area of the North region to serve communities in the North region and RIM area as alternative solutions.

The RUSEMARIE model's findings result in useful information for disaster planning groups and decision-makers but need refinement to provide more reliable risk evaluation, because of several uncertainties due to limitations in available evidence. These include using only one earthquake scenario, applying the model to only 2 types of vessels, having only limited accurate current data available.

This research provides a broader understanding of ship damage, and can be used to develop strategies for distribution of relief supplies and planning humanitarian logistics as future research. In addition, gathering more data about port infrastructure damage and vessel impacts, and validating the model using past event's information, would be fruitful areas of future work. Hence, this research uses ship availability information to understand the impacts of ships' emergency delivery to affected coastal communities.

Chapter 6
Conclusion

Estimating whether a ship will be damaged and comprehending the impact of earthquake-tsunami events on fleet availability for performing humanitarian relief operations, and is a critical component of developing evidence-based disaster preparedness and response strategies for coastal communities' emergency response logistics. This thesis presents a novel method for estimating the likelihood of vessel damage in such disasters, considering its function in humanitarian supply chain logistics during a natural disaster.

The Japan Association developed a tsunami damage framework that inspired this study to identify current maritime transportation system characteristics and past tsunami damage information. The criteria and information analyzed prompted the RUSEMARIE model, which evaluates whether a vessel in a particular area will likely be damaged and inoperable by an earthquake-tsunami event. The variables of the tsunami and the vessels included in the developed model were based on information from two loss probability damage investigations and differentiation for vessel groups.

The absence of earthquake-tsunami natural disasters in recent decades complicates research on ship damage in such events. Most research has focused on tsunami damage to static structures, but less knowledge is available for vessels. There is also a dearth of awareness of specific damage types and the magnitude of vessel damage, which may be attributed to the fact that earthquakes and tsunamis erase much evidence. This study aimed to provide a better understanding how these factors might be used together to provide better baseline information for disaster preparedness risk assessment and management. A knowledge-based model was created to estimate the damage to marine assets based on vessel movement data and simulated earthquake-tsunami data.

In summary this novel approach showed using the MVM model that ferries travel the same route multiple times per day, limited to along the Straight of Georgia, while tug-barges have multiple paths for the same ship all around Vancouver Island. The RUSEMARIE model showed that small boats are the most impacted by the earthquake-tsunami Cascadia megathrust event, with the region surrounding Gulf Island and confronting the Pacific Ocean having the highest damage probability. Vessels on the routes that link these regions, as well as the vessels that travel along them, are more likely to be damaged. Zone D was identified as the most impacted, and regions of South Island and Gulf Island had a high probability of having decreased capacity for emergency response logistics. One of the most important results is the estimate of ship damage, where it is found that at least 8 ships will not be available to assist with emergency logistics, due to these having a 95-100% damage risk. That information was reassessed after model criticality analyses, suggesting that at least 5 ships being unavailable is a plausible number to work with in disaster preparedness risk assessment.

Ships have been used to assist emergency operations in natural catastrophes, and research recommends lowering at least 5% of the fleet accessible. Nevertheless, the results indicate that there is a significant probability that a larger share of the fleet will be unavailable after a Cascadia-type earthquake-tsunami event. Vessels should journey to the Strait of Georgia and service towns in the North region and RIM area, while goods should be shipped to the Central region and trucked to the most affected regions. Isolated regions should be prioritized for air delivery, and the damage grid enables public and private decision-makers to devise improved ship safety measures.

The RUSEMARIE results provide useful information for disaster response planning organizations and decision-makers, but need refinement to provide a more reliable risk assessment. Extending ship classes could provide more insights into earthquake-tsunami damage and choices.

Applying the RUSEMARIE model to other earthquake-tsunami scenarios in different geographical areas could validate the proposed damage estimation model. This research used ship availability information to understand the impacts of ships' emergency delivery to affected coastal communities, which could be used in further research to assess the emergency supply capacity of the maritime system.

References

[1] A. Muhari, I. Charvet, F. Tsuyoshi, A. Suppasri, and F. Imamura, "Assessment of tsunami hazards in ports and their impact on marine vessels derived from tsunami models and the observed damage data," *Nat. Hazards*, vol. 78, no. 2, pp. 1309–1328, Sep. 2015, doi: 10.1007/s11069-015-1772-0.

[2] S. E. Chang and H. Dowlatabadi, "Transportation Disruptions and Regional Supply Chains: A Modeling Framework with Application to Coastal Shipping," *Adv. Spat. Sci.*, pp. 243–264, 2019, doi: 10.1007/978-3-030-16237-5_10.

[3] K. Ono, J. Tatsumi, and T. Nakao, "Possible mass and long distance ferry transportation for health and humanitarian logistics at a disaster scene," *Transp. Res. Procedia*, vol. 25, pp. 1180–1197, 2017, doi: 10.1016/j.trpro.2017.05.137.

[4] D. W. Mason and A. Zegers, "The Seismic and Tsunami Threat to Ships , Personnel , and Defence Infrastructure on Canada ' s West Coast," no. October, 2013.

[5] J. J. Clague, "Evidence for large earthquakes at the Cascadia subduction zone," *Rev. Geophys.*, vol. 35, no. 4, pp. 439–460, 1997, doi: 10.1029/97RG00222.

[6] J. J. Clague, P. T. Bobrowsky, and I. Hutchinson, "A review of geological records of large tsunamis at Vancouver Island, British Columbia, and implications for hazard," *Quat. Sci. Rev.*, vol. 19, no. 9, pp. 849–863, May 2000, doi: 10.1016/S0277-3791(99)00101-8.

[7] Alexa Tanner, Hadi Dowlatabadi, Stephanie E. Chang, Rodrigo da Costa, Xuesi Shen, "Resilient Coast : Liquid Fuel Delivery to British Columbia Coastal Communities," p. 35, 2017, doi: 10.14288/1.0360721.

[8] S. Chile *et al.*, "A Community Resilience Approach To Assessing Transportation Risk in Disasters," 2017.

[9] N. A. Errett, A. Tanner, X. Shen, and S. E. Chang, "Understanding the Impacts of Maritime Disruption Transportation to Hospital-Based Acute Health Care Supplies and Personnel in Coastal and Geographically Isolated Communities," *Disaster Med. Public Health Prep.*, vol. 13, no. 3, pp. 440–448, 2019, doi: 10.1017/dmp.2018.64.

[10] City of Victoria Planning and Development Department, "City of Victoria Official Community Plan," 2012. Accessed: Aug. 12, 2021. [Online]. Available: www.victoria.ca.

[11] S. Islam, F. Goerlandt, M. J. Uddin, Y. Shi, and N. S. F. Abdul Rahman, "Exploring vulnerability and resilience of shipping for coastal communities during disruptions: findings from a case study of Vancouver Island in Canada," *Int. J. Logist. Manag.*, vol. 32, no. 4, pp. 1434–1460, Oct. 2021, doi: 10.1108/IJLM-12-2020-0466/FULL/XML.

[12] Z. L. Chang S., Bristow D., Goerlandt F., Pelot R., Goodchild A., Lin C., "Planning for a Catastrophic Earthquake in British Columbia," 2020.

[13] A. Suppasri *et al.*, "Building damage characteristics based on surveyed data and fragility curves of the 2011 Great East Japan tsunami," *Nat. Hazards 2012 662*, vol. 66, no. 2, pp. 319–341, Nov. 2012, doi: 10.1007/S11069-012-0487-8.

[14] I. Charvet, I. Ioannou, T. Rossetto, A. Suppasri, and F. Imamura, “Empirical fragility assessment of buildings affected by the 2011 Great East Japan tsunami using improved statistical models,” *Nat. Hazards 2014 732*, vol. 73, no. 2, pp. 951–973, Mar. 2014, doi: 10.1007/S11069-014-1118-3.

[15] P. J. Lynett, J. Borrero, S. Son, R. Wilson, K. Miller, and J. B. S. S. R. W. K. M. PJ Lynett, “Assessment of the tsunami-induced current hazard,” *Geophys. Res. Lett.*, vol. 41, no. 6, pp. 2048–2055, Mar. 2014, doi: 10.1002/2013GL058680.

[16] S. Koshimura, T. Oie, H. Yanagisawa, and F. Imamura, “Developing Fragility Functions for Tsunami Damage Estimation Using Numerical Model and Post-Tsunami Data from Banda Aceh, Indonesia,” vol. 51, no. 3, pp. 243–273, doi: 10.1142/S0578563409002004.

[17] “What is an earthquake and what causes them to happen? | U.S. Geological Survey.” https://www.usgs.gov/faqs/what-earthquake-and-what-causes-them-happen (accessed Feb. 03, 2023).

[18] “Lists, Maps, and Statistics | U.S. Geological Survey.” https://www.usgs.gov/programs/earthquake-hazards/lists-maps-and-statistics (accessed Feb. 03, 2023).

[19] R. F. Goodwin and J. W. Good, “Making ports and harbors more resilient to earthquake and tsunami hazards,” *Proccedings 13th Bienn. Coast. Zo. Conf.*, 2003.

[20] “Seismic zones in Western Canada.” https://earthquakescanada.nrcan.gc.ca/zones/westcan-en.php (accessed Feb. 02, 2023).

[21] R. D. Hyndman and K. Wang, “The rupture zone of Cascadia great earthquakes from current deformation and the thermal regime,” *J. Geophys. Res. Solid Earth*, vol. 100, no. B11, pp. 22133–22154, Nov. 1995, doi: 10.1029/95JB01970.

[22] R. C. Witter *et al.*, “Simulated tsunami inundation for a range of Cascadia megathrust earthquake scenarios at Bandon, Oregon, USA,” 2013, doi: 10.1130/GES00899.1.

[23] R. C. Witter *et al.*, “Simulating Tsunami Inundation at Bandon, Coos County, Oregon , Using Hypothetical Cascadia and Alaska Earthquake Scenarios,” *Dep. Geol. Miner. Ind. State Oregon*, vol. Special Pa, p. 63, 2011.

[24] F. Shi *et al.*, “Task 3-Tsunami Modelling and Mapping report Capital Region, Coastal Flood Inundation Mapping Project,” 2020.

[25] A. M. Bell and D. N. Bristow, “Modelling the marine transport resilience of Vancouver Island in a Cascadia subduction zone earthquake scenario,” *https://doi-org.ezproxy.library.dal.ca/10.1080/23789689.2020.1845482*, 2020, doi: 10.1080/23789689.2020.1845482.

[26] K. Satake, K. Wang, and B. F. Atwater, “Fault slip and seismic moment of the 1700 Cascadia earthquake inferred from Japanese tsunami descriptions,” *J. Geophys. Res. Solid Earth*, vol. 108, no. B11, p. 2535, Nov. 2003, doi: 10.1029/2003JB002521.

[27] “Tsunamis | National Oceanic and Atmospheric Administration.” https://www.noaa.gov/education/resource-collections/ocean-coasts/tsunamis (accessed Feb. 03, 2023).

[28] J. F. Cassidy, G. C. Rogers, and R. D. Hyndman, "An Overview of the 28 October 2012 Mw 7.7 Earthquake in Haida Gwaii, Canada: A Tsunamigenic Thrust Event Along a Predominantly Strike-Slip Margin," *Pure Appl. Geophys.*, vol. 171, no. 12, pp. 3457–3465, 2014, doi: 10.1007/s00024-014-0775-1.

[29] H. M. Fritz *et al.*, "The 2011 Japan tsunami current velocity measurements from survivor videos at Kesennuma Bay using LiDAR," vol. 39, p. L00G23, Apr. 2012, Accessed: Aug. 24, 2021. [Online]. Available: https://agupubs.onlinelibrary.wiley.com/doi/full/10.1029/2011GL050686.

[30] I. M. Cheff, L. Nistor, and D. Palermo, "Tsunami vulnerability assessment of Canadian west coast communities based on evacuation capability," *Proceedings, Annu. Conf. - Can. Soc. Civ. Eng.*, vol. 3, pp. 1793–1803, 2016.

[31] Ø. Berle, B. E. Asbjørnslett, and J. B. Rice, "Formal Vulnerability Assessment of a maritime transportation system," *Reliab. Eng. Syst. Saf.*, vol. 96, no. 6, pp. 696–705, Jun. 2011, doi: 10.1016/J.RESS.2010.12.011.

[32] The Japan Association of Marine Safety Japan Maritime Center, "Research on Navigation Safety Measures in the Event of Major Earthquake/Tsunami Strikes," 2015.

[33] B. Øyvind, J. B. Rice, and E. A. Bjørn, "Failure modes in the maritime transportation system: A functional approach to throughput vulnerability," *Marit. Policy Manag.*, vol. 38, no. 6, pp. 605–632, 2011, doi: 10.1080/03088839.2011.615870.

[34] T. Tomita, T. Arikawa, and T. Asai, "Damage in ports due to the 2011 off the Pacific Coast of Tohoku Earthquake tsunami," *J. Disaster Res.*, vol. 8, no. 4, pp. 594–604, 2013, doi: 10.20965/JDR.2013.P0594.

[35] I. N. Robertson, "Vulnerability of Hawaii Commercial Port and Harbor Facilities to Tsunamis and Hurricane Storm Surge and Wave Action PROJECT REPORT for Hawaii Department of Transportation, Harbors Division," 2015.

[36] J. L. Bemley, L. B. Davis, and L. G. Brock, "Pre-positioning commodities to repair maritime navigational aids," *J. Humanit. Logist. Supply Chain Manag.*, vol. 3, no. 1, pp. 65–89, 2013, doi: 10.1108/20426741311328529.

[37] M. Vanneste *et al.*, "Submarine landslides and their consequences: What do we know, what can we do?," *Landslide Sci. Pract. Complex Environ.*, vol. 5, no. January, pp. 5–17, 2013, doi: 10.1007/978-3-642-31427-8_1.

[38] S. E. Chang and N. Nojima, "Measuring post-disaster transportation system performance: The 1995 Kobe earthquake in comparative perspective," *Transp. Res. Part A Policy Pract.*, vol. 35, no. 6, pp. 475–494, 2001, doi: 10.1016/S0965-8564(00)00003-3.

[39] S. Islam, F. Goerlandt, Q. M. H. Sakalayen, Y. Shi, and V. G. Venkatesh, "Developing a 'Disaster Scenario' to prepare for the possibility of disruptions to maritime transportation serving coastal communities of Vancouver Island," *Mar. Policy*, vol. 150, p. 105531, Apr. 2023, doi: 10.1016/J.MARPOL.2023.105531.

[40] S. J. Caldwell, "Coast Guard: Observations on the Preparation, Response, & Recovery Missions," Washington, DC, 2006. Accessed: Feb. 07, 2023. [Online]. Available: https://books.google.ca/books?id=Bm6uyI3E45gC&printsec=frontcover&hl=pt-PT&source=gbs_ge_summary_r&cad=0#v=onepage&q&f=false.

[41] F. Goerlandt and S. Islam, "A Bayesian Network risk model for estimating coastal maritime transportation delays following an earthquake in British Columbia," *Reliab. Eng. Syst. Saf.*, vol. 214, p. 107708, Oct. 2021, doi: 10.1016/J.RESS.2021.107708.

[42] Werner SD, *Seismic Guidelines for Ports* . Reston, VA: chnical Council on Lifeline Earthquake Engineering (TCLEE) Monograph No. 12, American Society of Civil Engineers, 1998.

[43] B. M. Sumer *et al.*, "Earthquake-Induced Liquefaction around Marine Structures," *J. Waterw. Port, Coastal, Ocean Eng.*, vol. 133, no. 1, pp. 55–82, Jan. 2007, doi: 10.1061/(ASCE)0733-950X(2007)133:1(55).

[44] P. J. Lynett, J. C. Borrero, R. Weiss, S. Son, D. Greer, and W. Renteria, "Observations and modeling of tsunami-induced currents in ports and harbors," *Earth Planet. Sci. Lett.*, vol. 327–328, pp. 68–74, 2012, doi: 10.1016/j.epsl.2012.02.002.

[45] S. E. Chang, "Disasters and transport systems: Loss, recovery and competition at the Port of Kobe after the 1995 earthquake," *J. Transp. Geogr.*, vol. 8, no. 1, pp. 53–65, Jan. 2000, doi: 10.1016/S0966-6923(99)00023-X.

[46] AECom Canada Ltd., "Modelling of potential tsunami inundation limits and run-up," 2013.

[47] S. A. Socolofsky and G. H. Jirka, "Large-scale flow structures and stability in shallow flows," *https://doi.org/10.1139/s04-032*, vol. 3, no. 5, pp. 451–462, 2011, doi: 10.1139/S04-032.

[48] R. S. Ludwin and A. Colorado, "Tsunami Whirlpools-observed in 2004 and remembered in First Nations art and myth," 2006, Accessed: Feb. 14, 2023. [Online]. Available: http://www.cdnn.info/industry/i041228e/i041228e.htm.

[49] J. C. Borrero, P. J. Lynett, N. Kalligeris, and P. L. N. K. JC Borrero, "Tsunami currents in ports," vol. 373, no. 2053, p. 20140372, Oct. 2015, Accessed: Aug. 24, 2021. [Online]. Available: https://royalsocietypublishing.org/doi/abs/10.1098/rsta.2014.0372.

[50] E. A. Okal, H. M. Fritz, R. Raveloson, G. Joelson, P. Pančošková, and G. Rambolamanana, "Madagascar Field Survey after the December 2004 Indian Ocean Tsunami," *https://doi.org/10.1193/1.2202646*, vol. 22, no. SUPPL. 3, Dec. 2019, doi: 10.1193/1.2202646.

[51] J. W. Gaythwaite, "Design of Marine Facilities for the Berthing, Mooring, and Repair of Vessels," *Des. Mar. Facil. Berthing, Mooring, Repair Vessel.*, Sep. 2004, doi: 10.1061/9780784407264.

[52] L. Dengler, B. Uslu, A. Barberopoulou, J. Borrero, and C. Synolakis, "The vulnerability of Crescent City, California, to tsunamis generated by earthquakes in the Kuril Islands region of the Northwestern Pacific," *Seismol. Res. Lett.*, vol. 79, no. 5, pp. 608–619, Sep. 2008, doi: 10.1785/GSSRL.79.5.608

[53] A. A. J. B. L. D. M. L. P. L. T. M. K. M. A. R. K. S. RI Wilson, "Observations and impacts from the 2010 Chilean and 2011 Japanese tsunamis in California (USA)," *Pure appl Geophys*, vol. 170, no. 6–8, pp. 1127–1147, Jun. 2013, doi: 10.1007/s00024-012-0527-z.

[54] J. Y. Cherniawsky, V. V. Titov, K. Wang, and J. Y. Li, "Numerical simulations of tsunami waves and currents for southern vancouver island from a Cascadia megathrust earthquake," *Pure Appl. Geophys.*, vol. 164, no. 2–3, pp. 465–492, Mar. 2007, doi: 10.1007/S00024-006-0169-0.

[55] A. Suppasri, A. Muhari, T. Futami, F. Imamura, N. Shuto, and A. M. T. F. F. I. N. S. A Suppasri, "Loss Functions for Small Marine Vessels Based on Survey Data and Numerical Simulation of the 2011 Great East Japan Tsunami," *J. Waterw. Port, Coastal, Ocean Eng.*, vol. 140, no. 5, p. 04014018, Sep. 2014, doi: 10.1061/(asce)ww.1943-5460.0000244.

[56] Y. Suga, S. Koshimura, and E. I. Kobayashi, "Risk evaluation of drifting ship by tsunami," *J. Disaster Res.*, vol. 8, no. 4, pp. 573–583, 2013, doi: 10.20965/jdr.2013.p0573.

[57] Y. Fujii, K. Satake, S. Sakai, M. Shinohara, and T. Kanazawa, "Tsunami source of the 2011 off the Pacific coast of Tohoku Earthquake," *Earth, Planets Sp. 2011 637*, vol. 63, no. 7, pp. 815–820, Sep. 2011, doi: 10.5047/EPS.2011.06.010.

[58] M. Nursey-Bray *et al.*, "Vulnerabilities and adaptation of ports to climate change," *J. Environ. Plan. Manag.*, vol. 56, no. 7, pp. 1021–1045, 2013, doi: 10.1080/09640568.2012.716363.

[59] D. Lee, S. S. Lee, and B. J. Park, "3-D geometric modeler for rapid ship safety assessment," *Ocean Eng.*, vol. 31, no. 10, pp. 1219–1230, Jul. 2004, doi: 10.1016/J.OCEANENG.2004.01.004.

[60] K. G. R. W. L. M. D. A. B. A. Y. B. J. B. M. C. K. C. PJ Lynett, "Inter-model analysis of tsunami-induced coastal currents," *Ocean Model*, vol. 114, pp. 14–32, Jun. 2017, doi: 10.1016/j.ocemod.2017.04.003.

[61] A. R. Admire *et al.*, "Observed and Modeled Currents from the Tohoku-oki, Japan and other Recent Tsunamis in Northern California," *Pure Appl. Geophys. 2014 17112*, vol. 171, no. 12, pp. 3385–3403, Feb. 2014, doi: 10.1007/S00024-014-0797-8.

[62] E. A. Okal, H. M. Fritz, P. E. Raad, C. Synolakis, Y. Al-Shijbi, and M. Al-Saifi, "Oman field survey after the December 2004 Indian Ocean tsunami," *Earthq. Spectra*, vol. 22, no. SUPPL. 3, 2006, doi: 10.1193/1.2202647.

[63] E. A. Okal, A. Sladen, and E. A. S. Okal, "Rodrigues, Mauritius, and Réunion Islands field survey after the December 2004 Indian Ocean tsunami," *Earthq. Spectra*, vol. 22, no. SUPPL. 3, 2006, doi: 10.1193/1.2209190.

[64] J. Choi, D. Lee, H. J. Kang, S. Y. Kim, and S. C. Shin, "Damage scenarios and an onboard support system for damaged ships," *Int. J. Nav. Archit. Ocean Eng.*, vol. 6, no. 2, pp. 236–244, Jun. 2014, doi: 10.2478/IJNAOE-2013-0175.

[65] "Tsunami Guideline Plan for Operators of Caribbean Ports," 2011.

[66] P. Lynett, A. Ayca, A. Keen, and M. Eskijian, "The Multi-Level Approach to Maritime Tsunami Response." .

[67] D. Mayne, S. Kunishige, K. Richards, G. Yoshimoto, and J. Greenly, "Hurricane and Tsunami Safety Manual," Hawai, 2013.

[68] O. Department of Geology and M. Industries, "WHAT TO KNOW ABOUT TSUNAMIS Tsunami Dangers." Oregon, USA, Accessed: Jan. 30, 2023. [Online]. Available: www.wrh.noaa.gov/pqr/.

[69] "What BOATERS should know Other resources for tsunami information in California How should boat owners PREPARE for tsunamis?," California, USA. Accessed: Jan. 30, 2023. [Online]. Available: www.tsunami.ca.gov/.

[70] S. Iwanaga and Y. Matsuura, "Safety of ships' evacuation from tsunami: Survey unit of the great east Japan earthquake," *Artif. Life Robot.*, vol. 17, no. 1, pp. 168–171, 2012, doi: 10.1007/s10015-012-0040-6.

[71] I. F. Muhari A, Suppasri A, Murakami H, Futami T, "Measuring fragility of ships based on numerical model of the 2011 East Japan tsunami," *Proc. Int. Sess. Coast. Eng. Conf. ,Kyushu, Japan*, vol. Dec 2013, 2013.

[72] "At Risk: The Human, Community and Infrastructure Resources of Coastal Louisiana on JSTOR." https://www.jstor.org/stable/25737051 (accessed Feb. 02, 2023).

[73] A. Rose and D. Wei, "ESTIMATING THE ECONOMIC CONSEQUENCES OF A PORT SHUTDOWN: THE SPECIAL ROLE OF RESILIENCE," *Econ. Syst. Res.*, vol. 25, no. 2, pp. 212–232, Jun. 2013, doi: 10.1080/09535314.2012.731379.

[74] "Port Recovery in the Aftermath of Hurricane Sandy Improving Port Resiliency in the Era of Climate Change on JSTOR." https://www.jstor.org/stable/resrep06221#metadata_info_tab_contents (accessed Feb. 02, 2023).

[75] T. Litman, "Lessons From Katrina and Rita: What Major Disasters Can Teach Transportation Planners," *J. Transp. Eng.*, vol. 132, no. 1, pp. 11–18, Jan. 2006, doi: 10.1061/(ASCE)0733-947X(2006)132:1(11).

[76] V. P. B. Valenzuela, M. Esteban, H. Takagi, N. D. Thao, and M. Onuki, "Disaster awareness in three low risk coastal communities in Puerto Princesa City, Palawan, Philippines," *Int. J. Disaster Risk Reduct.*, vol. 46, p. 101508, Jun. 2020, doi: 10.1016/J.IJDRR.2020.101508.

[77] S. Islam, F. Goerlandt, X. Feng, M. J. Uddin, Y. Shi, and C. Hilliard, "Improving disasters preparedness and response for coastal communities using AIS ship tracking data," *Int. J. Disaster Risk Reduct.*, vol. 51, Dec. 2020, doi: 10.1016/J.IJDRR.2020.101863.

[78] N. Tsunami Hazard Mitigation Program, "NTHMP Tsunami Information Guide." Accessed: Jul. 13, 2021. [Online]. Available: https://nws.weather.gov/nthmp/guide/.

[79] A. Pan, "Study on the decision-making behavior of evacuation for coastal residents under typhoon storm surge disaster," *Int. J. Disaster Risk Reduct.*, vol. 45, p. 101522, May 2020, doi: 10.1016/J.IJDRR.2020.101522.

[80] A. Deelstra and D. Bristow, "Characterizing Uncertainty in City-Wide Disaster Recovery through Geospatial Multi-Lifeline Restoration Modeling of Earthquake Impact in the District of North Vancouver," *Int. J. Disaster Risk Sci.*, vol. 11, no. 6, pp. 807–820, Dec. 2020, doi: 10.1007/S13753-020-00323-5.

[81] J. Scanlon, "Transportation in emergencies: An often neglected story," *Disaster Prev. Manag. An Int. J.*, vol. 12, no. 5, pp. 428–437, 2003, doi: 10.1108/09653560310507253.

[82] M. Hansen and S. Weinstein, "East Bay Ferry Service and the Loma Prieta Earthquake Permalink," Dec. 1991, Accessed: Feb. 01, 2023. [Online]. Available: https://escholarship.org/uc/item/5dg5n2kb.

[83] M. I. Burke and N. Sipe, "Urban ferries and catastrophic floods experiences and lessons learned in Brisbane, Australia, and New York City," *Transp. Res. Rec.*, vol. 2459, pp. 127–132, 2014, doi: 10.3141/2459-15.

[84] H. Nachtmann, E. A. Pohl, and L. Farrokhvar, "Decision Support for Inland Waterways Emergency Response," *http://dx.doi.org.ezproxy.library.dal.ca/10.1080/10429247.2012.11431942*, vol. 24, no. 3, pp. 3–14, Sep. 2015, doi: 10.1080/10429247.2012.11431942.

[85] K. H. Wilberg and A. L. Olafsen, "Improving humanitarian response through an innovative pre-positioning concept : an investigation of how commercial vessels can be used to store and transport relief items Supervisor :," 2012.

[86] "Measuring the Feasibility of Inland Waterway Emergency Response - ProQuest." https://www.proquest.com/docview/1190367661?pq-origsite=gscholar&fromopenview=true (accessed Jul. 13, 2021).

[87] M. Sharifyazdi, K. A. Navangul, A. Gharehgozli, and M. Jahre, "On- and offshore prepositioning and delivery mechanism for humanitarian relief operations," *Int. J. Prod. Res.*, vol. 56, no. 18, pp. 6164–6182, 2018, doi: 10.1080/00207543.2018.1477260.

[88] A. Dolcimascolo *et al.*, "TSUNAMI HAZARD MAPS OF THE PUGET SOUND AND ADJACENT WATERS-MODEL RESULTS FROM AN EXTENDED L1 Mw 9.0 CASCADIA SUBDUCTION ZONE MEGATHRUST EARTHQUAKE SCENARIO," 2021.

[89] F. Goerlandt, L. Souza Almeida, L. Rodrigues, and R. Pelot, "Towards a Modeling Toolbox for Multi-Modal Coastal Community Supply to Support Disaster Preparedness Risk Management in Canada," *Probabilistic Saf. Assess. Manag. PSAM*, vol. 16.

[90] G. Ryan, "Introduction to positivism, interpretivism and critical theory," *Nurse Res.*, vol. 25, no. 4, pp. 14–20, 2018, doi: 10.7748/NR.2018.E1466.

[91] "Current Census Division Boundaries - Datasets - Data Catalogue." https://catalogue.data.gov.bc.ca/dataset/current-census-division-boundaries (accessed Jan. 18, 2023).

[92] "Census Profile, 2016 Census - Vancouver Island and Coast [Economic region], British Columbia and British Columbia [Province]." https://www12.statcan.gc.ca/census-recensement/2016/dp-pd/prof/details/page.cfm?Lang=E&Geo1=ER&Code1=5910&Geo2=PR&Code2=59&SearchText=vancouver island&SearchType=Begins&SearchPR=01&B1=All&TABID=1&type=0 (accessed Jan. 18, 2023).

[93] "Focus on Geography Series, 2021 Census - British Columbia." https://www12.statcan.gc.ca/census-recensement/2021/as-sa/fogs-spg/Page.cfm?Lang=E&Dguid=2021A000259&topic=1 (accessed Jan. 18, 2023).

[94] N. Willems, H. Van De Wetering, and J. J. Van Wijk, "Visualization of vessel movements," *Comput. Graph. Forum*, vol. 28, no. 3, pp. 959–966, 2009, doi: 10.1111/j.1467-8659.2009.01440.x.

[95] M. Fournier, R. Casey Hilliard, S. Rezaee, and R. Pelot, "Past, present, and future of the satellite-based automatic identification system: areas of applications (2004–2016)," *WMU J. Marit. Aff.*, vol. 17, no. 3, pp. 311–345, 2018, doi: 10.1007/s13437-018-0151-6.

[96] C. Renso, S. Spaccapietra, and E. Zimányi, *Mobility Data: Modeling, management, and understanding*. 2012.

[97] L. Cheng, Z. J. Yan, Y. J. Xiao, Y. M. Chen, F. L. Zhang, and M. C. Li, "Using big data to track marine oil transportation along the 21st-century Maritime Silk Road," *Sci. China Technol. Sci.*, vol. 62, no. 4, pp. 677–686, 2019, doi: 10.1007/s11431-018-9335-1.

[98] L. Zhao, G. Shi, and J. Yang, "Ship Trajectories Pre-processing Based on AIS Data," *J. Navig.*, vol. 71, no. 5, pp. 1210–1230, 2018, doi: 10.1017/S0373463318000188.

[99] Y. Zheng, "Trajectory data mining: An overview," *ACM Trans. Intell. Syst. Technol.*, vol. 6, no. 3, pp. 1–41, 2015, doi: 10.1145/2743025.

[100] T. Devogele *et al.*, "Maritime monitoring," pp. 224–243, 2015.

[101] G. K. D. De Vries and M. Van Someren, "Machine learning for vessel trajectories using compression, alignments and domain knowledge," *Expert Syst. Appl.*, vol. 39, no. 18, pp. 13426–13439, 2012, doi: 10.1016/j.eswa.2012.05.060.

[102] L. Etienne, T. Devogele, and A. Bouju, "Spatio-Temporal Trajectory Analysis of Mobile Objects Following the Same Itinerary," *Int. Arch. Photogramm. Remote Sens. Spat. Inf. Sci.*, vol. 38, no. 3, pp. 86–91, 2012.

[103] "Freshwater Atlas Coastlines - Datasets - Data Catalogue." https://catalogue.data.gov.bc.ca/dataset/freshwater-atlas-coastlines (accessed Jan. 18, 2023).

[104] "BC Ports and Terminals - Datasets - Data Catalogue." https://catalogue.data.gov.bc.ca/dataset/bc-ports-and-terminals (accessed Jan. 21, 2023).

[105] "Cascadia megathrust fault map | U.S. Geological Survey." https://www.usgs.gov/media/images/cascadia-megathrust-fault-map (accessed Jan. 29, 2023).

[106] "Tsunami Notification Zones for BC - Datasets - Data Catalogue." https://catalogue.data.gov.bc.ca/dataset/tsunami-notification-zones-for-bc (accessed Jan. 29, 2023).

[107] "Get prepared for a tsunami - Province of British Columbia." https://www2.gov.bc.ca/gov/content/safety/emergency-management/preparedbc/know-your-hazards/earthquakes-tsunamis/tsunami (accessed Jan. 29, 2023).

[108] "Benthic Marine Ecounits - Coastal Resource Information Management System (CRIMS) - Datasets - Data Catalogue." https://catalogue.data.gov.bc.ca/dataset/benthic-marine-ecounits-coastal-resource-information-management-system-crims (accessed Jan. 30, 2023).

[109] AXYS Environmental Consulting Ltd., "British Columbia Marine Ecological Classification Update," 2002.

[110] T. Allen, "Calculate travel time for a tsunami | Learn ArcGIS." https://learn.arcgis.com/en/projects/calculate-travel-time-for-a-tsunami/#calculate-speed (accessed Jan. 30, 2023).

[111] D. Stevenson, "Tsunamis and Earthquakes: What Physics Is Interesting?," *Phys. Today*, vol. 58, no. 6, pp. 10–11, Jun. 2005, doi: 10.1063/1.1996451.

[112] Y. C. Altan and E. N. Otay, "Maritime Traffic Analysis of the Strait of Istanbul based on AIS data," *J. Navig.*, vol. 70, no. 6, pp. 1367–1382, 2017, doi: 10.1017/S0373463317000431.

[113] M. Lensu and F. Goerlandt, "Big maritime data for the Baltic Sea with a focus on the winter navigation system," *Mar. Policy*, vol. 104, no. January, pp. 53–65, 2019, doi: 10.1016/j.marpol.2019.02.038.

[114] L. Wu, Y. Xu, Q. Wang, F. Wang, and Z. Xu, "Mapping Global Shipping Density from AIS Data," *J. Navig.*, vol. 70, no. 1, pp. 67–81, 2017, doi: 10.1017/S0373463316000345.

[115] L. Zhang, Q. Meng, and T. Fang Fwa, "Big AIS data based spatial-temporal analyses of ship traffic in Singapore port waters," *Transp. Res. Part E Logist. Transp. Rev.*, vol. 129, pp. 287–304, 2019, doi: 10.1016/j.tre.2017.07.011.

[116] Y. T. Wen, C. H. Lai, P. R. Lei, and W. C. Peng, "RouteMiner: Mining ship routes from a massive maritime trajectories," *Proc. - IEEE Int. Conf. Mob. Data Manag.*, vol. 1, pp. 353–356, 2014, doi: 10.1109/MDM.2014.52.

[117] S. kai Zhang, G. you Shi, Z. jiang Liu, Z. wei Zhao, and Z. lin Wu, "Data-driven based automatic maritime routing from massive AIS trajectories in the face of disparity," *Ocean Eng.*, vol. 155, no. 1550, pp. 240–250, 2018, doi: 10.1016/j.oceaneng.2018.02.060.

[118] "Find Dwell Locations (GeoAnalytics)—ArcGIS Pro | Documentation." https://pro.arcgis.com/en/pro-app/latest/tool-reference/big-data-analytics/find-dwell-locations.htm (accessed Jan. 30, 2023).

[119] "Detect Incidents (GeoAnalytics)—ArcGIS Pro | Documentation." https://pro.arcgis.com/en/pro-app/latest/tool-reference/big-data-analytics/detect-incidents.htm (accessed Jan. 30, 2023).

[120] "Reconstruct Tracks (GeoAnalytics Desktop)—ArcGIS Pro | Documentation." https://pro.arcgis.com/en/pro-app/latest/tool-reference/geoanalytics-desktop/reconstruct-tracks.htm (accessed Jan. 30, 2023).

[121] L. Etienne, T. Devogele, M. Buchin, and G. McArdle, "Trajectory Box Plot: a new pattern to summarize movements," *Int. J. Geogr. Inf. Sci.*, vol. 30, no. 5, pp. 835–853, 2016, doi: 10.1080/13658816.2015.1081205.

[122] "Spatial Join (Analysis)—ArcMap | Documentation." https://desktop.arcgis.com/en/arcmap/latest/tools/analysis-toolbox/spatial-join.htm (accessed Jan. 30, 2023).

[123] "How Central Feature works—ArcGIS Pro | Documentation." https://pro.arcgis.com/en/pro-app/latest/tool-reference/spatial-statistics/h-how-central-feature-spatial-statistics-works.htm (accessed Jan. 30, 2023).

[124] "Calculate Field (Data Management)—ArcGIS Pro | Documentation." https://pro.arcgis.com/en/pro-app/latest/tool-reference/data-management/calculate-field.htm (accessed Jan. 30, 2023).

[125] N. Agrawal, *Natural disasters and risk management in Canada*, vol. 21. 2018.

[126] T. Aven, "Risk assessment and risk management: Review of recent advances on their foundation," *Eur. J. Oper. Res.*, vol. 253, no. 1, pp. 1–13, Aug. 2016, doi: 10.1016/J.EJOR.2015.12.023.

[127] "Near (Analysis)—ArcGIS Pro | Documentation." https://pro.arcgis.com/en/pro-app/latest/tool-reference/analysis/near.htm (accessed Jan. 30, 2023).

[128] "Cost Path Analysis - GIS Wiki | The GIS Encyclopedia." http://wiki.gis.com/wiki/index.php/Cost_Path_Analysis (accessed Jan. 30, 2023).

[129] "Generate Grid From Area (Defense)—ArcGIS Pro | Documentation." https://pro.arcgis.com/en/pro-app/latest/tool-reference/defense/generate-grid-from-area.htm (accessed Jan. 30, 2023).

[130] "Summary Statistics (Analysis)—ArcGIS Pro | Documentation." https://pro.arcgis.com/en/pro-app/latest/tool-reference/analysis/summary-statistics.htm (accessed Jan. 30, 2023).

[131] N. Agrawal, "Natural Disasters and Risk Management in Canada," vol. 49, 2018, doi: 10.1007/978-94-024-1283-3.

[132] F. Goerlandt and G. Reniers, "On the assessment of uncertainty in risk diagrams," *Saf. Sci.*, vol. 84, pp. 67–77, Apr. 2016, doi: 10.1016/J.SSCI.2015.12.001.

[133] F. Goerlandt and J. Montewka, "A framework for risk analysis of maritime transportation systems: A case study for oil spill from tankers in a ship–ship collision," *Saf. Sci.*, vol. 76, pp. 42–66, Jul. 2015, doi: 10.1016/J.SSCI.2015.02.009.

[134] L. Souza Almeida *et al.*, "Datasets of disrupted transportation networks on Canada's West Coast in a plausible M9.0 Cascadia Subduction Zone earthquake scenario," *Data Br.*, vol. 46, p. 108762, Feb. 2023, doi: 10.1016/J.DIB.2022.108762.

Appendixes

Appendix 1 – Subdivisions boundaries and table with population information.

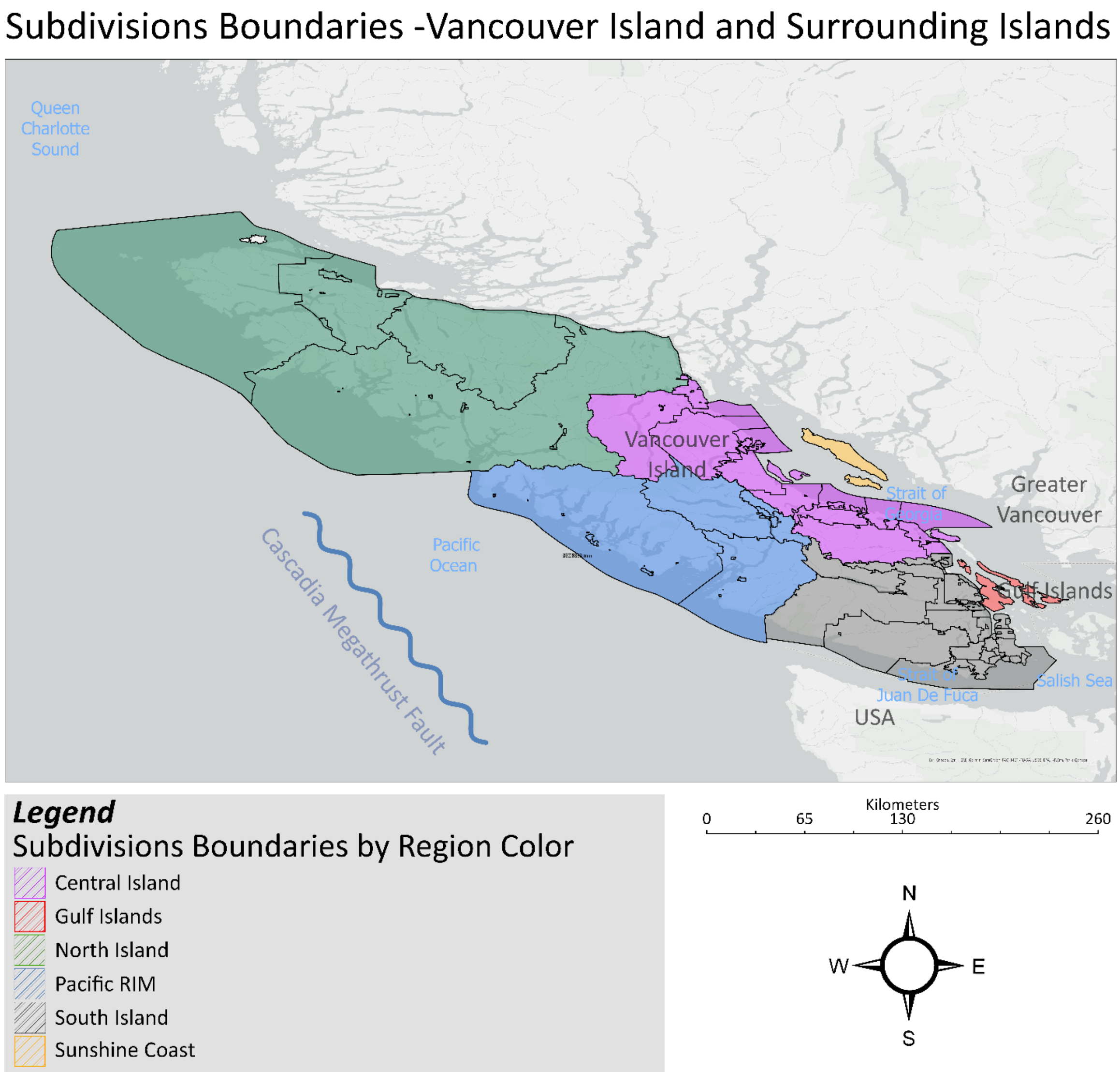

Figure 52 - Census subdivision boundaries and their respective regions' classification illustrated by different color categories.

Table 22 – 130 subdivisions' respective information - population, census division, and region.

Subdivision	Population	Census Division	Region
Powell River D	1,076	Powell River	Sunshine Coast
Powell River E	399	Powell River	Sunshine Coast
North Saanich	11,249	Capital	South Island
Sidney	11,672	Capital	South Island
Central Saanich	16,814	Capital	South Island
Saanich	114,148	Capital	South Island
Oak Bay	18,094	Capital	South Island
Victoria	85,792	Capital	South Island
Esquimalt	17,655	Capital	South Island
Colwood	16,859	Capital	South Island
Metchosin	4,708	Capital	South Island
Langford	35,342	Capital	South Island
View Royal	10,408	Capital	South Island

Highlands	2,225	Capital	South Island
Sooke	13,001	Capital	South Island
Juan de Fuca (Part 1)	4,670	Capital	South Island
Juan de Fuca (Part 2)	190	Capital	South Island
Cole Bay 3	332	Capital	South Island
Union Bay 4	94	Capital	South Island
East Saanich 2	1,689	Capital	South Island
South Saanich 1	822	Capital	South Island
Becher Bay 1	129	Capital	South Island
New Songhees 1A	1,842	Capital	South Island
Gordon River 2	111	Capital	South Island
T'Sou-ke	225	Capital	South Island
North Cowichan	29,676	Capital	South Island
Duncan	4,944	Capital	South Island
Cowichan Valley D	3,243	Capital	South Island

Cowichan Valley G	2,325	Capital	South Island
Lake Cowichan	3,226	Capital	South Island
Cowichan Valley H	2,446	Capital	South Island
Ladysmith	8,537	Capital	South Island
Cowichan Valley F	1,629	Capital	South Island
Cowichan Valley I	1,206	Capital	South Island
Cowichan Valley A	4,733	Capital	South Island
Cowichan Valley B	8,558	Capital	South Island
Cowichan Valley C	5,019	Capital	South Island
Cowichan Valley E	4,121	Capital	South Island
Halalt 2	168	Capital	South Island
Squaw-hay-one 11	35	Capital	South Island
Tsussie 6	103	Capital	South Island
Chemainus 13	735	Capital	South Island
Cowichan Lake	21	Capital	South Island

Malachan 11	158	Capital	South Island
Malahat 11	143	Capital	South Island
Oyster Bay 12	77	Capital	South Island
Theik 2	36	Capital	South Island
Est-Patrolas 4	23	Capital	South Island
Tzart-Lam 5	39	Capital	South Island
Cowichan	2,086	Capital	South Island
Port Alberni	17,678	Alberni-Clayoquot	Pacific RIM
Ucluelet	1,717	Alberni-Clayoquot	Pacific RIM
Tofino	1,932	Alberni-Clayoquot	Pacific RIM
Alberni-Clayoquot B	443	Alberni-Clayoquot	Pacific RIM
Alberni-Clayoquot D	1,616	Alberni-Clayoquot	Pacific RIM
Alberni-Clayoquot E	2,754	Alberni-Clayoquot	Pacific RIM
Alberni-Clayoquot F	1,935	Alberni-Clayoquot	Pacific RIM
Alberni-Clayoquot A	243	Alberni-Clayoquot	Pacific RIM

Alberni-Clayoquot C	677	Alberni-Clayoquot	Pacific RIM
Ahahswinis 1	119	Alberni-Clayoquot	Pacific RIM
Alberni 2	10	Alberni-Clayoquot	Pacific RIM
Anacla 12	82	Alberni-Clayoquot	Pacific RIM
Elhlateese 2	5	Alberni-Clayoquot	Pacific RIM
Hesquiat 1	5	Alberni-Clayoquot	Pacific RIM
Ittatsoo 1	274	Alberni-Clayoquot	Pacific RIM
Marktosis 15	622	Alberni-Clayoquot	Pacific RIM
Numukamis 1	5	Alberni-Clayoquot	Pacific RIM
Macoah 1	19	Alberni-Clayoquot	Pacific RIM
Opitsat 1	150	Alberni-Clayoquot	Pacific RIM
Tsahaheh 1	542	Alberni-Clayoquot	Pacific RIM
Klehkoot 2	15	Alberni-Clayoquot	Pacific RIM
Esowista 3	94	Alberni-Clayoquot	Pacific RIM
Refuge Cove 6	44	Alberni-Clayoquot	Pacific RIM

Gold River	1,212	Mount Waddington	North Island
Zeballos	107	Mount Waddington	North Island
Tahsis	248	Mount Waddington	North Island
Sayward	311	Mount Waddington	North Island
Strathcona A	764	Not applied	North Island
Houpsitas 6	181	Mount Waddington	North Island
Yuquot 1	5	Mount Waddington	North Island
Oclucje 7	30	Mount Waddington	North Island
Tsa Xana 18	187	Mount Waddington	North Island
Ehatis 11	88	Mount Waddington	North Island
Port McNeill	2,337	Mount Waddington	North Island
Port Alice	664	Mount Waddington	North Island
Port Hardy	4,132	Mount Waddington	North Island
Mount Waddington B	60	Mount Waddington	North Island
Mount Waddington C	750	Mount Waddington	North Island

Mount Waddington D	228	Mount Waddington	North Island
Fort Rupert 1	27	Mount Waddington	North Island
Tsulquate 4	431	Mount Waddington	North Island
Kippase 2	228	Mount Waddington	North Island
Quatsino Subdivision 18	224	Mount Waddington	North Island
South Pender Island Trust Area	235	Not applied	Gulf Islands
Saturna Island Trust Area	354	Not applied	Gulf Islands
North Pender Island Trust Area	2,067	Not applied	Gulf Islands
Mayne Island Trust Area	949	Not applied	Gulf Islands
Saltspring Island	10,557	Not applied	Gulf Islands
Galiano Island Trust Area	1,044	Not applied	Gulf Islands
Thetis Island Trust Area + Valdes Island	399	Not applied	Gulf Islands
Penelakut Island 7	452	Not applied	Gulf Islands
Denman Island Trust Area	1,165	Nanaimo	Central Island
Nanaimo B	4,033	Nanaimo	Central Island

Hornby Island Trust Area	1,016	Nanaimo	Central Island
Nanaimo	90,504	Nanaimo	Central Island
Lantzville	3,605	Nanaimo	Central Island
Nanaimo A	7,058	Nanaimo	Central Island
Nanaimo C	2,808	Nanaimo	Central Island
Parksville	12,514	Nanaimo	Central Island
Qualicum Beach	8,943	Nanaimo	Central Island
Nanaimo E	6,125	Nanaimo	Central Island
Nanaimo F	7,724	Nanaimo	Central Island
Nanaimo G	7,465	Nanaimo	Central Island
Nanaimo H	3,884	Nanaimo	Central Island
Nanaimo Town 1	360	Nanaimo	Central Island
Nanoose	230	Nanaimo	Central Island
Qualicum	74	Nanaimo	Central Island
Nanaimo River	371	Nanaimo	Central Island

Campbell River	32,588	Nanaimo	Central Island
Strathcona D (Oyster Bay - Buttle Lake)	4,396	Nanaimo	Central Island
Campbell River 11	381	Nanaimo	Central Island
Quinsam 12	294	Nanaimo	Central Island
Homalco 9	202	Nanaimo	Central Island
Comox	14,028	Nanaimo	Central Island
Courtenay	25,599	Nanaimo	Central Island
Cumberland	3,753	Nanaimo	Central Island
Comox Valley B (Lazo North)	7,095	Nanaimo	Central Island
Comox Valley C (Puntledge - Black Creek)	8,617	Nanaimo	Central Island
Comox 1	222	Nanaimo	Central Island
Comox Valley A	7,213	Nanaimo	Central Island

Appendix 2- ***Strength of evidence categories type definition and their levels descriptions***

Categories	Definition	Example	Level	Description of the level
Data	Input data and output data in models.	Tables, parameters, geographic data, area, information pieces, and other models' results.	Not applicable	Element is not data.
			Weak	Data is not available or unreliable.
			Medium	Data is available, but generalizations or modifications are made, and/or little data is available.
			Strong	Reliable data are available.
Model processes	Model processes are characterized by workflow/diagrams representing the GIS tools, calculations, and models' steps.	Calculations, GIS tools, intermediate results.	Not applicable	Element is not a model process
			Weak	Step processing gives poor accuracy, and the calculation poorly predicts the phenomena.
			Medium	Step proceeding is reasonable, and simple calculations have low phenomena deviation.
			Strong	Step processing gives good accuracy; the calculations are logical and predict the phenomena.
Assumptions	A decision made related to evidence, being this	Threat levels for Tsunami zones, ship damage	Not applicable	Assumptions are not made or elements based on evidence.

	choice assumed to be valid and/or logical.	distance near ports.	Weak	Strong simplifications with considerable application.
			Medium	Some simplifications are made, but medium application.
			Strong	Some simplifications are made, but low application.
Literature-based expert judgment	A decision related to evidence is based on expert judgment information from references (grey materials - such as guidelines, reports - or scientific papers).	Safe depth parameter, current areas.	Not applicable	Element is not an expert judgment.
			Weak	Lack of consensus and no literature review references.
			Medium	Lack of consensus but grey literature review references, such as field experience.
			Strong	Broad consensus and good literature review references.

Appendix 3 – *Importance levels descriptions*

Importance Level	Description of the level
Low importance	Low-importance elements mean they weak affect the results and do not contribute to biased results. The data is not part of the main calculation (variable); it is used to prep data and model calculation. Such as cleaning raw data, selecting information, boundary areas or import, joining tables, matching data sets, categorizing results.
Medium importance	Medium importance elements mean that they medium affect the results, indirectly contributing to bias. The data is not part of the main calculation (variable) but supports the primary data or model step does not contributes directly to final results but is a step previous to the main calculation.
High importance	High implication elements mean that they strongly affect the results, contributing to bias and deviation. The data is part of the main calculation (variable) or model step contributing directly to the final results.
Justification	How much would the results change if using a different data or model process?

Appendix 4 – Each vessel damage probability and categories.

Vessel ID	Status	Damage Probability	Color Code	Vessel Class
V1	Damage	58%	Orange	Medium Ferries
V2	Damage	57%	Orange	Medium Ferries
V3	Damage	55%	Orange	Medium Ferries
V4	Damage	36%	Yellow	Medium Ferries
V5	Damage	46%	Yellow	Small Ferries
V6	Damage	32%	Yellow	Medium Ferries
V7	Damage	42%	Yellow	Medium Ferries
V8	Damage	70%	Orange	Large Ferries
V9	Damage	100%	Dark Red	Large Ferries
V10	Damage	100%	Dark Red	Large Ferries
V11	Damage	76%	Light Red	Large Ferries
V12	Damage	34%	Yellow	Large Ferries
V13	Damage	41%	Yellow	Large Ferries
V14	Damage	30%	Yellow	Large Ferries
V15	Damage	61%	Orange	Large Ferries
V16	Damage	19%	Light Green	Large Ferries
V17	Damage	9%	Light Green	Large Ferries
V18	Damage	1%	Dark Green	Medium Ferries
V19	Damage	4%	Dark Green	Large Ferries
V21	Damage	96%	Dark Red	Medium Ferries
V22	Damage	100%	Dark Red	Medium Ferries
V23	Damage	100%	Dark Red	Small Ferries
V24	Damage	48%	Yellow	Medium Ferries
V25	Damage	33%	Yellow	Small Ferries
V26	Damage	1%	Dark Green	Medium Ferries
V27	Damage	100%	Dark Red	Small Ferries
V28	Damage	100%	Dark Red	Small Ferries
V31	NO Damage	0%	Dark Green	Small Ferries
V32	Damage	3%	Dark Green	Medium Ferries

V35	Damage	5%	Dark Green	Small Ferries
V36	Damage	19%	Light Green	Small Ferries
V37	Damage	53%	Orange	Small Ferries
V38	Damage	100%	Dark Red	Medium Ferries
V39	Damage	46%	Yellow	Medium Ferries
V40	Damage	36%	Yellow	Small Ferries
V41	Damage	69%	Orange	Large Tug-Barge combination
V42	Damage	27%	Yellow	Large Tug-Barge combination
V43	Damage	77%	Light Red	Large Tug-Barge combination
V44	Damage	53%	Orange	Large Tug-Barge combination
V45	Damage	57%	Orange	Medium Tug-Barge combination
V46	Damage	61%	Orange	Medium Tug-Barge combination
V47	Damage	51%	Orange	Medium Tug-Barge combination
V48	Damage	45%	Yellow	Large Tug-Barge combination
V49	Damage	42%	Yellow	Medium Tug-Barge combination
V50	Damage	67%	Orange	Medium Tug-Barge combination
V51	Damage	62%	Orange	Medium Tug-Barge combination
V52	Damage	26%	Yellow	Medium Tug-Barge combination
V53	Damage	47%	Yellow	Small Tug-Barge combination
V54	Damage	22%	Light Green	Small Tug-Barge combination
V55	Damage	31%	Yellow	Small Tug-Barge combination
V56	Damage	35%	Yellow	Small Tug-Barge combination
V57	Damage	76%	Light Red	Large Tug-Barge combination
V58	Damage	65%	Orange	Large Tug-Barge combination
V59	Damage	42%	Yellow	Medium Tug-Barge combination
V60	Damage	36%	Yellow	Medium Tug-Barge combination
V61	Damage	40%	Yellow	Medium Tug-Barge combination
V62	Damage	33%	Yellow	Medium Tug-Barge combination

Appendix 5 - ***Strength of evidence analyses***

*D=Data, M= Model processes, A= Assumptions, LB= Literature-based

		Categories *					
Code	**Evidence**	**D**	**M**	**A**	**LB**	**The justification that describes the reason for using this data or model process, and sometimes how it was utilized in the research**	**Overall Judgment**
M	**Marine vessel movement**						
M1	Select vessels					The vessels used in the research are based on the SIREN project database and its goals. They are data to be studied.	S
M2	AIS data					AIS data provided by Exact x and Literature-based information on being used to calculate ship trajectories.	S
M3	AIS data sampling					Sampling was performed because the AIS dataset was too large.	M
M4	AIS data Sample					Data represent the population.	S
M5	Cleaning AIS data					This step cleaned points at land and duplicated based, leading better dataset.	S
M6	Ports and terminals					Locate ports, terminals, and docks in the research area.	S
M7	Selecting Ports					Ports went through a selection process matching with AIS data.	M
M8	Ports selected					They are used to define routes' origin and destination.	S
M9	Coastline					They are used to clean outliers and avoid route overlay on land.	S

M10	Dwell Locations					Define ship stop locations to define origin and destination later.	S
M11	Remove Outliers					Remove dwell locations that are not near the coastline.	M
M12	Match Dwell with ports					They are used to match stop points with port information.	S
M13	Define Start and End trajectory points					Calculate where a route start and when it ends, assuming SOG information.	M
M14	Detect trajectories					Calculates different trajectories according to the point information.	S
M15	Reconstruct tracks					Draw a line of the tracks according to trajectories, reducing data, using detected trajectory ID distance parameter between points and time parameter with some assumptions.	S
M16	Clean tracks outliers					Clean some tracks that are too short of representing a track.	S
M17	Origin and Destination ports match with the track					Improve track information by adding origin and destination ports with simple calculations and generating itineraries.	M
M18	Homogenous Groups					Group tracks of the same ship according to the same itinerary.	S
M19	Centreline process					Create a centerline representing the path according to itineraries.	M
R	**RUSEMARIE**						
R1	Vessel tracks					Routes from the MVM model are good, but there is no LR that used them to analyze ship damage	M

R2	Path Distance Parameter					After some tests, the distance between points of 500 meters is used, despite of literature review about the correct distance between points to analyze the damage.	S
R3	Routes to Path					A processing step using pre-built software tools. Tools developed based on previous Literature	S
R4	Ports and Terminals Point Location					Same ports of MVM, port locations are based on points.	S
R5	Ports Distance Parameter					To be able to define damage near the port based on distance, the parameter was chosen based on tests, but there is no literature review saying the safe distance between the port and the vessel.	W
R6	Bridges Location					Reliable data based on the EMBC dataset; some assumptions were made to choose bridges that are in areas where ships navigate under.	S
R7	Bridges Distance Parameter					The parameter was chosen based on tests, but no literature review says the safe distance between the port and the vessel.	W
R8	Port and Bridge damage status					Damage information based on a study; some interpolation was made to add damage information to ports that were not in the referenced study.	M
R9	Calculation distance from port and bridges					The step used an ArcGIS tool that was developed according to studies.	S
R10	Vessel Safety Guidelines					Few guidelines about vessel safety were found, they have different	M

						information, so some assumptions were made, and most of the guides were grey Literature from governments.	
R11	Tsunami zones and alert levels					Some assumptions were made with high impact due to the RUSEMARIE model steps being different for each zone according to the assigned damage level. This assigned information was based on Literature about possible Cascadia Tsunami damages.	M
R12	Matching tsunami zones with points					Processing step using ArcGIS tool that is based on studies.	S
R13	Depth data					Bathymetric data is available from a reliable source, but in ranges, being inconsistent, leading to assumptions.	M
R14	Depth safe parameter					Safe depth parameter based on guidelines, but a higher parameter was chosen to fit at data due to data inconsistency.	M
R15	Coastlines					Data from a good source and used as a barrier to avoid overlay land, use according to the literature review.	S
R16	Central Point depth safe					A central point for depth area was created to be the end location of safe ship travel. No literature review specifies the central point to be used as the end of safe travel.	M
R17	Mean SOG definition					To calculate ship travel time to safe, the mean SOG from AIS data, one SOG calculated for ferries and the other for	M

						tugs. However, all ships of the same type receive the same SOG.	
R18	Calculation of ship Travel time to depth area					Processing made using ArcGIS tools indicated for this situation, being grey Literature. Assumptions about SOG mean impact travel time.	W
R19	Cascadia Megathrust Fault					Data is used to Tsunami travel path's initial location and calculate time.	M
R20	Depth maximum to velocity					The maximum range was used to calculate tsunami velocity, being the bathymetric area data in ranges, so an assumption with a high application.	M
R21	Tsunami Velocity					The tsunami velocity for each range was calculated using a simple formula using the maximum depth.	W
R22	Calculation Tsunami arrival time					Using Tsunami velocity and length to calculate time was made simply using the studied formula, despite a better model to calculate Tsunami time available.	W
R23	Comparing times					A simple calculation that compares two values, but assuming that if travel time is longer than arrival time, the point is damaged,	M
R24	Vessels Attributes					Vessel attributes, including size and tonnage, that impact one calculation step at RUSEMARIE is from a reliable database.	M

R25	Vessel size parameter					The size parameter to define small vessels are according to the literature review and grey material, but both consider the lack of the definition of small or diverge in size.	M
R26	Current area					The data with current velocity is based on a report, not having precise data; some assumptions were made to reproduce the current area.	M
R27	Current area overlay					Only points within the current area are classified as damaged. However, according to the literature review, vessels in these current areas will not always be damaged, depending on other vessel attributes.	M
R28	Damage or not process					The classification of damage or not in the RUSEMARIE model is according to conditional analyses of geographical elements. There is no literature on damage classification and conditional analyses.	M
R29	Damage extrapolation					Some points were missing damage classification, so an ArcGIS tool was used to extrapolate according to the proximity.	S
R30	Damage probability Calculation					The damage probability calculation was made using the count of damage points by the total number of points. Being this a simplification because there are other formulas to calculate probability.	M

I	**Impact Scenario Data**						
I1	Cascadia Megathrust Fault					Data available was Cascadia zone; for fault, some modifications and simplifications were made in the line.	M
I2	Tsunami Notification Zones					Reliable data based on government analyses.	S
I3	Tsunami impacts levels					Reliable data based on government information.	S
I4	Tsunami Zones match with impacts					When matching the zones with levels was a simple process with some assumptions based on a good literature review.	M
I5	Port and Bridge damage					Damage information from the reliable study, based on a good literature review.	S
I6	Port and Bridge damage levels extrapolation					Some ports were missing from the damage dataset, so extrapolation was made based on the Literature review.	M
I7	Currents velocity					Data is available only for some areas, not all studied areas; maximum velocity is considered, but papers lack consensus about maximum velocity.	M
I8	Current area definition					There was no area available,considerations are made, report information with some simplifications.	M
I9	Wave velocity calculation					Calculations use simple formulation, despite a better model at literature review, and have strong application at tsunami arrival time.	W

Appendix 6 – Importance analyses

Code	Evidence	Importance	Justification
M	**Marine vessel movement**		
M1	Select vessels	H	The analyses were made using these select vessels; a different selection could generate different results.
M2	AIS data	M	Raw AIS dataset.
M3	AIS data sampling	L	Sampling does not change route generation due number of points available.
M4	AIS data Sample	H	Input dataset used at MVM model.
M5	Cleaning AIS data	L	Pre-data step.
M6	Ports and terminals	L	Raw dataset.
M7	Selecting Ports	L	Process select ports that will be used.
M8	Ports selected	M	Ports used at MVM model.
M9	Coastline	L	Help avoid lines overpassing land; keep them in the sea.

M10	Dwell Locations	M	Knowing where the ships stop helps identify ports later.
M11	Remove Outliers	L	Sometimes ships stop in other areas that are not ports or terminals, away from the coastline, specifically tugs.
M12	Match Dwell with ports	L	Without a match, the Dwell are only areas.
M13	Define Start and End trajectory points	M	Knowing the start and end points is essential to detecting track information.
M14	Detect trajectories	M	Detect the sequence of points in a track; points will be mixed without it.
M15	Reconstruct tracks	M	Turn points to lines, decrease the number of data, and gets a better visualization of the track.
M16	Clean tracks outliers	L	Taking out small tracks could make data confused.
M17	Origin and Destination ports match with the track	H	Knowing the origin and destination ports is vital to track information.
M18	Homogenous Groups	M	A homogenous group is essential to generate itineraries that will support centreline generation.
M19	Centreline process	H	Generate the MVM output data paths.
R	**RUSEMARIE**		
R1	Vessel tracks	H	Core information is used to retrieve points.
R2	Path Distance Parameter	M	After testing the distance between points parameter, it affects the final results just a little.
R3	Routes to Path	H	The point data that will be analyzed and different

			point locations could generate other results.
R4	Ports and Terminals Point Location	L	Latitude and longitude are used as port locations.
R5	Ports Distance Parameter	H	Depending on the distance will generate more or fewer damage points near ports.
R6	Bridges Location	L	Latitude and longitude are used as bridge locations.
R7	Bridges Distance Parameter	H	Depending on the distance will generate more or fewer damage points near bridges.
R8	Port and Bridge damage status	M	Combined with proximity, it will define if the port will be damaged and, consequently, the point.
R9	Calculation distance from port and bridges	L	Simple step with low importance.
R10	Vessel Safety Guidelines	L	Used as a framework for RUSEMARIE development.
R11	Tsunami zones and alert levels	M	Essential because different levels end up in different calculations.
R12	Matching tsunami zones with points	L	Simple overlay step.
R13	Depth data	M	Safety depends on this data.
R14	Depth safe parameter	H	Parameter leads to damage or not in more than one zone.
R15	Coastlines	L	Avoid overlay of paths on land.
R16	Central Point Depth safe	M	Maybe considering a point near the border of a safe region, the travel time would be less.

R17	Mean SOG definition	M	Information calculates ship travel time and SOG results at different times.
R18	Calculation of ship Travel time to depth area	H	This is an essential calculation because the result can lead to damage compared to tsunami arrival.
R19	Cascadia Megathrust Fault	L	Used as a reference for the initial point of the tsunami.
R20	Depth maximum to velocity	M	Different depth result is the diverse velocity that impacts tsunami arrival time.
R21	Tsunami Velocity	M	Information used to calculate tsunami arrival time, different velocity results in different times.
R22	Calculation Tsunami arrival time	H	This is an essential calculation because the result can lead to damage compared to safe ship travel.
R23	Comparing times	L	Simple time comparison step.
R24	Vessels Attributes	L	Ship gross tonnage and type a selecting data.
R25	Vessel size parameter	H	Defining which parameter is used to identify small vessels is essential because it impacts the study vessels for current damage.
R26	Current area	H	Current area velocity defines the damage status; the outcome could be different if other data is used.
R27	Current area overlay	L	A simple step, current data is the critical part.
R28	Damage or not process	H	Simple condition steps, but this is the RUSEMARIE model outcome.

R29	Damage extrapolation	M	Help add information for points where the condition analyses were not performed, generating more data
R30	Damage probability Calculation	H	The calculation defines probability information.
I	**Impact Scenario Data**		
I1	Cascadia Megathrust Fault	M	Start point where the tsunami start is used to support the calculation of tsunami arrival time.
I2	Tsunami Notification Zones	H	The structural part of the RUSEMARIE model.
I3	Tsunami impacts levels	L	Support critical elements of the RUSEMARIE model but are not used directly.
I4	Tsunami Zones match with impacts	H	Tsunami zone impacts have been directly used in damage calculations types
I5	Port and Bridge damage	M	Define damage points near bridges and ports,
I6	Port and Bridge damage levels extrapolation	L	Processing is not part of the main calculation; it was used to generate input data.
I7	Currents velocity	H	Define an area if a small ship point was damaged.
I8	Current area definition	M	The area used together with current information.
I9	Wave velocity calculation	H	Velocity affects Tsunami arrival time, which leads to damage points.